

For Reference

NOT TO BE TAKEN FROM THIS ROOM

Ex LIBRIS
UNIVERSITATIS
ALBERTAEANAE





Digitized by the Internet Archive
in 2020 with funding from
University of Alberta Libraries

<https://archive.org/details/Liverman1981>

Pages 54 and 77 are not missing from this thesis, but
have been misnumbered.

THE UNIVERSITY OF ALBERTA

RELEASE FORM

NAME OF AUTHOR D.G.E.Liverman

TITLE OF THESIS Sedimentology and drainage history of a
glacier dammed lake, St. Elias
Mountains, Yukon Territory

DEGREE FOR WHICH THESIS WAS PRESENTED Master of Science

YEAR THIS DEGREE GRANTED Spring, 1981

Permission is hereby granted to THE UNIVERSITY OF
ALBERTA LIBRARY to reproduce single copies of this
thesis and to lend or sell such copies for private,
scholarly or scientific research purposes only.

The author reserves other publication rights, and
neither the thesis nor extensive extracts from it may
be printed or otherwise reproduced without the author's
written permission.

THE UNIVERSITY OF ALBERTA

Sedimentology and drainage history of a glacier dammed lake,
St. Elias Mountains, Yukon Territory

by



D.G.E. Liverman

A THESIS

SUBMITTED TO THE FACULTY OF GRADUATE STUDIES AND RESEARCH
IN PARTIAL FULFILMENT OF THE REQUIREMENTS FOR THE DEGREE
OF Master of Science

Geology

EDMONTON, ALBERTA
Spring, 1981

31-76

THE UNIVERSITY OF ALBERTA
FACULTY OF GRADUATE STUDIES AND RESEARCH

The undersigned certify that they have read, and recommend to the Faculty of Graduate Studies and Research, for acceptance, a thesis entitled Sedimentology and drainage history of a glacier dammed lake, St. Elias Mountains, Yukon Territory submitted by D.G.E.Liverman in partial fulfilment of the requirements for the degree of Master of Science.

Abstract

"Hazard Lake", located in the St. Elias Mountains, Yukon Territory, is an ice dammed lake formed by the surge of the Steele Glacier in 1966. Since 1975 it has annually catastrophically drained by means of a sub-glacial tunnel. During a four week field season in 1979, the final stages of lake filling, and the complete lake drainage were observed and measured. The discharge curve produced was similar to that produced by Clarke (1980b) for the 1978 event, showing that the physical parameters controlling the flood remain constant through time and supporting the floatation model of lake drainage. It is suggested that the low value of the Manning roughness coefficient, n' , calculated for the tunnel walls by Clarke is due to incomplete closure of the tunnel between events resulting in an erroneous input to the drainage model. A model for the historical development of ice dammed lakes is proposed, and tested against observation.

Lake processes were investigated while the lake was filling, and these suggest that the lake is unstratified, and the major inflow stream enters as underflow. Sections examined in the lake bottom after drainage show the deposition of a thick bed of laminated silts, usually directly overlying gravels, and overlaid by cross laminated and massive sands. The laminated silts are interpreted as being deposited by underflow during the nine years of lake stability. No evidence of an annual cycle is seen in this

facies, and this is explained in terms of the lake processes. The repeated filling and draining cycle appears to produce no permanent sedimentary record.

Acknowledgements

Many people assisted in numerous ways in the completion of this thesis. Dr. Ron May suggested the topic, obtained financial support, and furnished much advice and assistance throughout the study, especially with regard to computing. Gerry Groves was a capable and enthusiastic field assistant; he also assisted in some of the laboratory analysis. Dr Gary Clarke made an invaluable contribution, by supplying bathymetric data and maps, pre-publication copies of his papers, and most of all, through his own work on Hazard Lake. Dr John Shaw made many helpful suggestions during the writing of the thesis. Dr. Brian Jones and Norm Catto read and commented on early drafts of the thesis. My fellow graduate students in the geology department , particularly those of the "Quaternary group" provided much advice and help. To all of the above, much thanks.

The Arctic Institute of North America provided logistic support in the field. Financial support for the field work was through grants from the National Research Council and the Boreal Institute to Dr. May. During my stay at the University of Alberta, the geology department provided financial support by means of teaching assistantships, and inter-sessional bursaries.

List of symbols used in the text

A	Surface area of lake
D	Lake level (elevation above sea)
D _o	Maximum lake level
d	Lake depth
g	Acceleration due to gravity
h	Ice thickness
K	Constant
l	Tunnel length
n'	Manning roughness coefficient
p	Pressure of water film at glacier base
P _i	Glaciostatic pressure
P _w	Hydrostatic pressure
Q	Discharge
Q _a	Total outflow from lake
Q _i	Inflow to lake
Q _o	Discharge through overflow channel
Q _t	Discharge through tunnel
S	Cross sectional area of tunnel
s	Co-ordinate measured down glacier
V	Volume of lake
V _o	Maximum volume of lake
Z _o	Lake level
Z _b	Elevation of glacier base
Z _h	Elevation of glacier surface
ρ_i	Density of ice (0.91 kg/l)
ρ_w	Density of water (1.0 kg/l)

Table of contents

Chapter.....	Page
I. Introduction.....	1
A. Objectives of study.....	2
B. Location.....	3
C. Bathymetry.....	6
D. Historical development.....	8
II. Review of previous work.....	12
A. Descriptive work.....	12
B. Geomorphological effects.....	15
C. Theories concerning the propagation of the flood.....	17
D. Glacial lake and delta sedimentation...	32
III. Field and laboratory methods.....	37
A. Field work.....	37
B. Laboratory work.....	43
IV. Results.....	44
A. Lake and stream processes.....	44
B. Lake filling and drainage.....	58
C. Sections in the lake sediments.....	71
D. The Ekman sampler.....	84
V. Discussion.....	86
A. Lake drainage.....	87
B. A model for the historical development of dammed lakes.....	93
C. Lake processes.....	101
D. Interpretation of the lake sediments..	104

VI. Conclusions.....	118
VII. References.....	120
VIII. Appendices.....	126
1. Section descriptions.....	126
2. Grain size analysis data.....	138
3. Cumulative curve data.....	202
5. Lake water temperatures.....	204
5. Suspended sediment concentration, lake.....	207
6. Suspended sediment concentration, streams.....	209
7. Stage measurements, July 4th-22nd	210
8. Stage measurements July 18th	211
9. Estimates daily discharge.....	212
10. Discharge calculations and data.....	213
11. Distances of sections from source....	219
12. Sediment samples; descriptions and locations.....	220

List of Plates

Plate.....	Page
1:- Hazard Lake; before and after drainage.....	1
2:-View of lake vicinity.....	11
3:-Outflow stream.....	59
4:-Lake drainage.....	61
5:-Lake drainage 2.....	62
6:-The ice dam.....	69
7:-Slope failures.....	70
8:-Facies C.....	74
9:-Facies C.....	75
10:-Facies B3.....	76

List of Figures

Figure.....	Page
1:-Location map.....	4
2:-Map of lake vicinity.....	5
3:-Bathymmetry of Hazard Lake.....	7
4:-Sampling locations on lake.....	38
5:-Section locations.....	42
6:-Lake temperatures versus depth.....	54
7:-Suspended sediment versus depth.....	47
9:-Suspended sediment versus time.....	48
9:-Suspended sediment versus stage.....	50
10:-Stage versus time.....	52
11:-Stage variation, July 18th.....	55
12:-Lake level versus time.....	60
13:-Discharge against time.....	68
14:-Diagram of sections.....	80
15:-Discharge versus volume discharged.....	88
16:-Mean grain size versus standard deviation.....	114
17:-Mean grain size versus proximity.....	116
18:-Standard deviation versus proximity.....	117

List of Tables

Table.....	Page
1:-History of Hazard Lake.....	9
2:-Discharge results.....	51
3:-Hypsometric data.....	64
4:-Sections; facies sequences.....	79
5:-Section samples; Folk-Ward parameters.....	81
6:-Ekman sampler; Folk-Ward parameters.....	85
7:-Predictions of the historical model.....	102
8:-Facies; Mean grain size and sorting.....	113

Plate 1; Hazard Lake

The upper photograph shows the lake on the morning of July 9th, rapid drainage already commenced. The lower photograph shows the empty lake basin 48 hours later.



I. Introduction

Glacial lakes formed by glacial advance have the potential to empty catastrophically by means of the formation and rapid enlargement of a sub-glacial tunnel. This results in a huge, sudden and unpredictable increase in the discharge of streams carrying water from the glacier, a significant environmental hazard.

Most studies of the glaciolacustrine environment either concentrate on Pleistocene deposits, where the processes of sedimentation are unknown, or in modern glacial lakes where processes may be well studied but access to the resulting sediments is difficult. This particular type of lake enables the processes to be studied whilst the lake is full or filling, and the sediments to be well sampled after drainage has taken place.

This study reports the results of four weeks field work in July, 1979, on an ice dammed lake of this type.

A. Objectives of the study

The major objectives were:

1. To observe and measure the emptying of the lake with the aim of testing existing models.
2. To review the historical development of this and other lakes and to compare them with a history predicted by existing models.
3. To examine the processes operating in the lake while full, and the relationship of these to the sediments

- deposited, examined in detail after drainage.
4. To compare results with existing models of glacial lake sedimentation.

B. Location

Hazard Lake (an informal name: it has also earlier been described as North Fork Lake by Sharp, 1947) is located in a tributary valley of the Steele valley, in the Yukon Territory (UTM reference 7V ET4291; 61° 15' 24"N , 140° 12' 30"S), (Figure 1). The lake is retained by an ice dam formed by the Steele glacier (formerly known as Wolf Creek glacier), a major valley glacier over forty kilometres long. The lake occupies a U shaped valley surrounded by 3,500 to 4000 metre peaks. The major inflow stream is Hazard Creek, a meltwater stream derived from a number of glaciers on the slopes of Mount Wood, namely the Hazard glacier and the Rusty, Trapridge and Backe glaciers (Figure 2) .

The St. Elias Mountains are a major range, containing one of the largest icefields outside of the polar regions, and some of the highest mountains in North America, including Mount Logan, the highest in Canada. The area is extensively glaciated, with a number of very large valley glaciers. A large proportion of these glaciers are known to surge; that is on occasion the flow of ice increases radically, causing an advance of the toe of the glacier. Thus they are liable to dam the drainage and create ice dammed lakes. Collins and Clarke (1977) estimate that over

Figure 1: Location map

The scale of the map is 1:500,000. (from NTS sheets 11SG and 11SF). The inset shows the area in relation to Western Canada.

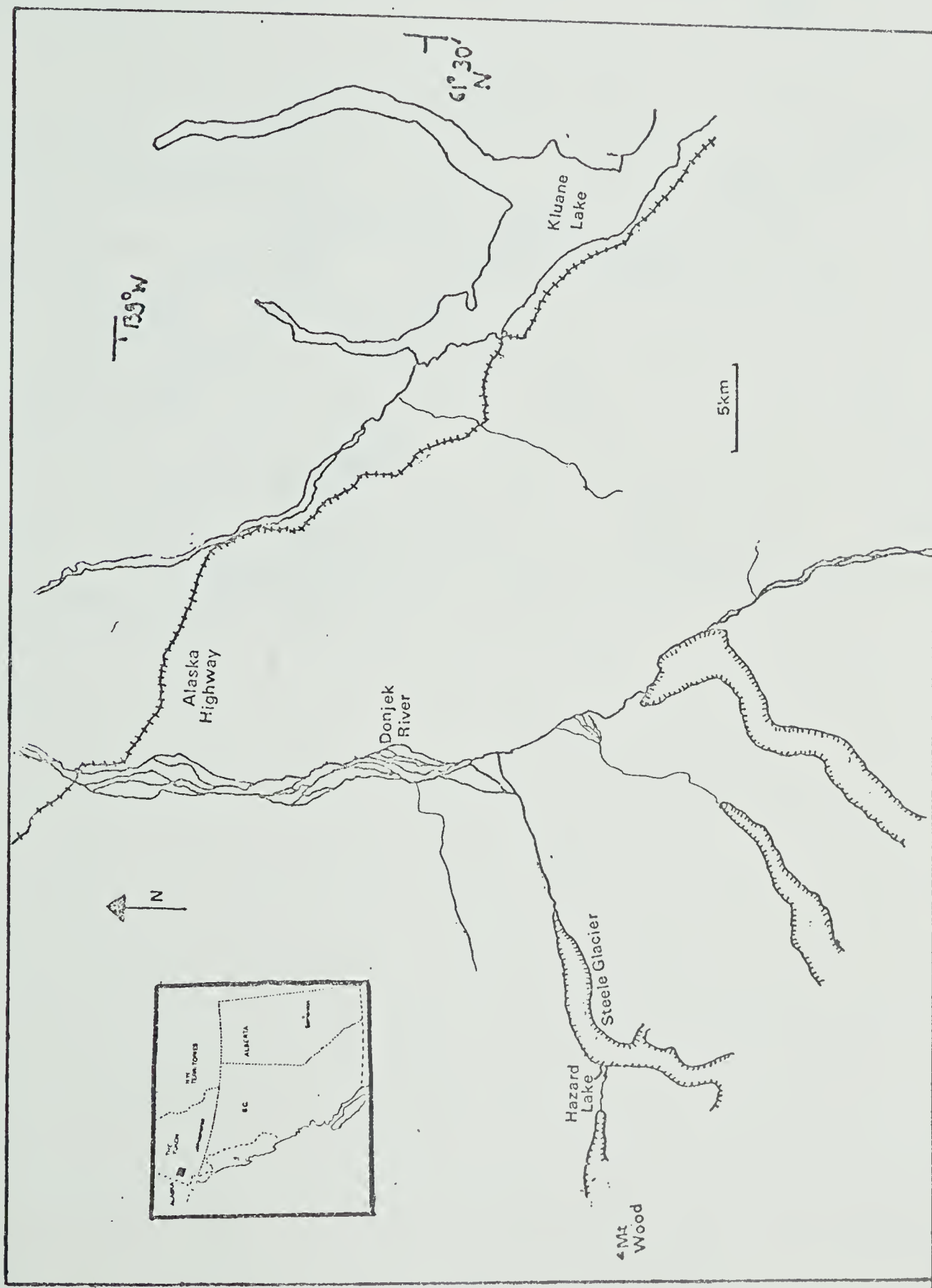
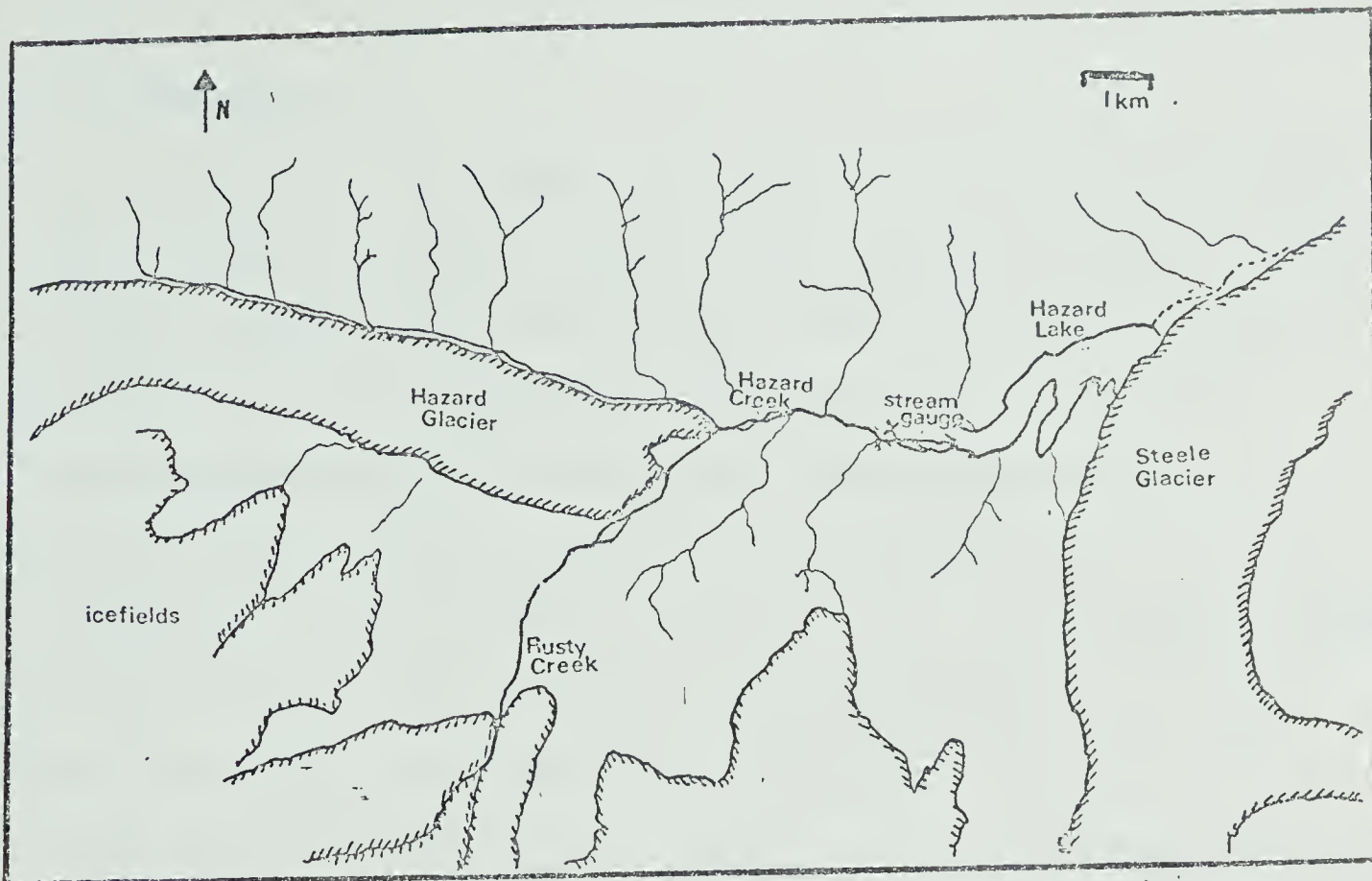


Figure 2: Map of vicinity of lake

Scale is 1:50,000. (from aerial photographs)



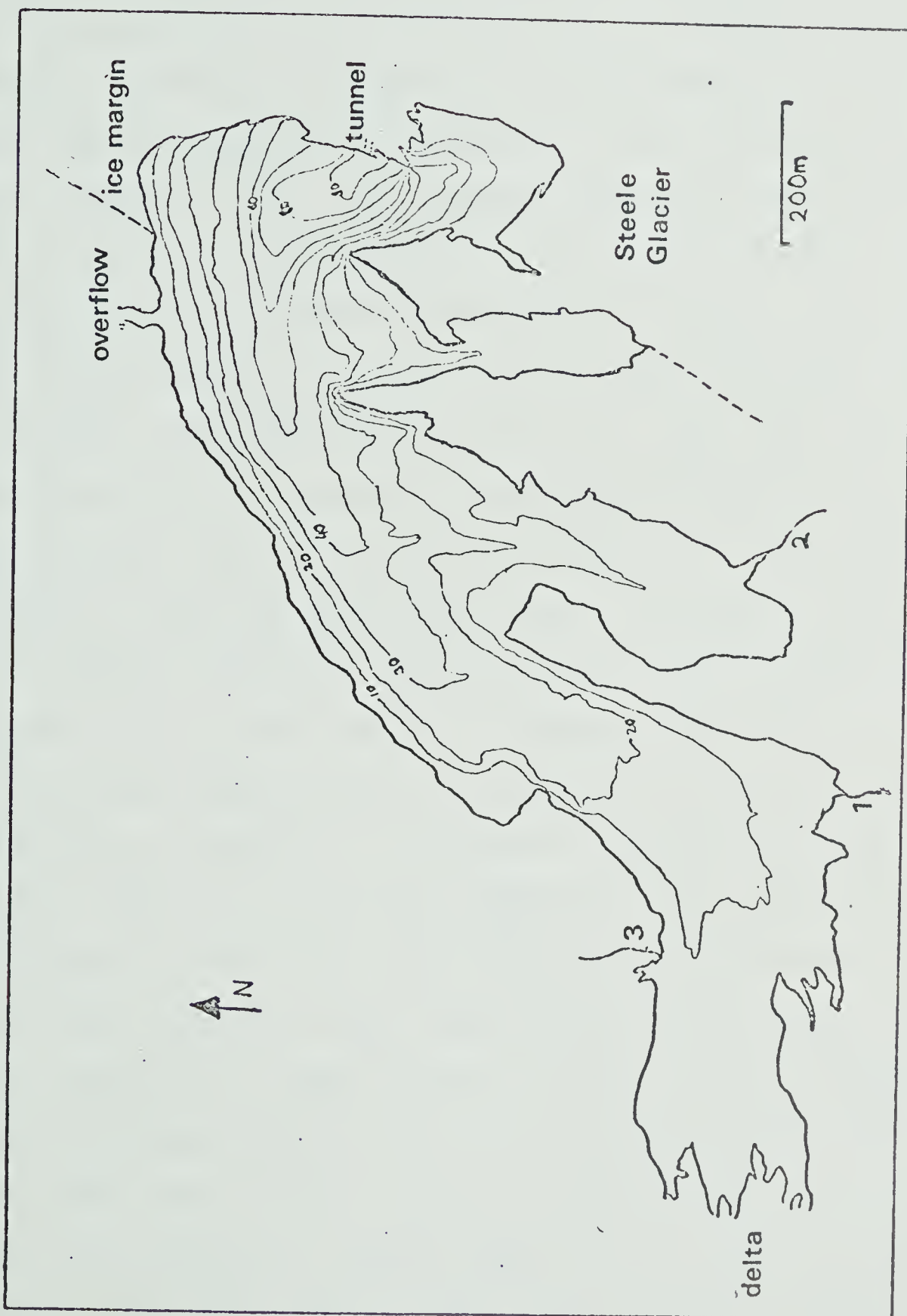
200 such lakes exist in the north east part of the St.Elias range alone. Hazard Lake was formed by the surge of the Steele Glacier in 1965-67 (Stanley, 1969, Wood, 1972).

C. Bathymmetry

Surveys of the lake were carried out in 1974 and 1979. Results of the earlier survey were reported by Collins and Clarke (1977), and those of the later by Clarke (1980a, b) (Figure 3). The lake is 2.1 kilometres long and has a maximum width of 0.5 kilometres. The average depth is 16 metres and the 1979 survey shows a maximum depth, in the vicinity of the ice dam, of 100 metres. The estimated volume is 20 million cubic metres. . The lake consists of three main sections; an extensive shallow area in front of the large delta of the inflow stream; a narrower deeper section, deepening up to the ice dam; and a narrow, shallow side arm, which contains a small delta, fed by meltwater from the Steele Glacier. The major inflow stream, Hazard Creek, enters the west end of the lake, and three minor inflow streams also contribute to the input, all building small deltas. When full the lake maintains a fixed level due to the presence of a rocky channel adjacent to the ice dam which acts as an overflow or spillway, forming a stream discharging along the margin of the Steele Glacier.

Figure 3: Bathymmetry of Hazard Lake

The scale is 1:10,000 and the contour interval is 10 metres (after Clarke 1980a).



D. Historical development of Hazard lake

The history of the lake has been outlined by Collins and Clarke (1977), and Clarke (1980a, b), using aerial photographs, published work, and the observations of field parties working in the area (Table 1). The Steele Glacier surged in 1965-67 resulting in a rapid advance of the ice front and a thickening of the ice in the vicinity of Hazard Creek, which at that time drained along the margin of the Steele Glacier. This resulted in the damming of the drainage, and the commencement of the filling of the lake. The lake reached its maximum level between September 1966 and August 1967 and remained full until late July 1975 when the lake drained sub-glacially beneath the Steele Glacier. The lake basin was observed to be empty in August 1976 but probably filled and emptied earlier in the year. It filled again between September and July 1977, only to drain between the 31st of July and the 5th of August 1977. The filling-emptying sequence was repeated in 1978, and was observed and measured, the results of which are given by Clarke (1980a, b). The actual emptying of the lake was witnessed for the first time during the field season of 1979, when rapid drainage occurred over the 9th and 10th of July. Previous to these recent fillings little is known. From the observations of the first parties in the area (Wood 1936, 1972; Sharp, 1947), and aerial photography it is clear that the lake basin remained empty for at least 30 years prior to the last surge of the Steele Glacier, and was

Table 1: History of Hazard Lake

After Clarke, 1980b.

DATE	EVENT	SOURCE
Autumn, 1965	Onset of surge of Steele glacier, lake basin empty	A.S. Post photography
August 1966	Basin partially filled	Canadian government photo A19647-42
September 1966	Basin partially filled	Canadian government photo A19739-35
Sept 1966-Aug 1967	Basin full, overflow operating	Canadian government photo A20128-13
Summer 1970	as above	photo A21523-77
Late July 1975	Tunnel drainage	R.B. Campbell
2-5 Aug 1977	Tunnel drainage after lake completely refilled	W.A. Wood and R.B. Campbell
8 August 1978	As above	Clarke (1980)
11 July 1979	As above	witnessed by author
26 June 1980	Tunnel drainage after incomplete filling	G.K.C. Clarke (pers. comm.)

unaffected by the small surge of 1940. However there is clear evidence of previous fillings in the form of terraces about 2-3 metres above the present maximum lake level, which could only be formed as part of a previous delta at a time of higher lake level. Also the existing delta is very extensive and would appear to be the product of a longer period of sedimentation than the thirteen years of recent fillings. Dating the sediments of this delta could lead to the dating of an earlier surge of the Steele Glacier.

Plate 2: view of lake vicinity

Hazard Lake viewed from summit of 3000 m peak to south of the lake. The lake basin is empty and the arrow indicates the ice dam.



II. Review of previous work

The phenomenon of catastrophic drainage of ice dammed lakes is common and is noticed wherever such lakes exist. Iceland, with historically a relatively large population, extensive glaciation, and a long literary tradition, possesses a good record of these events. The Icelandic language has the word 'jokulhlaup' especially to describe such occurrences, which indicates their importance as an environmental hazard. This word, which translates literally as "glacier burst", is now generally used in English language literature. Thorarinsson (1939) suggests that the earliest account of these floods is found in Icelandic literature, a description of the inexplicable rapid rise of a river blocking the path of travellers being found in the Sturlunga saga of the 13th century. Thorarinsson was able to trace the record of twenty eight jokulhlaups on the Skeidararsandur, from the end of the 14th century onwards.

Rabot (1905) catalogues examples in the Alps, Norway, Iceland, Spitzbergen, Greenland, and the Himalayas, with an emphasis on the Alpine examples, where jokulhlaups have caused extensive damage in the past. For example, Rabot describes the floods of a lake impounded by the Gretza glacier, which destroyed 600 houses and chalets in 1595, and cites many other cases in which stream channels were changed, large boulders transported, trees uprooted and property destroyed. Several of these have also been studied by later workers, such as the lakes of the Vatnajokull in

Iceland, the Gornersee, Switzerland, and Strupvatnet, Norway. This early work reflects the distribution of population in glaciated areas, but increased exploration and interest in glaciology has lead to examples being described from many parts of the world, bearing out Rabot's speculation that the phenomenon is found wherever ice dammed lakes exist. Norwegian examples are discussed by Strøm (1938), Liestøl (1955), Howarth (1968) and Whalley (1971). Patagonian examples are described by Nichols and Miller (1952), Greenland by Higgins (1970), Alaska by Lindsay (1966), Stone (1963a, 1963b), Marcus (1968); the Arctic by Maag (1963), Brook (1971), and Stone (1975). Canadian examples are Summit Lake, B.C. studied by Gilbert (1971, 1973), and Mathews (1965, 1973); Tulsequah Lake, B.C., studied by Kerr (1934) and Marcus (1960), and Hazard Lake itself.

A. Descriptive work

Most of the work on this type of lake has been descriptive. An examination of the work reveals the following general features.

1. Drainage is catastrophic, usually taking from a few days to a few hours from the observed commencement of drainage. Most records of the drainage are based on discharge measurements on outflow streams at the toe of the glacier.
2. Drainage is repeated a number of times, usually

annually, but the lake may be stable for longer periods between events.

3. Some lakes remain stable for a number of years before the first drainage.
4. Drainage is either by means of a tunnel in the ice at the base of the ice dam, or by erosion of the ice dam after the lake overtops the dam. The length of the tunnel formed depends on the distance of the lake from the toe of the glacier, and can be over 60 kilometres.
5. Drainage is not always complete, with the outflow being abruptly halted while water remains in the lake. Examples of this are given by Bjornsson (1975) and Whalley (1971).
6. Water balance calculations confirmed by dye tracing experiments described by Gilbert (1971, 1973) show that water may be transmitted from the lake to the glacial drainage system up to three months before catastrophic drainage.
7. Depths of lakes lie between 20 and 230 metres although deep lakes are rare.
8. The nature of lake drainage depends on the thermal conditions at the base of the glacier. If the glacier is frozen to its bed the lake will tend to drain by overtopping the dam and eroding a channel. The subglacial drainage typical of jokulhlaups only takes place if the glacier is wet based i.e. if a thin film of water exists at the base of the ice.

B. Geomorphological effects of jokulhlaups

Rabot (1905) indicated that it was likely that jokulhlaups were very frequent in periods of more extensive glaciation, and little attention had been paid to their possible effects of Pleistocene sediments. Seventy years later Embleton and King (1975) write

"Although present day jokulhlaups have been studied in Iceland, Norway, North America and elsewhere, recognition of possible Pleistocene jokulhlaups and their effects has advanced little"

It appears that there is now an increased awareness of the potential of these catastrophic floods, and there has been a reasonable amount of work. Clague and Mathews (1973) produced an empirical relationship between the total volume of the lake (V) and the peak discharge of the jokulhlaup (Q) by examining discharge records of modern examples. This was:-

$$Q(\text{max}) = 75 (V)^{0.67} \quad (1)$$

where Q is measured in cubic metres/second and V in millions of cubic metres. The extent and depth of Pleistocene ice dammed lakes can be estimated by the distribution and nature of the sediments deposited in them, and thus the maximum discharge of jokulhlaups possibly resulting from the lake can be calculated. Clague (1974) went on to apply this

result to sediments in glacial meltwater channels in the Rocky Mountain trench, B.C.. He estimated the peak discharge transporting the sediments deposited, and compared this to the discharges expected from ablation alone. He explained the resulting discrepancy by postulating jokulhlaups from glacial Lake Elk. He also suggests that the presence of jokulhlaups may be commonly recognised in other glacial meltwater channels.

Bretz (1923) examined the phenomenon of the channelled scablands of Montana, Idaho and Washington and suggested that the features observed there represent the results of huge floods. Later work by Pardee (1947) and Bretz (1969) indicates that these floods could be caused by jokulhlaups from glacial Lake Missoula. Birkeland (1964), working in Nevada, used the hypothesis of jokulhlaups from glacial Lake Tahoe to explain the transportation of boulders over three metres in diameter. More recently, in a study of the variation of grain size in varves, Shaw, Gilbert, and Archer (1978) suggested that the exceptional flows of jokulhlaups may be responsible for occasional findings of sand layers within the winter layer of a varve.

Despite this increasing interest in the effects of jokulhlaups there remains much work to be done in assessing their importance as a Pleistocene landforming agent.

C. Theories concerning the initiation and propagation of the flood

Any hypothesis concerning the phenomenon is constrained by the necessity of explaining the observations of the descriptive work outlined above. Rabot (1905) states:

"The causes which tend to form rock caverns go also to the formation of glacier cavities, namely, the pre-existence of fissures, erosion, corrosion and hydrostatic pressure, to which must be added the action of air above 32 degrees Farenheit. The waters of a glacial barrier or border lake, or of a subglacial or ice pocket lake in this way tend to scoop themselves out a passage through the mass of ice confining them."

This explanation fails to account for many of the salient features of the jokulhlaup, most importantly failing to account for the catastrophic and cyclical nature of the drainage.

The floatation hypothesis

This was outlined by Strøm (1938) and Thorarinsson (1939), and is based on the fact that ice is less dense than water. Thus if the lake water attains a sufficient level the ice barrier will float, allowing the escape of lake water at the base of the dam. Thorarinsson outlined the physics of the problem, stating that the lake level 'D' can be related to the ice thickness 'h' in a loosely defined "critical zone" ("that zone of the barrier, the lifting of which will

start the hlaup") as follows.

Floatation will take place when the glaciostatic (ice overburden) pressure becomes equal to the hydrostatic pressure. The glaciostatic pressure (P_i) is equal to $h\rho_i g$ where g is the acceleration due to gravity and ρ_i is the density of ice.

The hydrostatic pressure (P_w) is equal to $D\rho_w g$ where ρ_w is the density of water.

Thus the barrier will float when

$$P_i = P_w \quad (2)$$

or

$$D\rho_w g = h\rho_i g \quad (3)$$

thus:

$$D = \frac{h\rho_i}{\rho_w} \quad (4)$$

Substituting relevant values, it is found that the barrier will float when the lake level attains 0.91 the thickness of the ice in the critical zone. This is a simplified relation and takes no account of the bed and ice topography.

Thorarinsson points out that there are two variables controlling the initiation of drainage, the lake level and the thickness of the ice dam. Thus ice dammed lakes can be used as an indication of glacial thickness. For example, if

the retaining glacier has a mass balance of zero, the only variable is water depth and a jokulhlaup will occur every time the critical lake level is reached. If there is a positive mass balance, the required critical level will rise with time and eventually the lake may not drain catastrophically if there exists a constraint on its maximum depth, as is the case at Hazard Lake. If there is a negative mass balance, the relevant lake level will decrease, and eventually the lake will not fill at all. Thorarinsson thus suggests that the occurrence of jokulhlaups and the lake level required to produce them can be used as a predictor of past glacial regime, and attempts to estimate the extent of Icelandic glaciers in the Saga period in the light of the records of jokulhlaups.

The ice deformation hypothesis

Several criticisms were leveled at the floatation model. Whalley (1971) felt that outflow from the lake would occur as a basal sheet rather than as a localised tunnel. Glen (1954) suggested that once the ice dam had floated, the escape of water would result in insufficient water remaining in the lake to keep the dam afloat. Thus the maximum rate of discharge from the lake would be equal to the flow entering the lake and no catastrophic drainage could result. Glen went on to develop an alternative model for the formation of the tunnel, based on the deformation characteristics of ice under stress. Considering the situation at the base of the ice dam, there exists a vertical compressive stress (P_i) due

to the weight of the overlying ice given by:-

$$P_i = h \rho_i g \quad (5)$$

Also there exists a horizontal stress, normal to the dam, equal to the hydrostatic pressure (P_w). Now:

$$P_w = D \rho_w g \quad (6)$$

If D is approximately equal to h , then the horizontal stress exceeds the vertical by $h g (\rho_w - \rho_i)$. This is equivalent to a shear stress of half this value acting on planes at 45 degrees to the horizontal. If this stress is of sufficient magnitude, appreciable flow of ice will occur, leading in time to the breaching of the ice dam at the base. Using the approximation of perfect plasticity suggested by Nye (1951) and a yield stress of one bar, Glen calculated that this process would become significant at depths greater than 200 metres. As a general explanation this is obviously inadequate as they are known to occur in lakes, such as Hazard Lake, where the depths are much less than this value. Marcus (1960) also pointed out that the time required to form a tunnel of any length is unrealistic.

Hypotheses based on glacier hydrology

Whalley (1971), working on the glacial lake Strupvatnet, in Norway, rejecting the floatation hypothesis on the grounds that no perceptible lifting of the ice dam

was observed, and the ice deformation model as the lake is shallow, suggested that the internal drainage system of the glacier is important in initiating the jokulhlaup. He suggests that an enlargement of the drainage system during times of higher discharge as described by Stenborg (1969) taps the lake as it becomes hydraulically connected. It is difficult to explain the connection found between lake level, glacier thickness and draining events if this mechanism was universal, but it may be applicable in special cases. Rothlisberger (1972) found that he could explain the drainage of the Gornersee, Switzerland by his own model of the glacier hydrology. The piezometric head in the glacier varies seasonally, depending on the discharge through the internal drainage system. At times of low discharge the piezometric surface lies above the lake level; and at high discharge, below. Thus the lake will not empty at times of low discharge as there is no pressure differential acting away from the lake. The hydrology of glaciers is poorly understood but it seems that it may be an important factor in the drainage of some lakes.

These models explain the initiation but not the catastrophic nature of the drainage. In all cases it would be expected that, due to the pressure difference between the water in the tunnel and the glaciostatic pressure, ice deformation would tend to close the tunnel when formed.

Hypotheses involving frictional melting

Liestøl (1955) proposed a mechanism accounting for the

catastrophic nature of the drainage. He suggested that once a passage is established, the turbulent flow of water through the tunnel would cause frictional melting of the tunnel walls, thus enlarging the tunnel more rapidly than plastic deformation could close it. Mathews (1973) considered thermal conditions in the tunnel more closely and suggested that of the potential energy lost in the fall of water from the lake to the toe of the glacier, initially, ninety per cent is available for the melting of the tunnel walls, although this proportion would be smaller as the tunnel enlarged. Mathews derives an equation relating tunnel water temperatures to melting rates, and this was later improved by Gilbert (1973). This mechanism is compatible with either the floatation or the ice deformation models and answers Glen's criticism regarding the continuity of flow in the floatation model.

J.F.Nye (1976) proposed a modification of the floatation model, derived differential equations for flow in the tunnel leading to discharge: time relations and tested these against observation using the detailed survey of the ice dammed lake Grimsvotn, Iceland, reported by Bjornsson (1975). This paper represents the most successful attempt to explain the phenomenon of jokulhlaups.

The modified floatation model

This modification of the floatation model describes the critical zone of Thorarinsson (1939) precisely by taking into account the bed and ice topography. Nye

defines Z_b as the elevation of the glacier base, Z_h as that of the glacier surface. h equal to $Z_h - Z_b$ is thus the glacier thickness. The glacier is assumed to be wet based and thus the existence of a thin film of water at the base at a pressure p is postulated. If s is a coordinate measured down glacier then the pressure gradient at the base is given by:-

$$- d\phi/ds = -d/ds (\rho_w g Z_b + p) \quad (7)$$

If p is defined as being the ice overburden pressure, then :-

$$\phi = \rho_w g (Z_b + \frac{\rho_i}{\rho_w} h) \quad (8)$$

Now the hydrostatic pressure due to the lake is given by $\phi = Z_o \rho_w g$, where Z_o is the elevation of the lake level above the toe of the glacier. Thus the seal will be broken when the hydrostatic pressure is equal to the maximum value of the glaciostatic pressure, when:-

$$\frac{d}{ds} \left\{ \left(1 - \frac{\rho_i}{\rho_w} \right) Z_b + \frac{\rho_i}{\rho_w} Z_h \right\} = 0 \quad (9)$$

If the bed and ice topography are known then the value of s , and thus Z_b and Z_h can be found leading to the calculation of Z_o at the critical point by equating

hydrostatic and glaciostatic pressure.

Nye tested this model against the survey of Bjornsson (1975), and found that drainage took place with the lake level 20 metres below that expected (and 40 metres below that predicted by Glen's model). He explained this discrepancy by considering the effect of the ice already afloat before the seal is broken. This ice has a buoyant force acting on it and since it is mechanically connected to the ice in the region of the seal, it acts as a buoyant cantilever, serving to reduce the glaciostatic pressure at the base of the dam. The extent of this action is limited by the mechanical strength of the ice, and Nye using the assumption of perfect plasticity, estimated its magnitude as being twice the yield stress. This gives a pressure reduction in the order of two bars, roughly equivalent to the twenty metres of water required.

Conditions in the ice tunnel

Given that a tunnel can be formed, Nye goes on to examine conditions in the tunnel as water flows through it. He considers two main effects acting on the tunnel, the frictional heating and melting of Liestøl (1955), and plastic deformation acting to close the tunnel. Firstly he derives, from thermodynamical principles, a series of differential equations describing the geometry and flow of ice, the continuity of the system, the flow of water, the energy of the system, and heat transfer.

Using the results of Rothlisberger (1972) and Shreve (1972), it is assumed that the escape of water from the lake will take the form of a single channel at the base of the glacier. To obtain equations describing the main part of the jokulhlaup, the simplifying assumption that the plastic deformation of the ice is negligible during this phase of the drainage is made. This is justified on the grounds of goodness of fit of the results to observation. Simplifying the original equations he arrives at the following equation:-

$$\frac{dQ}{dt} = K Q^{1/2.5} \quad (10)$$

where Q is the discharge, t is time, and K is a value that is a function of position and time. It can be shown that K (a measure of tunnel roughness) is essentially constant, and if $t=0$ is chosen as the time at which Q becomes theoretically infinite, and Q is the average discharge over the length of the tunnel, then the equation can be integrated to give:-

$$Q = (-4 / Kt)^{4/5} \quad (11)$$

Thus the exponential increase in discharge is well explained. If this equation is compared to the record of the jokulhlaup of 1973 obtained by Rist (1974) an

extremely good fit of observation to theory results. A regression of $\ln(Q)$ against $\ln(-t)$ gives an exponent of -4.00 ± 0.06 , and realistic values for K .

Closure of the tunnel

Grimsvoth is one of the examples in which the jokulhlaup terminates before the reservoir is exhausted. Nye states that the cause of closure is a rapid increase in the rate of plastic deformation of the tunnel walls. The magnitude of the force acting on the tunnel walls is dependent on the pressure difference between the water in the tunnel and the glaciostatic pressure of the overlying ice. As the lake level drops and the jokulhlaup approaches a peak the pressure in the tunnel drops rapidly. Nye shows that the rate of plastic deformation of the tunnel walls is proportional to:-

$$\{ 1 + (t'_0 / t')^3 \}^3 \quad (12)$$

where t' is the time remaining before the discharge becomes theoretically infinite (equal to $-t$). Thus the deformation rate initially remains fairly stable, as the quantity t'_0/t' is close to 1, but increases rapidly as t' becomes small, the rate being approximately proportional to t'_0 / t' to the ninth power. At this point the jokulhlaup will terminate when the rate of closure by ice deformation overcomes the enlargement due to melting. This point is not always reached before the

reservoir is exhausted but in the cases where the lake drains completely the tunnel will close if the flow of water through the tunnel (the discharge of the input streams) is insufficient to maintain a high enough melting rate to overcome plastic deformation. If this closure does not occur immediately it will usually follow in the fall when the discharge of the streams drops as freeze up progresses.

Thus Nye identifies three phases in the propagation of the jokulhlaup.

1. The dam is breached when a sufficient lake level is reached, and flow commences in the tunnel. At this point plastic contraction of the tunnel and expansion by melting are of the same order of magnitude. However, Nye shows that the situation of a tunnel draining a reservoir at fixed pressure is essentially unstable and this leads to the next stage.
2. In this phase the melting rate far exceeds the plastic closure of the tunnel, giving rise to the full catastrophic flood of the jokulhlaup, the discharge of which can be approximated by the equations given earlier.
3. In the final phase the plastic deformation rate rapidly increases to overtake the melting rate and close the tunnel.

Nye has developed a comprehensive model which seems to

well explain the main features of the Grimsvotn jokulhlaup and should have general application.

Clarke (1980a, b) attempted to generalise these results by applying the model to further measured jokulhlaups, the July 1978 event at Hazard Lake and the 1965 and 1967 events at Summit Lake B.C. He generalised the model by considering the effects of reservoir geometry on the jokulhlaup. He was also able to include the effects of plastic closure on the tunnel. Clarke makes a number of assumptions

1. The crucial part of the tunnel in controlling the characteristics of the flood is that part in the region of the seal to the lake. This assumption is justifiable in that the glaciostatic pressure which affects the rate of tunnel closure through deformation is at a maximum at this point.
2. The seal is considered to be close to the lake, and thus the pressure in the tunnel is approximately equal to the hydrostatic pressure in the lake.
3. The shape and roughness of the tunnel do not vary with position along the tunnel.
4. The potential gradient in the tunnel is given by the average over the length of the tunnel i.e. the elevation difference between the lake level and the toe of the glacier divided by the distance from the lake to the toe.

A major departure from Nye is the consideration of lake

geometry. The volume is related to the discharge by:-

$$\frac{dV}{dt} = Q_i - Q_a \quad (13)$$

where t is time, Q_i is the inflow into the lake, and Q_a is the flow out of the lake. $Q_a = Qt + Q_o$ where Qt is the volume discharged through the subglacial tunnel, and Q_o is the discharge from the overflow when the lake is full. Clarke solves the equations of Nye under these conditions with the additional information that the volume in the lake (V) may be related to the lake level (D) by the equation:-

$$D / D_0 = (V/V_0)^m \quad (14)$$

where D_0 is the maximum lake depth, V_0 is the maximum volume and m is dependent on the geometry of the reservoir, being equal to 1 for a vertically sided reservoir, and smaller as the slope of the walls decrease. The results of this simulation are to produce an estimate of the only unknown parameter in the model, the Manning roughness coefficient, n' , a measure of the roughness of the tunnel walls. Nye reports a value of n' of $0.12 \text{ m}^{0.33} \text{s}$ for Grimsvotn, and Clarke obtains values of $0.08 \text{ m}^{0.33} \text{s}$ for Summit Lake, and $0.009 \text{ m}^{0.33} \text{s}$ for Hazard Lake. The expected range according to Nye is 0.01

to $0.1 \text{ m}^{0.33} \text{s}$, and thus the value for Hazard Lake is surprisingly low. Clarke (1980b) states that it might be possible to obtain such a value for a polished tunnel of ice, but this has never been investigated experimentally. He also suggests that this low value may indicate faults in the input of the model, and pinpoints the potential gradient as a source of possible error. The assumption that the entire tunnel is closed and reopened every year may be incorrect, and thus the potential gradient over the length of the tunnel might be greater than that used in the model.

Clarke also tested the model by fitting the discharge results to a relationship:-

$$Q_t = c (V_o - V)^p \quad (15)$$

where c is a constant of proportionality, and p , a constant, is predicted by Nye's model, if tunnel closure is neglected, to be 1.33. He obtains a value of 1.12 for p at Hazard Lake, again possibly explicable by the estimate of potential gradient, and for the analysis of the Summit Lake events, three markedly different results for the three jokulhlaups studied. Some of this variability is due to the quality of the data, but definite differences exist. If the Nye model is correct, and all inputs to the model remain the same then the characteristics of the floods resulting should be

identical. Clarke suggests that these inconsistencies may be due to:

1. The hydrological conditions in the glacier, as described by Whalley and Rothlisberger above.
2. Tunnel collapse, and engorgement of ice and other material.
3. Varying degrees of closure of the tunnel from event to event.

Clarke concludes that calibration of the Nye model is difficult, in the light of the apparent variability of n' .

Finally, Clarke investigated the relationship between reservoir geometry, rate of tunnel closure due to ice deformation and peak discharge. He shows that termination of the flood through plastic deformation is more likely in a steep sided reservoir than in a shallow sided reservoir. This is because in a shallow sided reservoir, most of the volume is stored at a high elevation in the lake and thus the hydrostatic pressure, and the pressure in the tunnel will only fall sharply towards the end of the flood, when the reservoir is nearly exhausted. Thus increasing rates of creep closure and steep reservoir sides serve to reduce peak discharge.

D. Glacial lake and delta sedimentation

Sedimentation in glacial lakes has been the subject of much attention in the past. Accordingly this review of the literature will be brief. Most of this work has been related to the rhythmic bedding known as varving. There has been much discussion over the mode of deposition of these sediments, and concerning the cyclical variation in the depositing agents. The suggestion that each coarse-fine couplet comprising a varve represents the deposit of one year's sedimentation was first made by De Geer (1912), who also proposed that the coarse layer was deposited by current flow along the lake bottom during the summer months. This flow is suggested to be a result of a density difference between the stream water entering the lake and the lake water caused by temperature differences between the two. The fine layer is deposited from suspension during the winter when inflow ceases due to freezing. The role of these density flows was doubted by later workers such as Antevs (1931) on the grounds that these flows had not been observed to occur in the field, and also many lakes did not possess the temperature stratification required by the hypothesis. Kuenen (1951) showed that density flows were likely to occur in glacial lakes as the density differences were more due to suspended sediment content than temperature differences. Field measurements showed that this difference was usually high enough for these flows to occur. Agterberg and Banerjee (1969) recognised three genetically separate parts of a

single varve.

1. The coarse silt/sand layer, deposited directly from the turbidity current.
2. The lower part of the clay layer, deposited from suspension as the turbidity current stagnates
3. The upper part of the clay layer, formed from deposition from suspension over winter in the absence of further inflow.

This explanation is now generally accepted as the mechanism of deposition of these sediments, but the nature of the turbidity currents themselves appears to be variable.

Gustavson (1975) observed the occurrence of density currents as a continuous underflow during the melt season. However, Gilbert (1975) stated that in the example under investigation major density flows were a rare event occurring only a few times during the melt season and were probably due to slumping of material from the delta front. Underflow was an intermittent but frequent event. The continuous underflow model would result in varves, rhythmic bedding that is, in fact, annual. However, if underflow is discontinuous, then it is possible that either no "varves" or more than one "varve" may be deposited in a single melt season. This second situation may be rare; the annual nature of varves in thick sequences has been well supported by pollen analysis, and by radiocarbon dating. But this possibility does exist and more work is required to delineate the conditions in which the two types of underflow

occur. Shaw, Gilbert and Archer (1978) show that major flow events may occur in the winter months also, resulting in coarse layers within the 'winter' part of the varve, and further complicating the situation.

Sturm (1979) relates the nature of the processes operating in the lake to the sediments deposited. The main parameters that he considers are the mode of influx of suspended matter, and the state of stratification in the lake. Uniform, continuous influx of suspended sediment into a lake cannot give rise to varves or laminated sediments of any kind. Discontinuous pulses of suspended sediment will give different results according to the state of stratification of the lake. If the lake is unstratified, then the sediments will form simply by settling under Stoke's law, and will be laminated, each lamination reflecting a pulse of suspended sediment influx. If stratification exists during the summer months, varves will be deposited. Thus this model allows the prediction of sediments deposited under known hydrological conditions and vice versa.

Work by Wankiewicz (1979) suggests that wind produced bottom currents may be important in glacial lake sedimentation. A steady wind over the lake surface produces a return current in the opposite direction on the lake bottom. The velocity of these currents may be estimated and it can be shown that moderate winds can produce a current sufficient to maintain material as coarse as silt in

suspension.

Thus the sediments of the lacustrine environment are well studied, as are those of the glacio-fluvial environment. However the transition between the two, the deltaic and proximal lacustrine situation, is less well understood. In this situation the sediment supply is greater and the system is more sensitive to variations in flow strength in the inflow stream. In the lacustrine environment, only the annual cycle in discharge is apparent, but Gustavson, Ashley and Boothroyd (1975) believe that three orders of cyclicity in discharge may affect the deltaic environment.

1. The annual cycle, as mentioned above.
2. A second order cycle, related to short term weather changes, from a few days to a few weeks.
3. The diurnal variation in discharge due to the daily temperature fluctuations.

Thus sedimentary features can be explained in terms of any of these three variations in discharge. Gustavson, Ashley and Boothroyd went on to examine the sedimentary sequences in glaciolacustrine deltas, using the work of Jopling and Walker (1968), and recognised a repeated sequence of sedimentary structures which they relate to a cyclical variation in discharge. This sequence, lying between winter clay layers marking one years deposition, is of a thin unit of type B ripple drift cross lamination overlain by a relatively thick unit of type A, which grades back into type

B, itself grading into draped lamination. This reflects the increase and subsequent decrease in current strength over the melt season. Ashley (1975) shows how these deltaic sediments can grade into lacustrine rhythmically bedded deposits, as the silt/sand component of the varve thickens as the delta is approached. Shaw (1975) explains more proximal sequences in terms of frequent movement of the paths of distributary channels on the delta, as well as discharge variation.

Thus the role of turbidity currents in the lacustrine environment is major, although the extent, frequency, flow patterns, initiation, and distribution in present day lakes needs to be better understood before lacustrine sedimentation can be better understood. The frequent variation in discharge, the changing of channel position and the large sediment supply leads to complexity in the deltaic environment that does not easily lead to a simple, generally applicable, model. It appears that the continuous density flow of water entering the lake is an important agent in the deposition of sediment. This can be integrated with models of proximal varve formation to explain the grading from deltaic to lacustrine sediments.

III. Field and laboratory methods

A. Field work

Measurement of lake processes

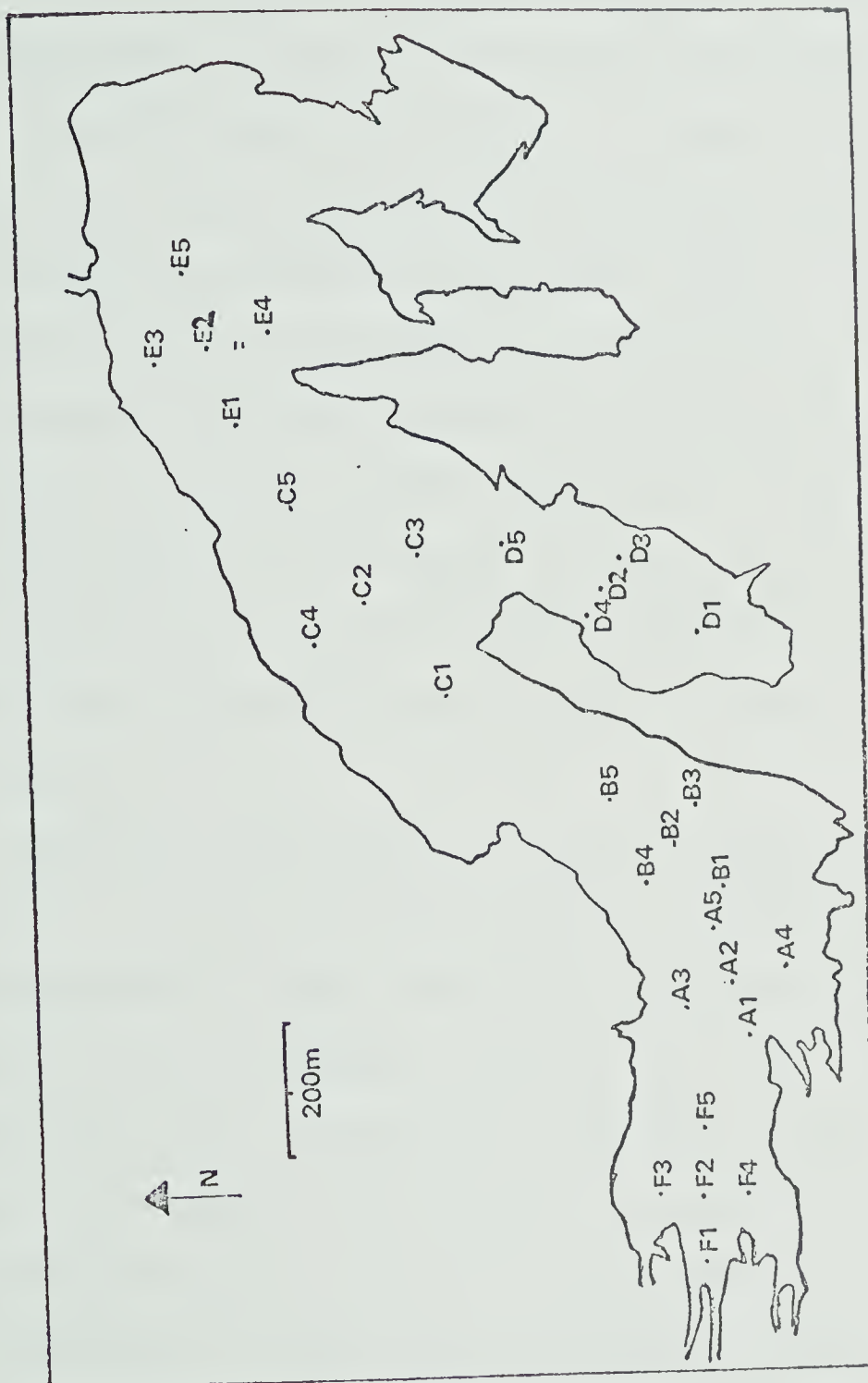
The aim of this part of the study was to gain insight into the processes operating in the lake. Measurements were made of:

1. Lake water temperatures
2. Inflow stream water temperatures
3. Stage level of inflow streams.
4. Current strength of inflow streams.
5. Suspended sediment content of inflow streams.
6. Suspended sediment content of lake water.
7. Lake bottom sediment samples.

A sampling grid was erected for use in investigation of lake bottom sediments and water. This grid was constructed so as to give as complete a spatial coverage as possible and consisted of six groups of five sites, a total of thirty (Figure 4). Sampling was incomplete in the field due to the premature drainage of the lake. Previous indications were that the lake would drain around the end of July but the commencement of rapid drainage on the 8th of July meant that a complete sampling was not possible. Navigation on the lake was by a system devised by the author. Sampling was from a rubber boat and the position of the sample sites was located using a system of double marker flags on the shore. A number of pairs of flags were placed on the shore, using a map

Figure 4: Sampling locations on lake

Scale is 1:10,000



prepared by S.Collins, T.Tight, M.Smith and T.Berkstresser in 1974, and a Brunton compass. Each pair of flags were placed so as to define a line of sight across the lake, and each sampling point was at the intersection of two such lines. Positioning of the raft on such a line was made using the principle of parallax; when the two flags appeared to be on a line of sight, the craft was on the line defined by the flags. The flags were constructed of dowling, survey tape, and orange nylon material and were readily visible at distances up to 1.5 kilometres if binoculars were used. Positioning using this method was very precise, to within probably 2-3 metres but the accuracy is very dependent on the positioning of the flags. In this case survey techniques were rudimentary, but with better methods, this technique could prove useful for work on small lakes with a small field party.

Samples of lake water were collected at 5 metre depth intervals using a Van Dorn sampler. Temperature of the water was measured by simply inserting a mercury glass thermometer (accurate to 0.5 degrees Celcius) into the sample immediately after collection, the specific heat of water being high enough to make any errors due to cooling/warming of the water by the air or shallower water negligible. One liter samples of water were collected in plastic bottles to be later analysed for suspended sediment content. The original aim was to filter these samples in the field but the filtering apparatus available proved to be inadequate

and thus the number of samples taken was limited by the number of bottles, resulting in only a partial sampling of suspended sediment. These samples were later processed in the laboratory.

Sampling of the bottom sediments was carried out using an Ekman grab sampler. As mentioned above sampling was limited by the premature disappearance of the lake. The sampler in general worked well, but was adversely affected by sediments coarser than sand. In these circumstances the sediment prevented the full closure of the jaws of the sampler, and most of the finer sediment escaped as the sampler was being recovered. The sampler was emptied into a large plastic sample bag, and the sample allowed to settle in camp. Excess water was then syphoned off and the sediment allowed to air dry.

A stream gauge was established two days after start of field work and monitored daily. The stream was also closely observed for a continuous period of thirteen hours. The stage level was measured and suspended sediment samples taken every hour and the strength and distribution of the current flow was measured over the period of an hour using a Price current meter.

Observation of lake level

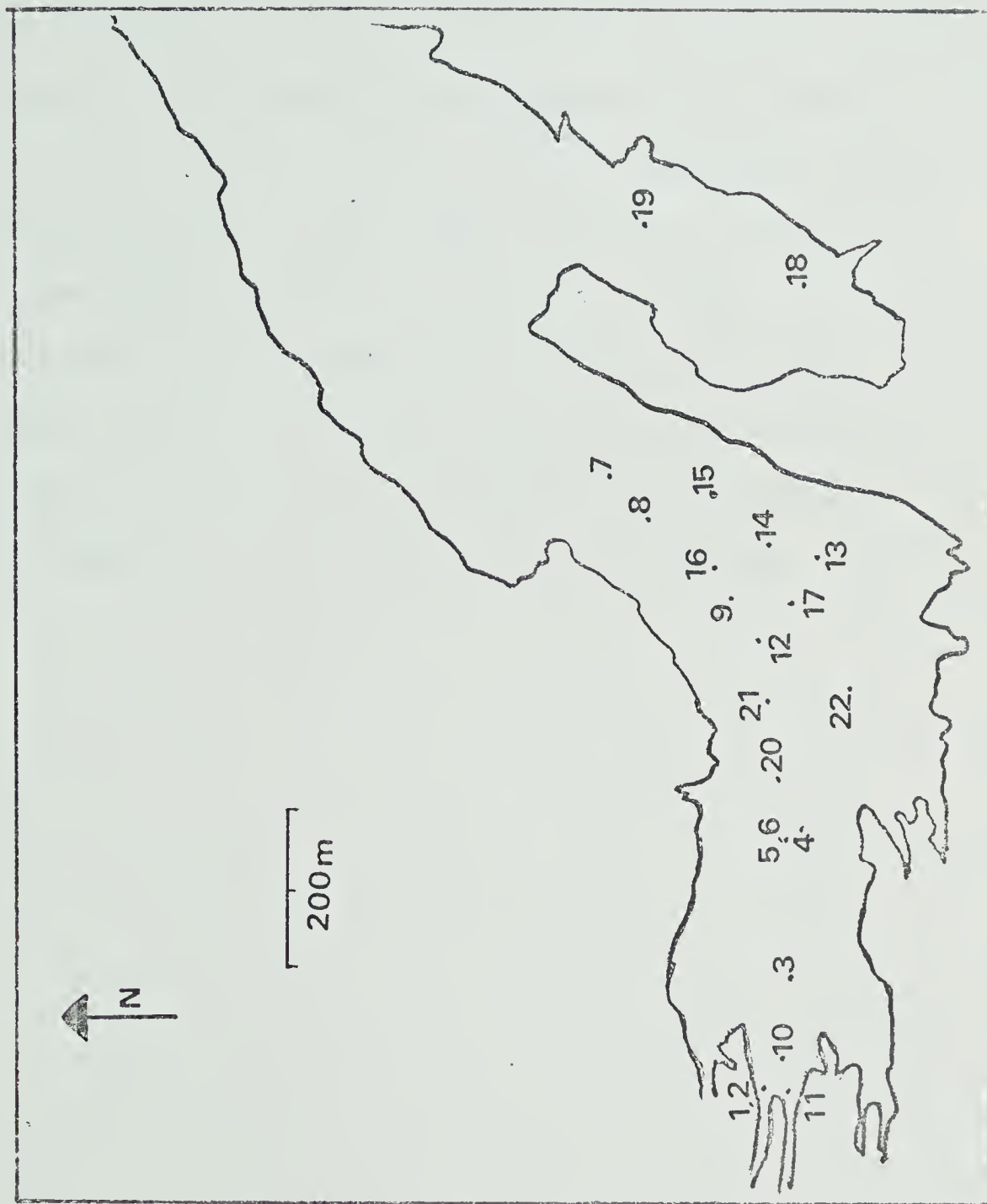
The lake level was closely monitored using a simple survey method. On arrival at the lake, a simple gauge, consisting of a length of dowling marked in centimetres, was inserted in the lake, and the lake level measured relative

to an arbitrary zero point. When drainage commenced this single gauge had insufficient range to cope so once the level fell to near the base of the gauge, a second gauge was inserted deeper in the lake, and the tendency of water to lie horizontally used to level between them. This process was repeated as the level continued to drop but became impractical as drainage became extremely rapid. At this stage drawdown was estimated using a number of scaled photographs, from which measurements were later obtained.

Sampling after drainage

Sampling of lake bottom sediments commenced soon after drainage. Twenty two sites were chosen so as to give as full a coverage of the lake bottom as possible (Figure 5). No sampling took place in the east end of the lake where steep sides to the lake led to slumping and washing down of most sediment, leaving little preserved. Most sampling therefore took place in the west end of the lake, and choice of sites here was limited by the semi-liquid nature of the bottom sediments. The sediments had a high water content and were thus very mechanically weak making work on them difficult and sometimes hazardous. However, the lake bottom was dissected by a number of streams, and these eroded their way through the bottom sediments. Along the banks of these streams, the sediments lost much of their water content, making work possible. Twenty two sections were exposed using a shovel to trench the sediments, and these were measured, described, photographed and sampled, a total of forty four

Figure 5: Map of section locations.
Scale is 1:10,000



samples being collected.

B. Laboratory work

The sediment samples collected with the Ekmann sampler, and directly from the lake bottom were subjected to a grain size analysis, using a combination of sieving and hydrometer methods, and procedures recommended by Krumbein and Pettijohn (1938) and Folk (1959). Suspended sediment was analysed using a simplified version of the method recommended by Østrem and Stanley (1969). The ashing procedure was not used, the filter paper simply being weighed before filtering, and again after drying. This method is likely to be slightly less accurate but has the advantage of being rapid and requiring less equipment.

IV. Results

A. Lake and stream processes

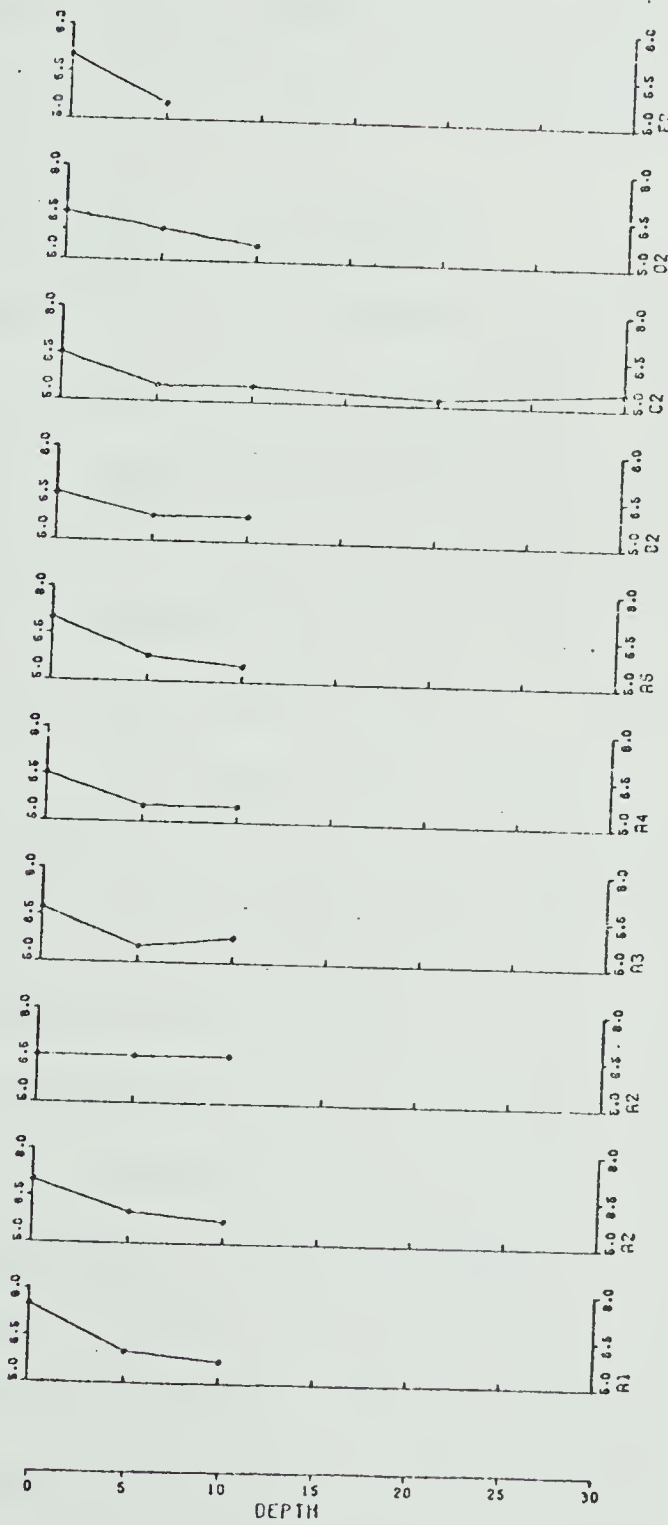
The factors affecting processes investigated were lake and stream temperatures ; suspended sediment content of lake and streams; discharge of inflow streams. As previously mentioned, equipment and time were insufficient for an adequate examination of these factors affecting sedimentation. However, using the results obtained in combination with previous work which outlines the expected behaviour over time of glacio-fluvial and lacustrine systems some useful order of magnitude results can be obtained.

Temperature

A full coverage, as originally planned, was only possible on sample grid A, sampling on other grids (B-E) being limited to one location. The results are summarised in Figure 6, and tabulated in Appendix 4. They show a small range, the coldest temperature recorded being 5 degrees, at 10 m and 20 m, sample station E2, and the warmest, 7.5 degrees, at the surface, station A1. Thus the lake appears to be essentially isothermal, but a small degree of stratification occurs between the surface and deeper waters. The surface water is 1-2 degrees warmer than the water at 5 m. There is a discernable trend with depth, temperatures decreasing slightly with depth in most cases, and only increasing in one example, station C2. The magnitude of this effect is small, however, being at the most a difference of

Figure 6: Graph of lake temperatures and depth

Temperatures are measured in degrees centigrade, depth in metres. For sample locations see Figure 4.



2 degrees. There is also a trend towards slightly cooler water temperatures at depth in the deeper parts of the lake, stations E2 and C2.

The temperature of the inflow stream was not monitored closely due to the breakage of the thermometer during field work. However, three measurements were made at an earlier stage. These were all taken in the late afternoon and show temperatures of 5.5, 6 and 6.5 degrees for July 4th, 6th and 7th respectively.

Suspended sediment, lake water

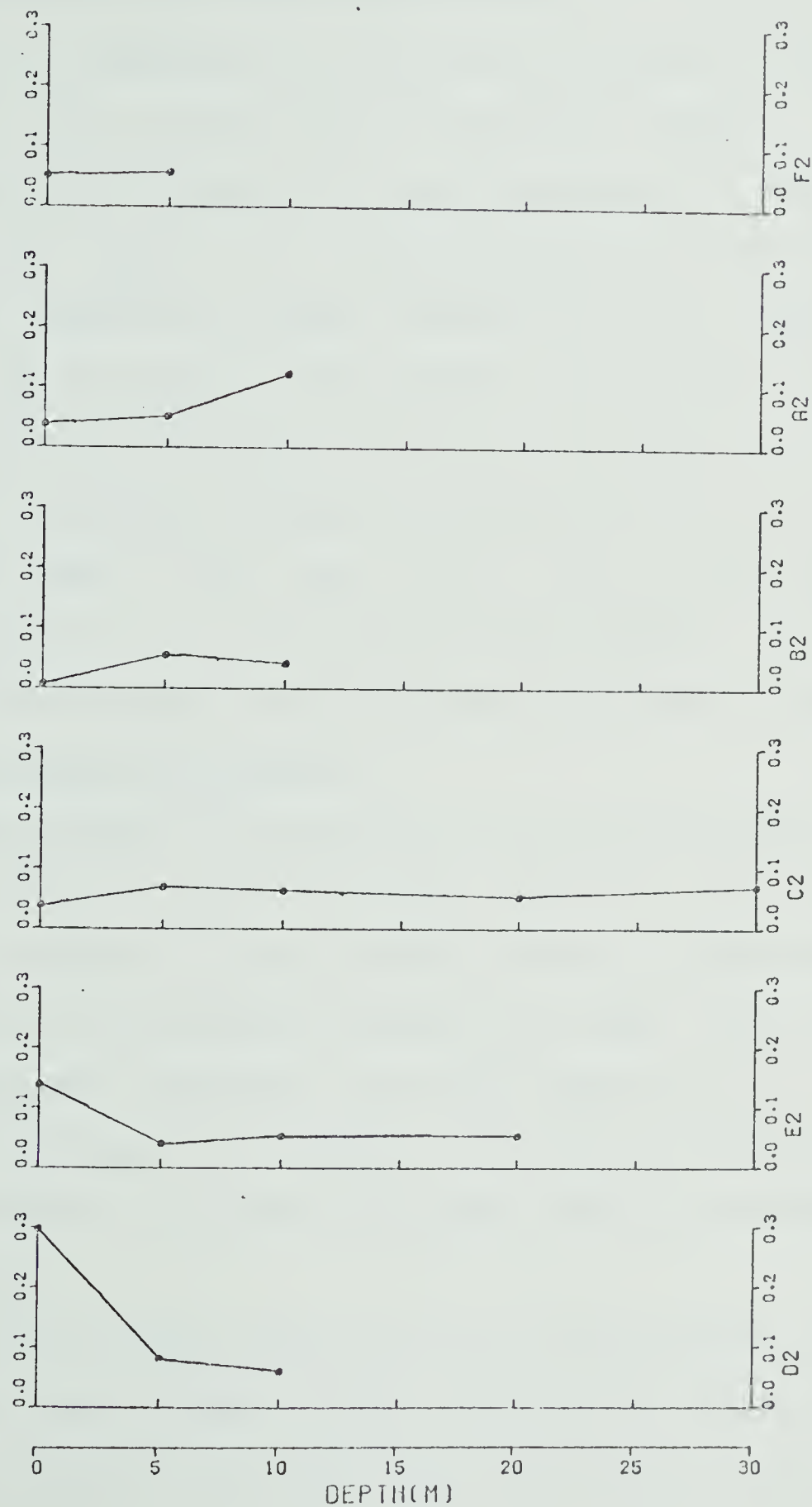
The results of the analyses performed are summarised in Figure 7, and tabulated in Appendix 5. No clear pattern is recognisable. Sample points D2 and E2 show particularly high sediment concentrations at the water surface, as does A2, only close to the lake bottom, at a depth of 10m. Sample B2 showed a very low concentration at the surface, of 0.007 grams/liter. Apart from these apparently anomalous results, the other samples were similar in sediment content, showing no consistent trend with depth or position with regard to the main sources of sediment. It is worth noting that the suspended sediment concentration of location C2 increased close to the lake bottom, as did the water temperature.

Suspended sediment, inflow streams

Appendix 6 gives the results of a detailed sampling of Hazard Creek and single samples from the three largest streams also contributing to the waters of the lake. Figure 8 shows the variation of suspended sediment concentration

Figure 7: Graph of suspended sediment against depth

Suspended sediment is measured in g/l and depth in metres.
For sample locations see Figure 4.



with time in Hazard Creek, on July 18th. There is a general increase in concentration from morning to afternoon, with the highest values being recorded between 14:00 and 16:00 hours. The maximum value obtained was 1.957 grams/liter. This is in agreement with the results quoted by Church and Gilbert (1975) which show that maximum sediment concentration precedes maximum discharge by a few hours on a given day. Figure 9 is a graph showing the relationship between suspended sediment concentration and stage on July 18th, and it appears that a direct relationship exists. The correlation coefficient for this relationship is 0.86.

The suspended sediment concentration for the minor streams shows a high range, from 0.186 to 2.879 grams/liter. The weather on July 8th was overcast and wet, resulting in a higher than normal sediment content in these streams.

Stream stage and discharge

Measurements were made on four inflow streams, Hazard Creek, and three minor streams (Figure 3). For Hazard Creek a daily record of stage and one series of measurements leading to a discharge estimate were made. Insufficient time and equipment prevented the establishment of a stage/discharge relationship. For each of the minor streams an estimate of discharge was made from the measurements obtained.

Table 2 shows the results of the discharge estimates for the four streams. Figure 10 shows the variation in stage over the twenty three days that the level was monitored, and

Figure 8: Graph of suspended sediment against time

These are the results from samples taken on July 18th.

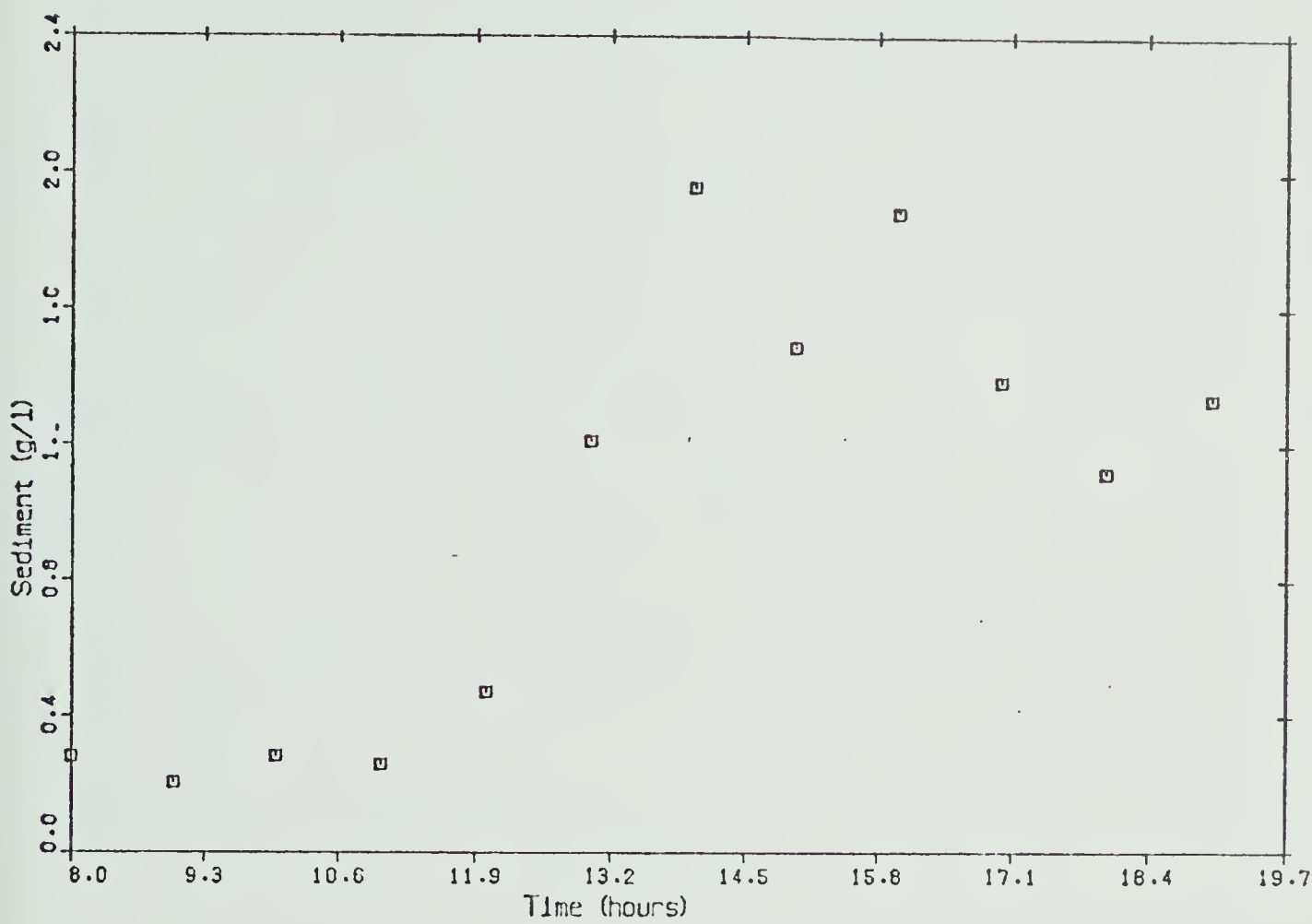


Figure 9: Graph of suspended sediment against stage

Results of measurements and samples taken on July 18th, 1979.

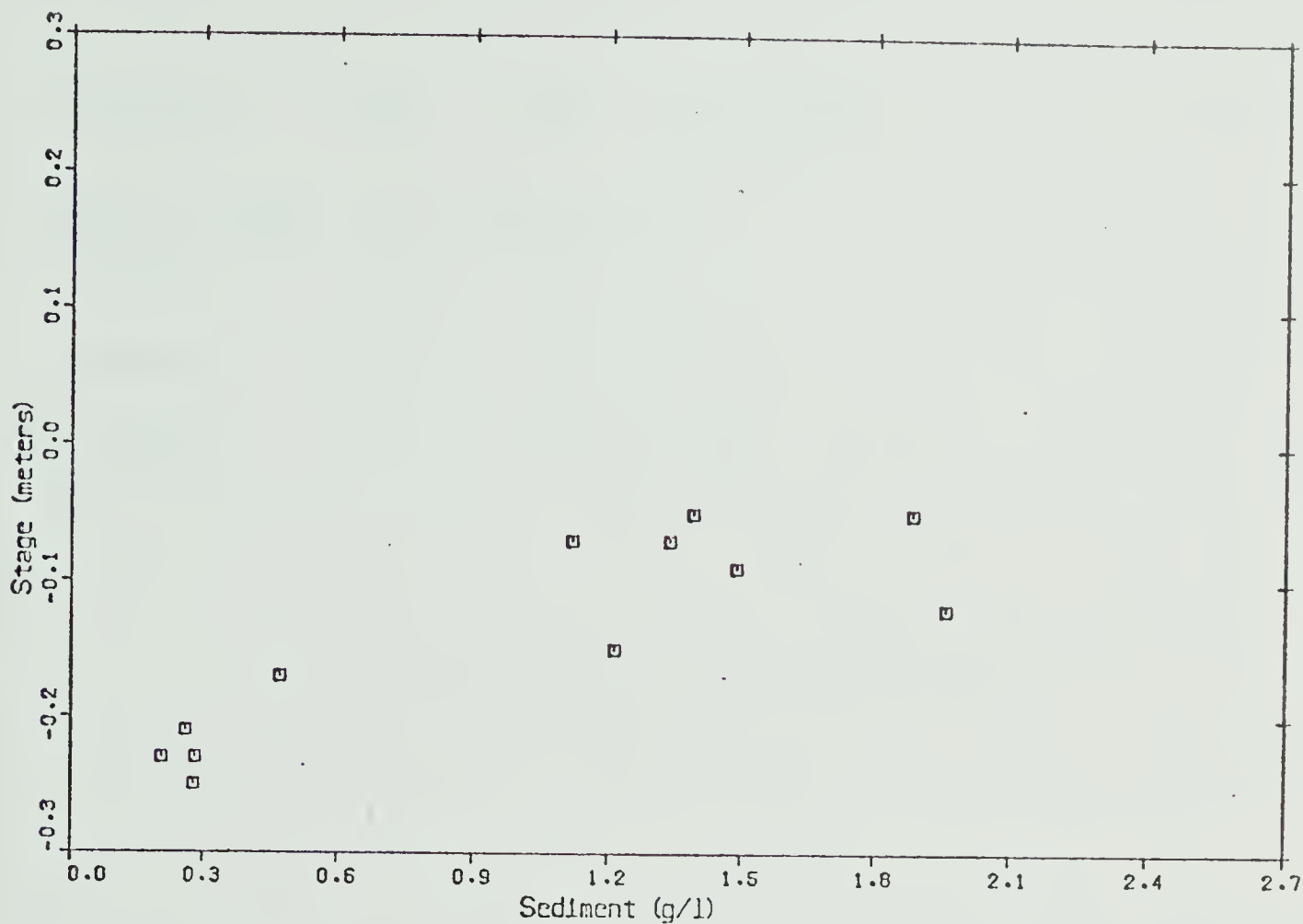


Table 2: Discharge results

Location	Date	Time	Discharge (m ³ /s)
Hazard Creek	July 18	09.30	6.0
Stream 1	July 8	13.20	0.21
Stream 2	July 8	14.00	0.17
Stream 3	July 8	16.00	0.39

Figure 10: Graph of stage against time

This records the variation in stage from July 4th to 25th.

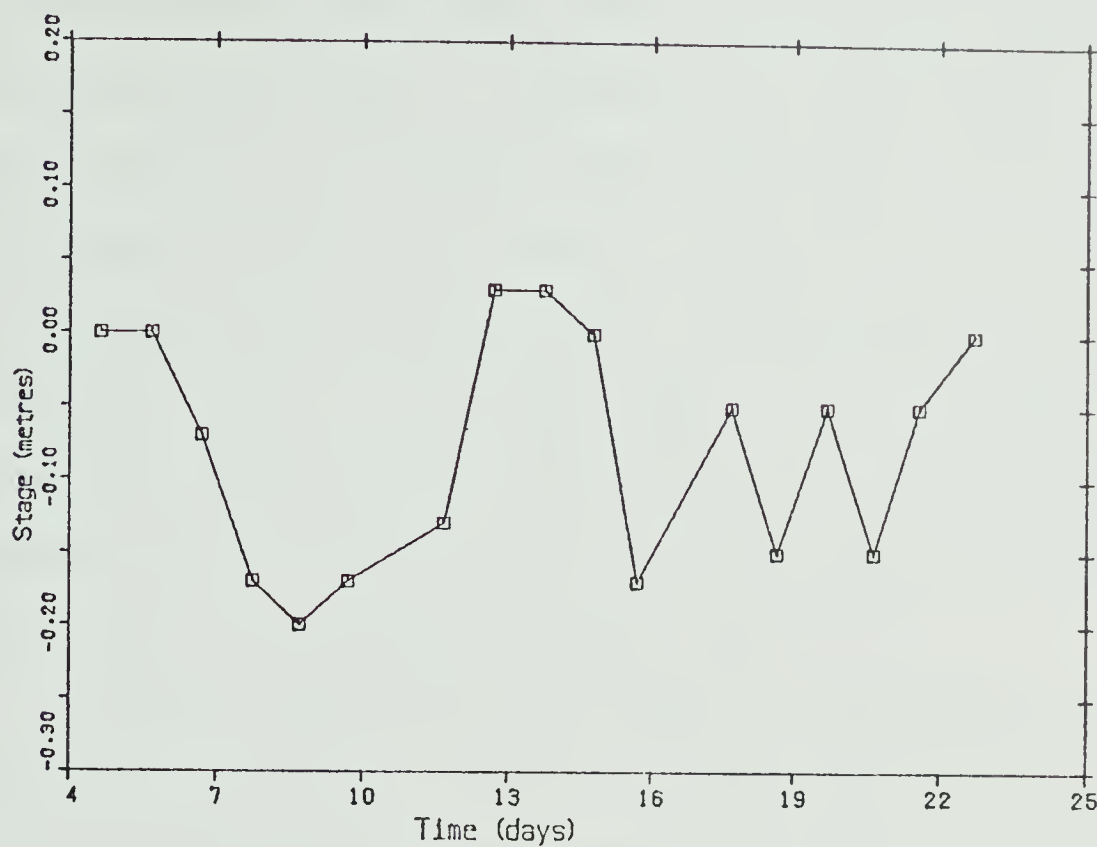
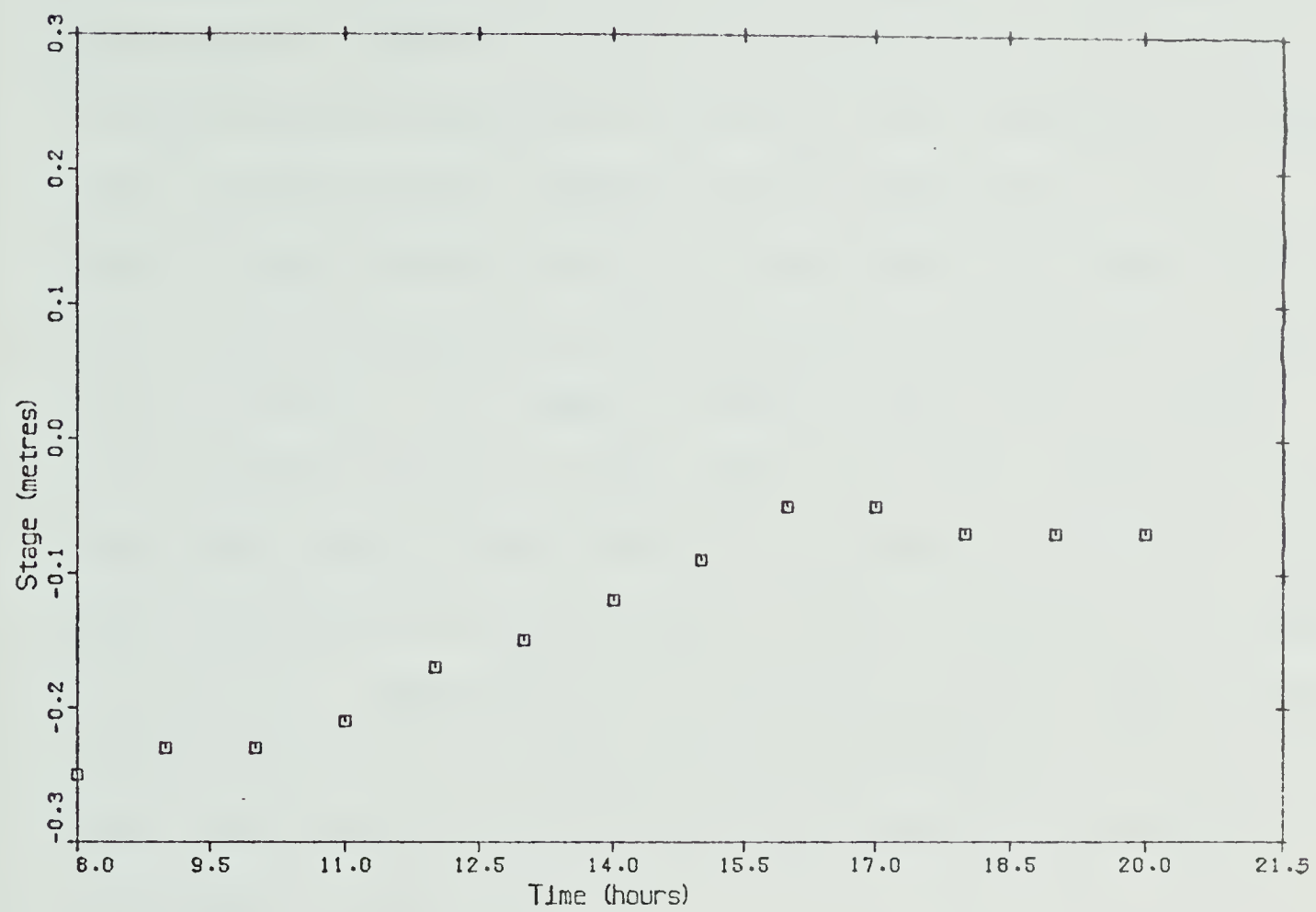


Figure 11 shows the stage variation over a thirteen hour period on July 18th. These results are tabulated in appendices 7 and 8 respectively. Examination of the weather log kept in the field shows that high stage appears to correlate with highs in temperature, rather than precipitation. This agrees with the results quoted by Church and Gilbert (1975) that most of the variation in run off can be explained by air temperature, this being the most important factor in melting rates. The daily measurements of stage were made between 15:40 and 19:00 hours, and an examination of Figure 11 shows that these levels must be very close to the peak for that day.

Further examination of Figure 10 indicates that the discharge measurement made for Hazard Creek was made at a time of low stage; in fact lower than any stage measurement made during the daily monitoring of the stream. To obtain an estimate of the peak and mean daily discharge, a comparison with results quoted by Church and Gilbert (1975) is made. An examination of their Figures 3 and 4 shows that minimum discharge occurs in the early to mid morning, and peak discharge is in the late afternoon. Thus it is reasonable to assume that the discharge measurement made was close to the minimum discharge for that day. This is supported by visual observations of stream flow over the delta of Hazard Creek; the timing of the discharge measurement was chosen to be at the lowest possible stage so as to facilitate wading of the stream. Examination of Church and Gilbert's Figure 8 shows

Figure 11: Stage variation, July 18th



the minimum discharge was approximately half the mean discharge, and one third to one quarter of the peak discharge. Although the use of this result for estimates of discharge of Hazard Creek may not be strictly justifiable, the estimates produced may be shown to be reasonable in the light of other work. Support for this approach is the detailed hydrological study of Rusty Creek by Faber (1972). Rusty Creek is a major contributor to the waters of Hazard Creek (Figure 2). He reports results which show a similar relationship between minimum, mean and peak discharge on a given day. Using these results it can be estimated that the peak discharge of Hazard Creek on July 18th was in the order of $22 \text{ m}^3/\text{s}$, equivalent to a stage of -0.05 m. The minimum discharge was $6 \text{ m}^3/\text{s}$ equivalent to a stage of -0.23 m. The mean stage was 0.13 m, which can be equated to the mean discharge of $12 \text{ m}^3/\text{s}$.

July 18th was a day of above average discharge (Figure 10). The peak stage level on July 18th was -0.05 m as opposed to a mean peak stage of -0.09 m. Now making a further simplifying assumption, a linear interpolation between the stage/discharge estimates made leads to an estimate of $17 \text{ m}^3/\text{s}$ for the peak discharge over the period the stream was monitored (July 4th to July 22nd). Using the relationship between peak and mean discharge established earlier, it would appear that $8.5 \text{ m}^3/\text{s}$ is a reasonable estimate for the mean discharge of Hazard Creek over this period. Thus the mean daily discharge over this period is

estimated to be $7.3 \times 10^5 \text{ m}^3$. It may be argued that the above reasoning rests on rather shaky ground, due to its reliance on a number of simplistic assumptions regarding the behaviour of glacial streams. However, the result obtained is testable against other data. As mentioned above, Faber (1972) made a detailed hydrological study of Rusty Creek, a major tributary of Hazard Creek. He reports results of $2.0 \times 10^5 \text{ m}^3$ for the mean daily discharge in the period July 19th to August 19th, 1967; and $1.8 \times 10^5 \text{ m}^3$ for the period July 9th-August 15th, 1968. The estimate for the daily discharge obtained above is $7.3 \times 10^5 \text{ m}^3$. Examination of aerial photographs allows estimates of the drainage basin areas of Rusty Creek, and Hazard Creek to be made. Rusty Creek constitutes approximately 15% of the drainage basin of Hazard Creek. Thus the estimate of discharge made in this study for Hazard Creek appears to be reasonable.

The measurements of the discharges of the minor inflow streams were made on July 8th, the day on which the lowest stage level was measured on Hazard Creek. The weather was cool, and wet, with considerable rain at the altitude of the lake, probably falling as snow at higher elevations. It might be expected that the contribution of the minor streams to the total inflow would be anomalously high. This is because their source is mainly precipitation, whereas that of Hazard Creek is snow and ice melt. Melt would be at a minimum in such weather as evidenced by the low stage, whilst discharge due to precipitation would be high. An

estimate for the peak discharge of Hazard Creek on the 8th can be made by methods similar to those above and yields a figure of $8 \text{ m}^3/\text{s}$. Thus the minor streams contribute at the most 10% of the total inflow, and probably normally much less, and are thus not considered in the effects of inflow on lake drainage.

B. Lake filling and drainage

When measurement of the lake level commenced on the morning of July 1st the lake had not yet attained its maximum level, and overflow was not occurring. The lake level rose at approximately two centimetres an hour until the morning of the 3rd, when the outflow was observed to be operating. The lake level fluctuated over a 20 cm range for the next five days until the morning of the 8th at which point it was observed to have dropped 30 cm below the maximum level attained. By 8:25 on the morning of the 9th the level had dropped 71 cm in the last 15 hours, and it was assumed that rapid drainage had commenced. From this point onwards the lake level was closely monitored, with measurements being made at least every hour apart from a four hour period between 1:30 and 5:30 on the 10th. Figure 12 is a graph plotting lake level in metres below maximum against time in hours from an arbitrary zero point of 17:00 hrs on July 1st. By 17:55 on July 10th the lake level had dropped over 12 m and the original survey method had to be replaced by photographic methods. This method became

Plate 3: Outflow stream

Outflow stream flowing after the lake attained maximum level, July 3rd. The Steele Glacier is visible in the background, damming the lake.



Figure 12: Plot of lake level against time

The drawdown is measured relative to the maximum lake level achieved. The zero point on the time axis is the time of the first measurement, 17:00 on the 1st of July.

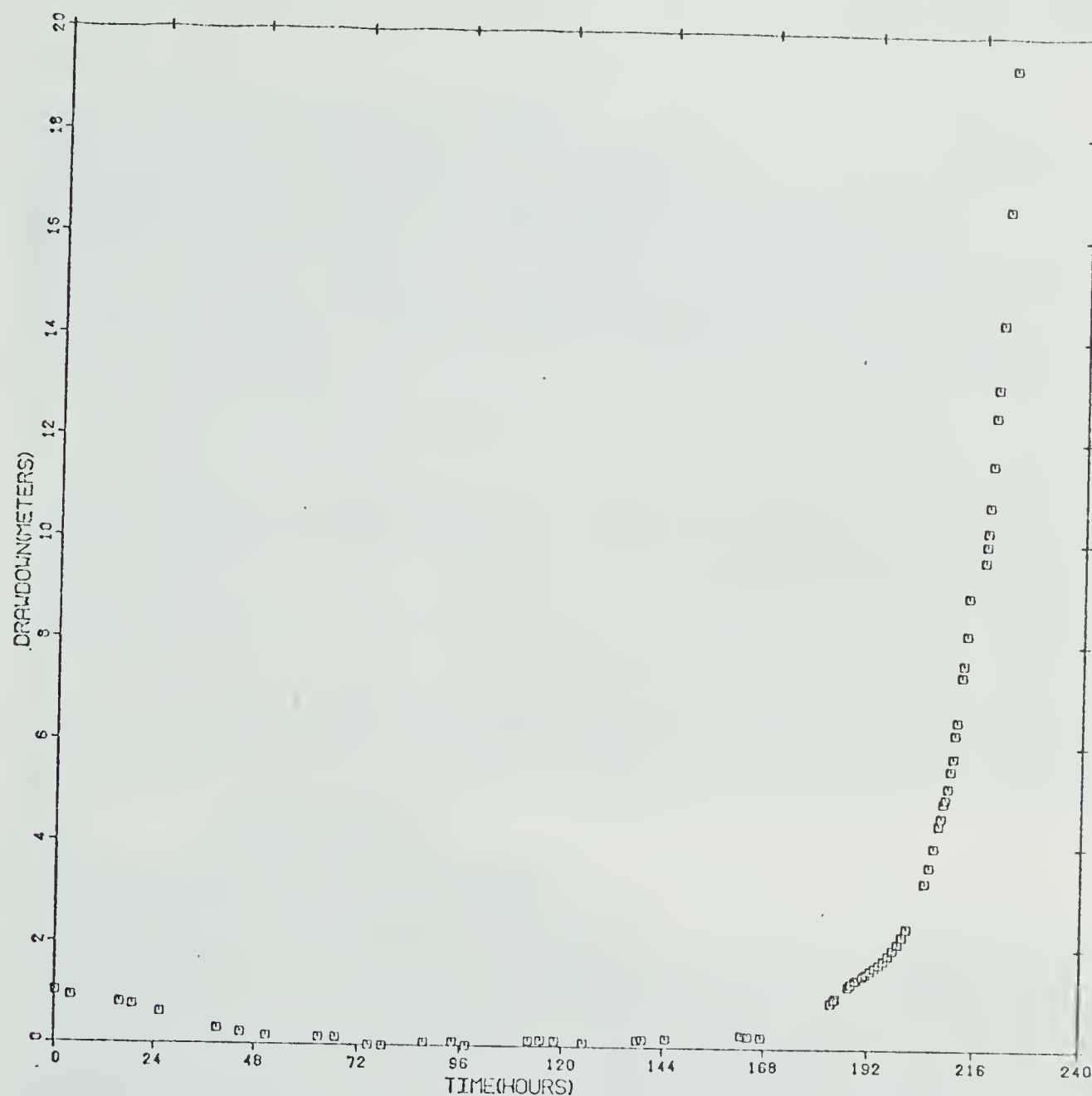


Plate 4: Lake drainage.

The upper photograph was taken at 06:30, July 10th, at which point the lake level was 3.63 m below the maximum level attained. The lower photograph was taken at 14:00 on the same day. In the intervening time the lake level has dropped 4 m. Many small strand lines are visible on the lake shore to the left of the photographs. The photographs were taken adjacent to stream 1 looking eastwards towards the delta of Hazard Creek.



Plate 5: Lake Drainage 2

The upper photograph was taken at 18:05, July 10th, at which point the lake level was 13 m below the maximum attained. The second photograph was taken at 22:00 the same day, the lake level then standing 27 m below maximum. Both pictures are from the same location, the delta of stream 1, looking North.



impractical after 23:00 due to lack of light. Drainage became complete sometime between this time and 05:30 on the 11th.

To convert lake levels to discharge the variation of surface area with depth is required. The area of the lake at 5m depth intervals was obtained from the results of a survey made by G.K.C.Clarke and others in 1979 (Clarke 1980a, b), and is tabulated in Table 3. To obtain area estimates for intermediate values the statistical technique of regression analysis was used, which gives a best fit straight line through the data points. An examination of the raw data obviously shows that a simple linear model would not be effective, and thus a semi-logarithmic transformation was applied. This proposes that the relationship between depth (d) and surface area (A) is of the form:-

$$A = ab^d \quad (16)$$

where a and b are constants. If logarithms are taken of both sides of the equation it is transformed to:-

$$\ln(A) = \ln(a) + d \cdot \ln(b) \quad (17)$$

This is a linear relationship between the natural logarithm of the surface area and the depth. A correlation coefficient of -0.9989 was obtained for this relationship, and the regression yielded values of -0.6050 for $\ln(b)$ and 11.691 for $\ln(a)$. The residuals show no trend. Thus the

Table 3: Hypsometric data, Hazard Lake

After Clarke, 1980a

Contour Elevation (m)	Water depth (m)	Contour Area (m ²)
1674	0	1274000
1669	5	873700
1664	10	622700
1659	15	461800
1654	20	349700
1649	25	263700
1644	30	206600
1639	35	144200
1635	40	105100

relationship between the two variables can be expressed by the equation:-

$$\ln(A) = 11.691 - 0.06050(d) \quad (18)$$

An F test showed this to be significant at alpha = 0.01. Thus, using this equation, a value of surface area can be estimated for any given depth.

At any instant the discharge into or from the lake (Q) is given by:-

$$Q = dd/dt (A_d) \quad (19)$$

where A_d is the surface area at depth d , and t is time. The rate of change of depth with time is difficult to measure directly, and is estimated by the following procedure. Given two measurements at times t^1 and t^2 , the depths at these points being d^1 and d^2 respectively, the change in depth over the time $t^1 - t^2$ is $|d^1 - d^2|$. Thus the average rate of change in depth over this time is:-

$$|d^1 - d^2| / t^1 - t^2 \quad (20)$$

An estimate of the instantaneous discharge at a time halfway between t^1 and t^2 ($t^{1/2}$ is given by:-

$$Q^{1/2} = A_{\frac{1}{2}} \{ (d^1 - d^2) / (t^1 - t^2) \} \quad (21)$$

where $A_{\frac{1}{2}}$ is the surface area at a depth halfway between d^1

and d^2 . This figure is the overall discharge from the lake, Q_a . In order to estimate the discharge through the tunnel (Q_t) the inflow to the lake from Hazard Creek and other streams must be known (Q_i). Clarke (1980a) estimates this to be a steady $5 \text{ m}^3/\text{sec}$. The data collected from the inflow streams allows an improvement on this estimate to be made. Appendix 9 is a list of estimates of Q_i on a daily basis. These were made using the information of peak, mean and minimum discharge and the corresponding stage levels. Using the information obtained on July 18th an approximate stage/discharge relationship can be established, using a linear interpolation for the values between the three data points. This is then scaled against the mean discharge over the total period of time of stage measurement. Ideally a more accurate stage/ discharge relationship would give a more precise estimate of these quantities, and a further correction might be made for the variations between days. However, it was felt that the accuracy of the data did not allow a correction of this degree of precision in this case. Despite the uncertainties in the estimates of discharge, this represents an improvement on Clarke's estimate, as shown by the fact that when the correction is applied to give $Q_t = Q_a + Q_i$ there are no negative values of Q_t , which would occur if Clarke's correction was used. Estimation of Q_t whilst the lake was at its maximum level was impossible due to the fact that the amount of water flowing out of the lake by the stream along the margin of the Steele is unknown.

(Q_o).

The volume remaining in the lake at a given time is calculated by the method of Clarke (1980b), where the volume of the lake (V) is related to the depth of water above the seal to the lake by equation 14 (page 29). 'm' in this equation is calculated by Clarke (1980a) using regression methods as being 0.06 for Hazard Lake. The volume discharged from the lake at a given time is approximately V_o - V and is tabulated in Appendix 10 along with data pertaining to discharge calculations, total discharge, inflow to the lake and tunnel discharge. Figure 13 is a graph of discharge against time.

Early measurements of lake level are probably fairly accurate, the main errors being due to difficulty in obtaining an accurate reading when the lake surface was disturbed by waves. As the lake commenced to drain rapidly, it would be expected that the error in measurement would increase due to the frequent repositioning of the gauges. The photographic method used for the final stages is not very accurate, and errors of up to ten per cent are likely.

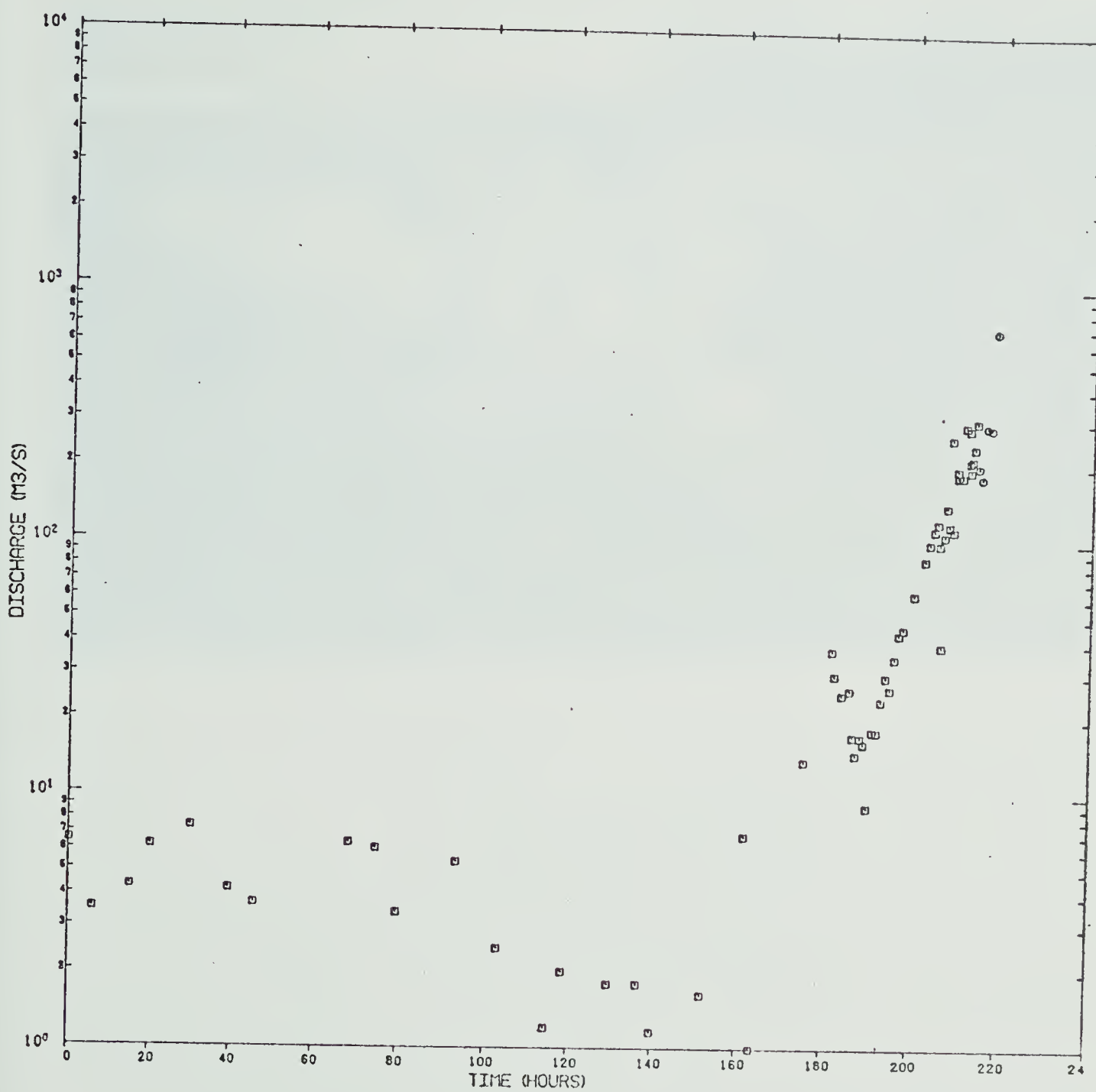
Visual observations

Two notable effects of the rapid drawdown were observed. The rapid fall in lake level resulted in the formation of many small slope failures in the sediments exposed as the lake level dropped. Plate 7 shows two examples, both being rotational movements.

The second observation of note was the formation of

Figure 13: Discharge/time, lake draining

Discharge is the overall discharge from the lake in this case.



)

Plate 6: The ice dam

The ice dam portrayed shortly after drainage, looking south. The tunnel is clearly shown at the base of the dam, as is the tide mark showing the maximum lake level. The dam is 100 m high. At the base of the dam many ice blocks can be seen, formed by collapse of the dam after removal of the buoyant effect of the water.



Plate 7: Slope failures

The example of the upper photograph was observed on the south side of the delta of Hazard Creek. The lower photograph shows a failure close to the delta of stream 1 (bushes in picture are approximately 1m high).



many small strandlines (Plates 4 and 5). These formed in a very brief period, as the top two metres of the lake banks were observed to be free of them in the short period as the lake was filling, but were clearly marked by them during drainage. On drainage, many more strandlines were visible, some of a considerably greater size than those originally observed. Embleton and King (1974) cite examples of these described by Stone (1963a) and others and suggest that they form during drainage, specifically in periods of slow rather than catastrophic drainage. This example shows that this is not the case at Hazard Lake. It is suggested that these 'terracettes' are formed during the filling of the lake at times of low inflow, and thus times of static lake level, and the rapid drainage prevents erosive forces acting to the same extent as during slow drainage, resulting in their preservation. The rapidity of formation observed in this case casts considerable doubt on work that attempts to relate relatively minor terraces to major variations in lake level, such as that of Brook (1971), and Stone (1963a).

C. Sections in lake sediments

Written descriptions of the sections constitute Appendix 1. The locations of the sections are displayed in Figure 5. Appendix 12 is a list of samples taken from the sections. To facilitate description a number of major facies will be described, into which the sediments of the sections will be classified. These to some extent follow those of

Shaw (1975), but differ in detail. The facies are:-

1. Gravel (A)
2. Cross bedded sand (B1)
3. Massive sand (B2)
4. Cross laminated sand (B3)
5. Graded bedded sand (B4)
6. Laminated silts (C)
7. Clays (D)

The general features of each facies are described below.

A- Gravel

This facies is common and is usually found towards the base of sections. Structure is difficult to discern, but horizontal bedding is visible in some examples, as is imbrication of the pebbles. Sorting is variable but generally poor. Clasts are well rounded.

B1- Cross bedded sand

This facies is rare, only being found in two sections. Where seen, the sets of the cross bedding appeared to be tabular. The units of cross bedding are between 1 and 5 cm in thickness, and contain beds 0.5 to 1 cm thick.

B2- Massive sand

This facies consists of massive sands, internally structureless. Bedding thickness ranges from 0.01 to 0.50 m, and the facies is common in the sections.

B3- Cross laminated sand

This facies is also common, and consists of ripple

drift cross laminated sand. It is found in most sections close to the sediment source. Both types A and B of Jopling and Walker (1969) are found, as is the draped lamination of Gustavson, Boothroyd and Ashley (1975). Type B cross lamination appears to be more common. Some apparently massive beds were assigned to this facies on the grounds that the only structure visible, at the contact with the overlying unit, was rippled. The internal structure of the sediment was commonly difficult to see, due to the water soaked nature of the sediment. Sets of laminae were between 1 and 3 cm thick, and the laminae were themselves between 0.2 and 3 mm thick.

B4- Graded bedded sand

This facies was common, and this in combination with its use as an indicator of flow conditions, justifies its inclusion as a separate facies. The thickness of the beds involved was variable, from 0.5 to 10 cm, and the material involved varied from coarse sand to silt.

C- Parallel laminated silts

This facies was common, and formed the major component of sections relatively distant from the sediment source. The lamination was generally flat lying but was observed to be draped over boulders on the lake bottom (Plate 8). Individual laminae were of a thickness of 0.5-2 mm, and examination of samples under the

Plate 8: Facies C

Laminated silts (facies C) draping over a boulder at the base of section D7. The photograph shows the sharpness of the contact between facies C and A.



Plate 9: Facies C

Close up of laminated silt facies in section D7.



Plate 10: Facies B3

Draped lamination in cross laminated sand facies B3, section D11.



binocular microscope showed that each lamina is graded, from fine sand/silt to silt/clay. Minor faulting was observed in these sediments in several localities.

D- Clays

This was a distinctive facies, usually found at the top of the section. The clays were usually massive but sometimes showed horizontal lamination. The unit was generally thin (1-2cm), and draped underlying structures.

Facies associations

Table 4 is a list of facies transitions found in the sections, from bottom to top of sections. Figure 14 is a diagram showing the sections described. The samples taken are listed in Appendix 12, with their locations. It can readily be seen that facies A and D are most commonly found at the base and top of the sections respectively. The transition from facies A to C at the base of the section is common. Facies B4 appears to be closely associated with facies B2.

Grain size analysis

The raw data from the grain size analysis is given in Appendices 2 and 3. Table 5 is a list of samples and their graphic Folk-Ward parameters. Three duplicate analyses were performed to investigate the usefulness of the four measures in interpretation to be made. Insufficient duplicate analyses were made to allow a full statistical analysis of the variability due to laboratory analysis. However, the

Table 4: Facies sequences in sections

The sequences listed below are from the bottom of the sections described upwards.

Section	Sequence
D1/2	B2-B3-B2-A-B2
D3	A-B2-C-B3
D4	A-C-B4-B3-B2
D5/6	B2-B3-C-B2-B4-C-B4-D
D7	A-C-B2-B4-B2-B1-B4-B2-D
D8	A-C-A-B2
D9	A-C-B2
D10	A-C-B4-B2-B4-B2-A-D
D11	A-B2-B4-B3-B1-B2
D12	A-C-B3-C-B2-C-B2-D
D13	A-C-B2
D14	A-C-D
D15	A-C-B2-D
D16	A-C-B2-D-B3
D17	A-C-D
D18	A-C-B4-B2-D
D19	A-C
D20	C-B2-D
D21	C-B2-D
D22	C-D

Figure 14: diagram of sections, arranged in order of proximity to source

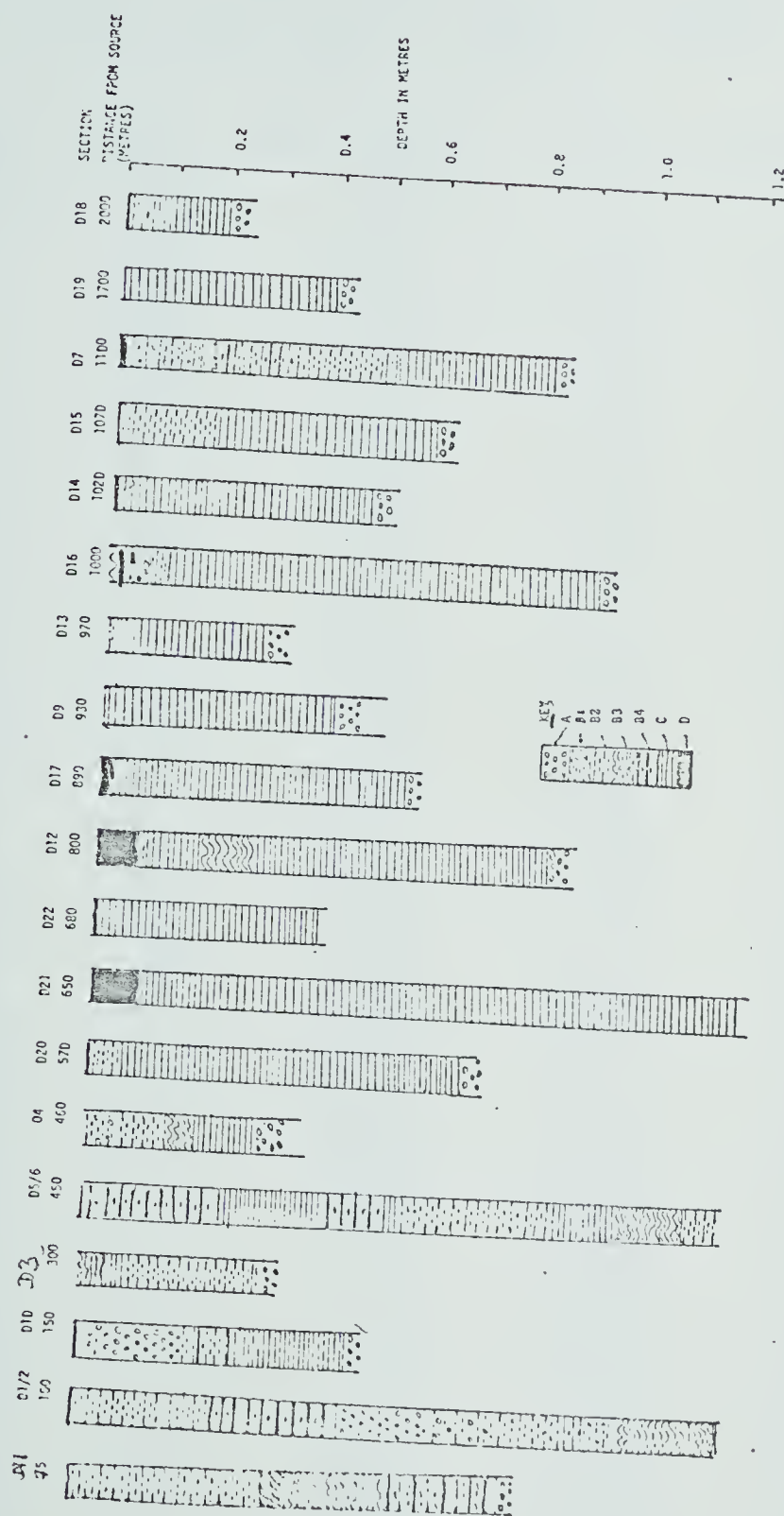


Table 5: Folk-Ward parameters, section samples

Sample numbers refer to the section from which the sample taken i.e. sample D12B is from section D12. The measures given are Folk-Ward parameters, calculated by graphic methods. Mean grain size and sorting are measured in phi units. Duplicate sample numbers indicate replicate analyses. These are tabulated separately.

Sample number	Facies state	Mean grain size	Sorting	Skewness	Kurtosis
D1A	B2	2.27	1.12	-0.01	1.33
D1C	B2	4.57	1.91	0.38	2.49
D2A	B2	3.23	1.19	0.07	1.29
D2B	B3	3.27	1.15	0.08	1.11
D3A	B2	1.93	0.97	0.11	1.34
D4A	C	5.50	1.79	0.40	1.81
D5A	C	4.97	1.92	0.53	2.10
D6A	C	5.03	2.07	0.47	1.98
D6B	B2	1.47	0.64	-0.06	1.08
D7A	C	8.33	2.74	0.36	0.87
D7B	C	8.27	2.61	0.47	0.91
D7C	C	8.33	2.78	0.35	0.86
D7D	C	7.90	2.96	0.34	1.05
D9A	B2	7.20	2.97	0.49	1.04
D9B	C	7.60	2.95	0.53	1.04
D9C	C	7.33	2.62	0.50	0.94
D9E	C	6.63	2.29	0.43	1.45
D10A	B4	4.47	1.26	0.48	2.05
D10B	C	5.53	1.97	0.59	1.97
D11A	B4	4.53	1.17	0.30	1.80
D12A	B3	3.30	0.94	-0.03	1.06
D12B	C	6.63	2.37	0.64	2.02
D12C	C	6.77	2.61	0.59	1.44
D12D	C	6.40	2.14	0.49	1.56
D12E	C	6.73	2.55	0.60	1.74
D12F	C	6.83	2.47	0.58	1.82
D12G	C	7.03	2.39	0.51	1.83
D13A	C	7.53	2.55	0.09	0.96
D14A	C	7.13	2.80	0.34	1.10
D16A	C	6.37	2.45	0.45	1.50
D16B	C	7.40	2.96	0.48	0.97
D16C	C	7.73	2.79	0.50	0.96
D17A	C	7.17	2.58	0.55	1.53
D19A	C	8.90	2.95	0.15	1.01
D20A	C	6.37	2.19	0.51	1.48
D20B	C	5.43	1.86	0.37	2.00
D20C	C	6.40	2.47	0.57	1.50
D20D	C	6.37	2.34	0.53	1.53
D20E	C	6.53	2.42	0.53	1.78
D21A	C	6.57	2.64	0.63	1.45

D22A	C	7.23	2.68	0.47	1.41
------	---	------	------	------	------

Replicate samples

Sample	Facies	Mg	Sorting	Skewness	Kurtosis
D9D	C	7.70	2.65	0.43	1.07
D9D	C	7.53	2.66	0.44	1.90
D15A	C	7.80	2.70	0.44	1.01
D15A	C	7.93	2.77	0.45	0.91
D18A	C	7.33	2.45	0.49	1.68
D18A	C	7.10	2.18	0.36	1.51

measures skewness and kurtosis show considerable within sample variation and this, combined with the lack of any trend with facies, or sample location, leads to the rejection of the use of these measures in interpretation. This agrees with the results obtained by Swan, Clague and Luternauer (1978) who reject these two measures as unreliable. The large within sample variation appears to be due to the use of the tails of the grain size distribution in the calculation of these parameters, which are subject, for a number of reasons, to greater error in laboratory analysis. Thus only the mean grain size and graphic standard deviation will be used in the interpretation of these results.

Trends in grain size

Much of the sampling concentrated on one facies, the laminated silts, which was found in most sections and was the predominant facies in many. Most of these samples were channel samples, although in sections D9, D12, and D20 samples were taken at intervals throughout the unit, to investigate variation with depth in this facies. For section D20 a channel sample through the whole unit was taken also and these results can be used to test whether a channel sample is representative of the unit as a whole. The channel sample D20A had a mean grain size of 6.37 phi, and the samples D20B-E an average mean grain size of 6.18 phi. The sorting of D20A was 2.27 phi and the average of samples B-E was 2.19 phi. Considering the variability of replicate

analyses, it can be concluded that channel samples taken were representative of the characteristics of the unit as a whole.

An examination of the stratified samples taken in sections D20, D9, and D12 shows no consistent trends in mean grain size or sorting with depth. However, an examination of the field notes made shows that definite trends can be recognised. For instance, section D12 shows a trend from bottom to top of an initial abrupt fining followed by a gradual coarsening, and an abrupt fining at the top of the section. This trend is repeated in sections D8, 10, 11, 15, 18, and 21. Sections D20 and D16 are probably similar, but the base of the section is not exposed. Sections D3, 4, 9, and 13 are also similar but do not show the abrupt fining at the top of the section. Sections D14, 17, 19, and 22 have similar trends and show a consistent fining upward trend. Sections D5/6 and D1/2 show more complex variation (in both of these cases the two sections are considered to be one continuous section).

D. Results from the Ekmann sampler

The results of grain size analysis performed on samples collected with the Ekmann grab sampler are given in Table 6. These results show little relation to the results obtained from sampling of the lake bottom after drainage. The reproducibility of the sampling is also in doubt, considering the disparate results from location A2. Another

Table 6: Folk-Ward parameters, Ekmann sampler

This table lists the results of the grain size analyses performed on samples collected with the Ekmann sampler. The measures tabulated are graphic Folk-Ward parameters. Mean grain size and sorting are measured in phi units.

Location	Mean grain size	Sorting	Skewness	Kurtosis
A1	5.30	2.01	0.59	1.82
A2a	5.83	1.87	0.42	0.84
A2b	6.23	2.04	0.69	2.36
A3	5.83	2.11	0.35	1.89
A4	5.07	2.38	0.20	1.81
A5	6.83	2.46	0.48	1.74
B1	6.67	2.33	0.46	1.26
B2	2.90	2.25	0.24	1.20
B5	6.47	2.95	0.35	1.23
C2	7.00	3.11	0.19	1.24
E2	9.50	2.66	0.15	0.92
F2	4.93	1.76	0.41	2.05

major problem with this type of sampling in this case is that considering the complexity of the upper part of the sections measured after drainage, the samples can only be realistically interpreted if it is known exactly what is being sampled. The sampler scrapes off sediment from the lake bottom which may be from a number of sedimentary units. The internal structure is not preserved well, and thus these samples are impossible to relate to the sediments seen after drainage. The sampler is also seriously affected by any material coarser than silt that sticks in the jaws resulting in the washing out of fine material. The use of some sort of coring device would have yielded more useful information as the sediment would be recovered as part of a stratigraphic sequence that could be related to the sediments seen after drainage, allowing an investigation of the effects of the drainage on the sediments deposited.

V. Discussion

A. Lake drainage

The objective of the measurements made of lake drainage was to test the existing models for the drainage of these types of lakes. Clarke (1980a) states

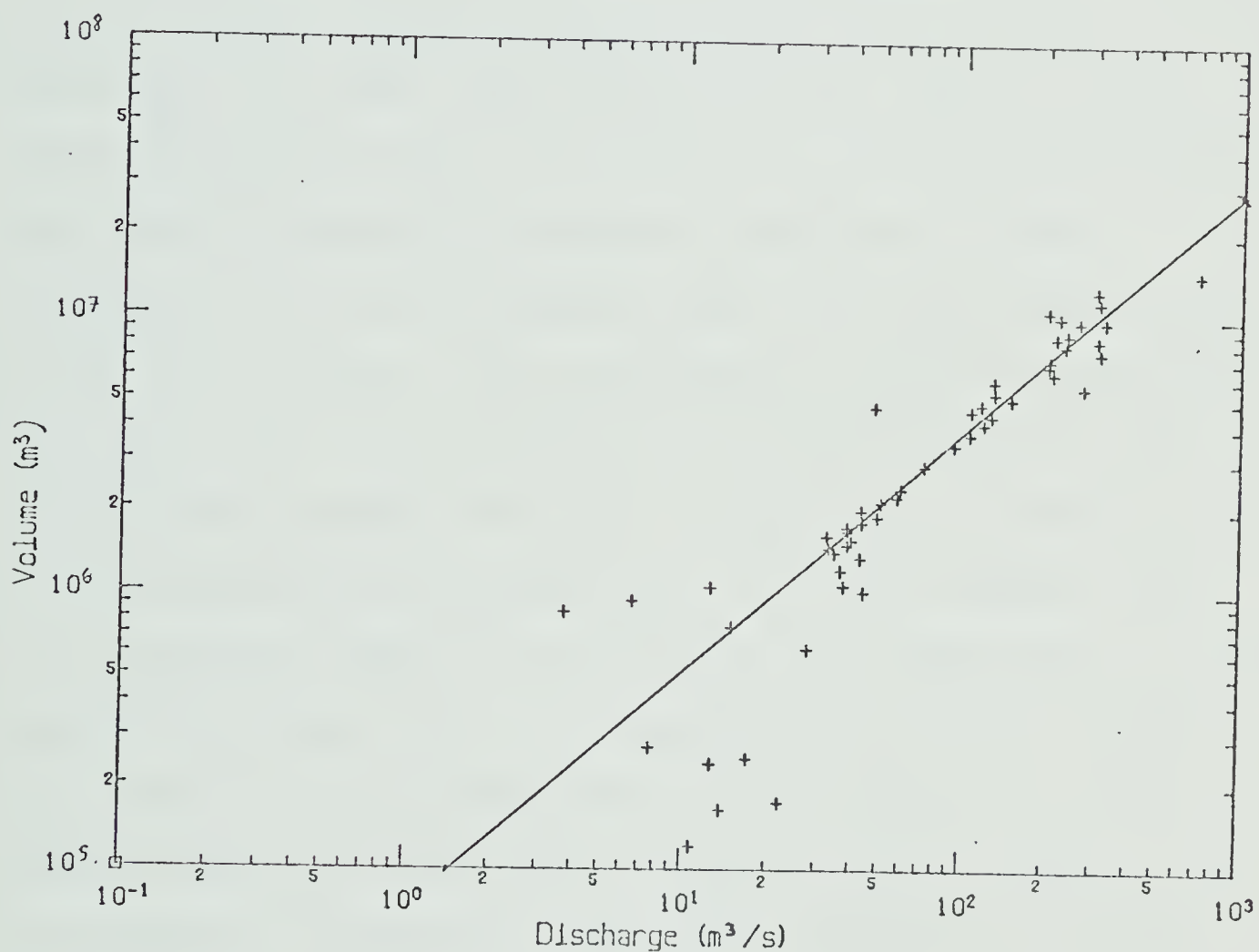
"If successive floods differ significantly, even when all external influences appear similar the Nye model must be incomplete in some important way."

Clarke published the results of the detailed measurements of the 1978 jokulhlaup from Hazard Lake, and a comparison of his results with those reported in this study constitutes a test of the Nye model. As far as possible the discharge results have been treated in a simliar manner to those of Clarke, although it is suggested that the estimates of input to the lake from inflow streams is superior in this case. Clarke fits his data to the relationship of equation 15 (page 30) by means of a regression of $\log(V_0 - V)$ against $\log Q$. His results are a value of 1.1174 for p and -5.343 for $\log c$. Figure 15 is a logarithmic plot of Q against $V_0 - V$ for the data of Appendix 10. A regression analysis was performed on this data, and an examination of the residuals showed that a simple linear fit was not applicable, the data being best described by one equation for the first fourteen data points, which are highly influenced by the accuracy of the correction (Q_i) applied, and another equation for the rest of the data. The regression analysis for the later part of

Figure 15: Graph of discharge/ volume discharged

The regression line obtained in this study is marked on the graph. Clarke's result from the 1980a paper is indistinguishable from this line on the scale of this plot. The equation is:-

$$\text{Log } (Q) = 1.134 \{\text{log } (V-V_0)\} - 5.477.$$



the flood, from 10:00 on the 9th of July to the termination of the flood, involving 75% of the volume of the lake, yielded values of 1.134 for p and -5.477 for $\log c$. An F test on the regression gives a value for F at degrees of freedom 1,35 of 318.6, a significant result at alpha = 0.01. The residuals showed no trend.

This represents an extremely close agreement with the data of Clarke, despite the use of different methods of measuring lake level. This result is very useful in the light of Clarke's report of results from three jokulhlaups from Summit Lake where successive events were highly variable. This result indicated that the model used may be at fault in some way. The closeness of the results reported here shows that the characteristics of the 1978 and 1979 events were virtually identical, supporting the model of Nye for the growth of the jokulhlaup. This also suggests that the assumptions made in the model do not always apply in the instance of Summit Lake, as hypothesised by Clarke (1980a). This result supports the unusually low value of n' , the Manning roughness coefficient found by Clarke (1980a, b) in his computer simulation of the 1978 discharge. As Clarke comments, this value is difficult to explain in physical terms, despite the fact it may be theoretically possible for a polished tunnel in ice. However, the work of Shreve (1972) indicated that the stable position of a tunnel carrying water through ice is at the base of the glacier, and therefore must have an interface with material other than

ice, making this value of n' unrealistic. The alternative explanation that the assumptions made in the inputs of the model are incorrect is preferred here. As Clarke suggests, parts of the tunnel may remain open from one event to another, acting to increase the potential gradient which is a primary input to the model. The potential gradient in this case is the gradient in the region of the seal. Clarke uses the spatial average from the mouth of the tunnel to the toe of the glacier. However, if the seal is close to the lake, as is likely in this case, the potential gradient is liable to be greater. This is because Hazard Lake sits in a relatively minor tributary valley to the Steele Valley. The valley of the Steele Glacier is probably of the typical U shape, and thus the steepest part of the tunnel will be the initial section, from the wall to the floor of the valley. If the tunnel closed partially, it would be in this region also, as the ice thickness is greatest at this point. Thus for the opening of the tunnel, after the first drainage event, the potential gradient as estimated by Clarke is likely to be an underestimate. This has the effect on the hydrograph of a more rapid increase in discharge. This is analogous to the effect of a smoother outflow tunnel, and thus may explain the low value of n' .

It would appear that this hypothesis is likely given the observation of G.K.C. Clarke and R.W. May (R.W. May, University of Alberta, personal communication) that the lake basin was still empty in late September, 1978, after the

drainage event of August 8th. This indicates that in the region of the seal, the area at which plastic deformation would be a maximum, the tunnel was still open after six weeks. It would not seem unreasonable to assume that the tunnel remained open over most of its length in the ten to eleven months between the jokulhlaup and the reopening of the tunnel.

However, further work is required on the closure of the tunnel before the model can be calibrated with any degree of certainty. This closure should be possible to model as the behaviour of ice under stress is well known, and this in combination with a sufficient knowledge of ice and bed topography should enable an estimate to be made. Thus a constraint can be made on the value of the potential gradient input to the model, and the prediction of n' can be improved. A possible test of this hypothesis of partial closure could be made if the records of a number of jokulhlaups are available from a given lake. The value of n' produced from a model such as Clarke's should be noticeably different for the first drainage of such a lake (for instance the 1975 event at Hazard Lake). Subsequent events should show similar results if the time period elapsing between outbursts is the same, as the closure of the tunnel is time dependent. This hypothesis is also supported by the only other values of n' calculated for jokulhlaups. Nye reports $n' = 0.12 \text{ m}^{0.33} \text{ s}$ for the 1973 event of Grimsvotn, where the period between events is five years and plastic

closure stops the jokulhlaup before exhaustion of the reservoir. This would indicate that the tunnel is probably completely closed in this case. Clarke (1980a) reports $n' = 0.08$ for the 1967 flood of Summit Lake. The interval between events in this case was two years, and it might be expected that the tunnel was closed over a greater proportion of its length than at Hazard Lake, giving a higher value of n' . It is therefore hypothesised that the value of n' is not as variable as Clarke (1980b) suggests, most of the variability in discharge records being due to different degrees of closure of the tunnel. It seems possible that the value of n' of 0.12 reported by Nye may be generally applicable, but discharge prediction is difficult unless the tunnel geometry is known. However, for the first event after an initial period of stability following the formation of the lake, the estimate of potential gradient used by Clarke and Nye would be valid, and thus the model should be useful in predicting discharge records for this event, probably the most important from the point of view of environmental hazard. Subsequent peak discharges would be expected to be greater if the tunnel does not close completely.

It is concluded that the Clarke-Nye model is a good one for predicting the discharge record at Hazard Lake. The close matching of the 1978 and 1979 records show that the model is applicable through time for a given lake. No firm conclusions can be drawn regarding the general applicability

of the model, but it seems probable that further work on modelling the behaviour of the ice tunnel after drainage may allow this. The peak discharge predicted by the Nye model is $620 \text{ m}^3/\text{s}$, and the maximum discharge measured in 1979 was $706 \text{ m}^3/\text{s}$, which is compatible if the accuracy of the observation of lake level is considered (plus or minus 10%).

B. A model for the historical development of ice dammed lakes

In this section a general model will be developed for the history of ice dammed lakes, and this will be applied to Hazard Lake. This is useful in that it provides an explanation of the sequence of events observed in studied ice dammed lakes, and allows prediction of the future development of these and other examples. The floatation hypothesis is accepted for the initiation of the jokulhlaup. Thus the main two variables to be modelled are the glaciostatic pressure (P_i) and the hydrostatic pressure (P_w).

Glaciostatic pressure

This is given by $P_i = \rho_i gh$ where h is the glacier thickness. The glaciostatic pressure is at a maximum in the region of the seal, and all predictions refer to the glacier thickness at this point. The position of the seal is that point at which $d\phi/ds = 0$, where ϕ is given by equation (8). The ice thickness h is controlled by the mass balance of the glacier. Generally the mass balance at the critical point

will be initially positive, and the glacier will thicken, impounding the lake. The mass balance will subsequently be negative, allowing the seal to be breached and the jokulhlaup mode of drainage to take place. This is not always the case as in the situation where the ice dam is continuing to thicken but not as fast as the increase in hydrostatic pressure is possible, although all known examples are dammed by an ablating glacier. In the case of a surge dammed lake, the ice thickness will increase rapidly for the duration of the surge, and then, due to the thermal imbalance caused by the surge, ablate steadily until thermal equilibrium is achieved. This ablation can be described by the equation

$$h = h(\max) - a t \quad (22)$$

where $h(\max)$ is the initial thickness of the ice at the end of the surge, a is the ablation rate, and t is time elapsed from the surge end. If the lake was not in existence prior to the surge then it will cease to exist before the glacier reattains equilibrium.

Hydrostatic pressure

Hydrostatic pressure is given by equation (6) (page 20). D in this equation is related to the volume of the lake by equation (15) (page 30). The volume at any given time is given by:

$$V = \int Q_i dt - \int Q_t dt - \int Q_o dt \quad (23)$$

where Q_i is the discharge of the inflow streams, Q_t is the discharge through the sub-glacial tunnel, Q_o is the discharge of an alternative outflow of water if in existence, and $t = 0$ is the time at which the lake is sealed. Thus the variation in hydrostatic pressure, which can be observed directly by measuring the lake level, can be related to the discharges through the tunnel and of the inflow streams. Q_i is usually easily measured if a discharge/stage relation is established, and the stage is monitored over the period of the lake's existence. Q_o can be estimated by similar means, but Q_t has to be obtained by the equation above, (25), given that Q_i and Q_o are known. The discharge through the tunnel is predicted by the model of Nye (1976). The tunnel drainage follows three phases.

1. The rates of enlargement and closure are balanced in the initial stages. The exact relationship of discharge to time has not been investigated but Nye (1976) shows that this is an unstable situation, leading to the next stage.
2. The rate of enlargement through melting becomes dominant, giving rise to the catastrophic flood typical of drainage. The discharge is related to the volume of the lake by equation (15) (page 30).
3. If the reservoir is exhausted then the tunnel will later close. The lake will be resealed after a period during which $Q_t = Q_i$. Depending on the geometry of the lake, and the rate of plastic closure, the lake may be

resealed before the reservoir is exhausted. This occurs when the rate of closure through creep becomes dominant.

Thus the variation of hydrostatic and glaciostatic pressure can be modelled and the history of a given lake can be predicted if sufficient information exists. Two possibilities are outlined below, the first a situation where the lake level is unconstrained, that is where the lake water has no alternative mode of escape; the second possibility is that where the lake level has a maximum possible value.

Lake level unconstrained

1. The glaciostatic pressure increases due to the surge of the glacier, to a maximum ice thickness of $h_{(\max)}$. If the glaciostatic pressure exceeds the hydrostatic pressure, then the basin will be sealed and a lake will start to form.
2. The glaciostatic pressure will decrease at a rate of a_{g_i} , and the hydrostatic pressure will increase at a rate of $\rho_w g D \{ (Q_i / V_o) - (Q_t / V) \}$ until the two become equal, at which point tunnel drainage commences. The hydrostatic pressure is then governed by:-

$$P_w = \rho_w g D \{ (Q_i / V_o) - (Q_t / V) \} \quad (24)$$

The integral of Q_i from 0 to t with respect to time is the volume of water supplied by the inflow stream from the start of the melt season to time t . When Q_t exceeds

Q_i the lake level will start to fall and the catastrophic flood will ensue.

3. Depending on reservoir geometry and rate of creep closure of the tunnel, the jokulhlaup will either terminate before exhaustion of the reservoir through resealing of the tunnel or the reservoir will be exhausted and the tunnel will reseal at a later date.
4. This sequence of events will be repeated until the ice dam is too low to retain the lake, or the feeder stream finds an alternative course.

Lake level constrained

1. The initial formation is as above.
2. The lake will fill until the hydrostatic pressure attains the maximum possible value i.e. $D = D_0$, at which point the lake level will be fixed.
3. The lake will remain stable until the glacier ablated to the point where $P_w = P_i$ and tunnel drainage will be initiated.
4. The lake level will start to fall when $Q_i = Q_t$, and the jokulhlaup will follow.
5. The sequence of events will be repeated with tunnel drainage being initiated at increasingly earlier stages of lake filling until Q_t exceeds Q_i before $D = D_0$, at which point the history becomes that of a lake with no constraint on lake level.

Application of the model to Hazard Lake

Application is in some ways difficult due to the fact

that data is incomplete, but some useful results can be obtained and the weaknesses in data collection can be pinpointed. The inputs to the model that are known with a reasonable degree of certainty are:

1. The ablation rate of the ice dam, reported by Collins and Clarke (1977) to be 2.65 m/year (from measurements made over one year only).
2. The exact dates of drainage in 1978 and 1979, and approximate dates for other events.
3. The date and duration of the surge of the Steele Glacier, stated to be 1965 to Summer, 1967, by Stanley (1969).
4. The discharge estimates for the inflow streams reported in this study.
5. The geometry and volume of the lake as reported by Clarke (1980a,b), with $V = 19,790,000 \text{ m}^3$ and $m = 0.06$.
6. The elevation of the surface of the Steele Glacier in the vicinity of the ice dam (1705 m.a.s.l) and the maximum lake level (1674m.a.s.l) (Clarke, 1980b)

From this data a number of deductions can be made. The initial thickness of the glacier after surge, h , can be calculated as follows. From the floatation hypothesis, drainage will take place under the conditions of equation (4) (page 18).

In 1975, $h - D = 31 \text{ m}$, and thus $h = 344 \text{ m}$. If the ablation rate is 2.65 m/year then the thickness after surge = 369 m. If the lake was not in existence prior to the surge

then the value of h must have been such as to be equivalent to a value of d less than 161 m. This gives a value of h of 180 m, the maximum thickness prior to the surge. This assumes that the glaciostatic pressure remains the control on the filling of the lake, although in fact Hazard Creek is known to have found an alternative drainage channel along the margin of the Steele Glacier. By similar methods the date at which the lake will cease to exist can be predicted to be when h reattains 180m, in 2045. There are considerable uncertainties in predicting the variation in Q_i . These are the main data lacking in the application of the model, as only one discharge measurement was made in the course of this study. However, using the arguments outlined earlier, and the work of Faber (1972) on Rusty Creek, a basic model for this variation can be set up. Faber shows that peak discharge for the year occurs in mid July. Break up in the area is in mid May and freeze up mid September. Peak discharge in 1979 was measured at $1.04 \times 10^6 \text{ m}^3/\text{day}$, based on a mean daily discharge of $12\text{m}^3 / \text{s}$. The simplest possible model is of a linear increase from 0 at break up to the discharge maximum on the 15th of July, followed by a linear decrease back to 0 at freeze up. This is clearly an oversimplification but in the absence of better data is used as an input to the model.

Using these data, a number of events can be predicted.

1. The date of initiation of tunnel drainage, and the critical lake level.

2. The volume of the lake at this point
3. The date of drainage of the lake

The lake level at which drainage occurs is predicted from the knowledge that in 1975, $d = 338 \text{ m}$ was the critical level for tunnel formation. If the ablation rate of the ice dam is 2.65 m/year then the critical lake level decreases by 2.38 m/year . The decrease in lake volume at this point can be calculated by equation (14) (page 29). The date of creation of tunnel drainage can be predicted from knowledge of the critical lake level and the filling rate of the lake. The volume at the critical level is V and this is equal to $Q_i dt$. In this case $Q_i = ct$ where $t = 0$ is May 15th, and $c = (1.04 \times 10^6 / 60) \text{ m}^3/\text{day}$ until July 15th, and $(-1.04 \times 10^6 / 60) \text{ m}^3/\text{day}$ subsequently. Thus

$$V = c t^2 / 2 \quad (25)$$

and thus the date of tunnel drainage can be predicted.

Q_t is not known in the earlier stages of drainage, but a simple model may be substituted for its behaviour as an illustration of the application of the model. If it is considered that Q_t varies linearly from zero at the initiation of the tunnel until $Q_i = Q_t$, the slope of this line can be obtained using the 1979 data, where tunnel formation occurred 18 days before $Q_i = Q_t = 12 \text{ m}^3/\text{s}$. Thus the variation of $Q(t)$ can be predicted, and the date of rapid drainage is where $Q_i = Q_t$. $Q_i = ct$, and $Q_t = b(t - t_q)$ where c

is defined as above, $b = (1.04 \times 10^6 / 18) m^3/day$, and t_a is the number of days between breakup and tunnel formation.

These predictions are given in Table 7. The faults in the model are apparent when this is compared to Table 1, the actual chronology of events concerning the lake. However, the fault probably lies in the assumptions made regarding Q_i and Q_t . Q_i varies in character from year to year, a high melt year in 1977 resulting in an earlier date of drainage than in 1978. The simple linear model for variation in discharge over the melt season used here is, from consideration of the behaviour of other glacial streams, not a particularly accurate one. However, the results do approximate to reality, and with better input data, the predictions should be reliable.

C. Lake processes

A glacial stream entering a lake may do so in three ways (Bates, 1953).

1. Underflow, if the density of the inflow stream exceeds that of the lake water.
2. Interflow, if the densities of the lake water and inflow stream are equal.
3. Overflow, if the density of the stream water is exceeded by that of the lake.

The density difference between the lake water and the waters of Hazard Creek can be easily estimated. The temperature difference is considered to be negligible, the differences

Table 7: Predictions of the historical model

These are the results as calculated by the methods outlined in the text. d is the elevation in metres above the seal at which point drainage will commence. V is the volume of the lake at this stage in $m^3 \times 10^6$. D(t) is the date at which tunnel drainage will commence and D(l) is the date at which the jokulhlaup will occur.

Year	d	V	D(t)	D(l)
1975	338.0	19.79	July 3	
1976	335.6	17.00	June 30	July 20
1977	333.2	14.55	June 27	July 14
1978	330.8	12.41	June 24	July 11
1979	328.5	10.67	June 21	July 9
1980	326.0	9.63	June 18	July 1
1983	318.9	5.57	June 11	June 20
1985	314.1	3.99	June 7	June 15

of less than one degree giving a density difference of less than 0.1 g/l. The suspended sediment content is more variable. The lake water had a mean suspended sediment content of 0.04 g/l, and the inflow stream had values ranging from 0.206 g/l to 1.88 g/l. These values can be converted to actual densities by assigning a specific gravity of 2.65 to the sediment, and calculating the weight of water displaced by the sediment. This shows that the density difference between lake and stream waters is a minimum of 0.103 g/l and a maximum of 1.146 g/l. Bell (1942) states that a density difference of 0.01% is sufficient to give underflow. The density difference approaches this value at the minimum but is in general much higher. Thus underflow is the most likely mode of entry of the inflow stream. The characteristics of this underflow will depend on the variation in the discharge and suspended sediment content of the waters of Hazard Creek. It will thus vary widely in magnitude on a diurnal basis, and may not operate at discharge minimum, and low suspended sediment concentrations. Thus the effect of stream inflow is of a daily turbidity flow. that suspended sediment concentration appeared to be related to discharge although the exact form of this relationship was not investigated. The variation of discharge with time follows three periodic fluctuations. Firstly, a daily variation, apparent from the results reported earlier in this study; secondly a longer period variation related to weather conditions, apparent again in

the stage/time graph of Figure 10, and thirdly, the annual variation from 0 at break up to a maximum in mid summer to 0 again at freeze up.

Examination of the results of temperature and suspended sediment content for the lake show that the lake is essentially unstratified. The presence or absence of stratification is an important control on the nature of the sediments deposited.

D. Interpretation of the lake sediments

Firstly the effects of repeated filling and emptying on the sediments are considered. Theoretically this should take the form of a transgressive to regressive sequence. At a given point, the mean grain size should initially grade from coarse to fine, whilst the lake is filling, and subsequently rapidly grade from fine to coarse as the lake empties. If a record exists of the repeated draining events, this pattern should be repeated a number of times. However, this trend is only seen once in the sections examined. This is best explained by considering the bulk of the sediment constituting the sections to be the product of the initial period of stability following the first filling of the lake. This hypothesis is supported by the volume of sediment in existence, over one metre in relatively distal positions, and the short period of time available for sedimentation during cyclic drainage (one to two months as opposed to nine years). This indicates that much of the sediment deposited

in recent fillings is eroded during the drainage, and while the lake is empty. Erosion was observed on steep slopes in the lake, where little sediment was preserved during drainage.

A model for sedimentation

The main agent of sediment input to the lake is underflow from the inflow stream as a turbidity current. This is considered to be a daily event during the melt season, and the magnitude of the flow is dependent on the discharge of the inflow stream, which varies according to the pattern outlined above. As the lake filled the effect would be of an increasing distance from the source of sediment, the inflow stream. After filling this would be constant for the period of stability, and then decrease rapidly during drainage. The effects on the sediments of this source movement are controlled by the effects on current velocity. It would be expected that current velocity would decrease exponentially with distance from source if the slope remains constant. Thus the sediments should show the effects of two variations in the depositing current, the variations in magnitude due to variation of discharge of the source stream, and the variations due to the change in position of the source.

The facies states outlined earlier are characteristic of deposition in definite flow conditions. These are in order of relative current strength A, B1, B3, B2, C, D. The grain size of facies A precludes deposition from underflow.

Facies B4 would be deposited in declining currents, of similar strength to those depositing facies B2 and C. Thus the probable position of deposition of the sediments is indicated. The gravel facies is deposited by stream flow; the sand facies B1-B3 are deposited by underflow in proximal positions; B4 is deposited in declining flow conditions in relatively proximal positions; C is deposited by underflow in distal positions; D is deposited from suspension in times of little underflow activity.

The variation in the underflow can account for the characteristics of some of the sediments. The laminae of facies C are probably due to the diurnal variation in input resulting in a sequence of increasing and declining flow, giving rise to the grading seen. This hypothesis may be tested in the following manner. An examination of Plate 9 and other photographs allows an estimation of the mean thickness of the laminae. If this is divided into the thickness of the section, this gives the number of laminae in the section. This should be equal to the the number of active days during the deposition of the facies which can be estimated, given that these sediments are the product of the nine years of stability, to be 1090 days. The estimated number of laminae is 985, providing strong support for the hypothesis. Further support for the existence of underflow was the observation of a sharp break between the waters of the inflow stream and the lake at the point of entry of the stream as the stream water "dives" beneath the lake water.

Examination of Plate 8 shows that laminae thin as they drape over a boulder. If deposition was from suspension from overflow or interflow, the laminae would not show this variation in thickness, and thus deposition from suspension in a bottom current is likely. In the sampling of the lake waters, an increase in suspended sediment concentration and temperature was observed near to the lake bottom at sample position C2. This point is located in the centre of the lake basin, and these observations may indicate the detection of turbid flow on the lake bottom. No evidence was observed for the effects of the longer term cycles on these deposits and this will be discussed later.

These laminated sediments are not considered to be the product of wind generated bottom currents. The uniformity in thickness, and the absence of any other sedimentary structures makes this unlikely, as it would require winds of a very high degree of regularity in strength and duration. This particular location is subject to wide variation in wind.

The model can be applied to explain the characteristics of the sections measured. Sections D4, 8, 9, 13, 15, 16, 17, 18, 19, 20, 21, and 22 all show the same general characteristics; gravel at the base of the section, unconformably overlain by laminated silts, which themselves grade into sand facies B2 or B4; overlying this is the clay facies D draped over the underlying sediments. The most complete example is D18, but all the above sections show at

least part of this sequence. This can be interpreted in the following manner. Initially, before the filling of the lake, the valley was filled by a braided stream. The gravels are interpreted as being the product of sedimentation in this environment and thus were deposited prior to the formation of the lake. On filling a transition to a lacustrine environment occurs. It might be expected that the sediments should grade from the coarse gravels to the laminated silts, but this is only seen in one section, D3. This sharp transition would be possible if the turbid underflow was confined during filling to one major channel, possibly the existing stream bed. The effects of this underflow during this period would thus be confined to this channel, until the lake attained its maximum level. At this point the position of inflow would become relatively stable, resulting in very high rates of sedimentation at this point. This may have choked the confining channel and allowed the underflow to migrate over the delta surface, allowing sedimentation over a large part of the lake basin, and the deposition of the laminated silts. An alternative hypothesis is that during the period of filling, underflow was not the predominant process. This is certainly likely in the early stages, as the lake water would initially have a high suspended sediment concentration, close to that of the inflow stream, and interflow or overflow could result. Thus initial sedimentation could be by deposition from suspension, and the sediments would not show the effects of

current action.

When drainage commenced, the source moved closer to the point of deposition, resulting in the observed grading into sand facies, due to the increasing power of current flow. The degree of this effect depends on the position of the section relative to the source. Sections D14, 17, and 22 are exposed in positions some distance from the main stream flow reestablished after drainage. Thus they are unaffected by the increasing current activity during drainage, and the sequence seen is simply from laminated silts to clay. Section 13 is exposed close to the inflow of minor stream 1 and the other sections are exposed close to Hazard Creek. Thus they are affected strongly by current activity during drainage. It might be expected that these sections should show effects of an increasing current, followed by a decrease as the stream abandons the area as drainage progresses. This is to some extent seen, but the situation is complicated by the fact that these sediments at the top of the sections could have been deposited in any of the drainage events, or be the product of more than one drainage. Also the effects of erosion are difficult to gauge. The clay draped over some of the sections is deposited during drainage, in the final stages, where sediment is washed down as the lake level drops. In the areas unaffected by stream action the effect of drainage is analogous to a very slow current, that washes fine material from the sediment, and redeposits it as drainage becomes

complete. This was observed to occur at the lake margins during drainage.

Sections D7, 10 and 12 show thicker and more complex sequences at the top of the section. These can be explained by the hypothesis that these locations were exposed to a greater variation in the amount of stream flow. In the case of section D10 it would seem that the section was at some time in the path of an active stream channel, later abandoned. This results in a grading upward into gravel, followed by a return to sand facies as the flow declined. The characteristics of the other sections can be explained in a similar fashion. Sections 1/2, 5/6 and 11 show considerable complexity, and do not possess the laminated silt facies. These sections are exposed very close to the inflow of the stream at maximum lake level, being covered by one to two metres of water at the most. It is suggested that these are typical glaciolacustrine deposits, showing frequent alternation between sand facies, and evidence of relatively high current flow, being the only sections containing facies B1 and B3.

One feature that requires some explanation is the lack of evidence for any annual cycle in the laminated silt facies. It is possible that sampling on a finer scale than that done in this study, say every two centimetres or finer, may have revealed grain size trends with depth. Certainly the cases where several samples were taken at different depths such as section D12 reveal that the sediments are

quite variable. The absence of varves as such is easily explained. The "winter" section of the varve is deposited from suspension in times of very low inflow. In this case virtually no inflow takes place for seven months of the year. The amount of sediment that can be deposited in this time can be calculated. The average suspended sediment content of the lake water is 0.04 g/l. Considering a water column with a height of 10m and an area of 100 cm². then 4g of sediment is contained within it. If this is entirely deposited during the winter, and assuming a density of 1.5 g/cm³ (J. Shaw, University of Alberta, personal communication), this results in a bed less than 0.2 mm thick, unrecogniseable in the sedimentary record at this level of sampling. However, at lake depths of 100 m, this would produce 2 cm of sediment. No sediment was preserved in the deeper portions of the lake, and thus this was not observed. Thus the absence of stratification on the lake, and the shallow depths, mean that insufficient sediment is held in suspension to allow the deposition of recognisable varves.

Several predictions can be made from this sedimentary model that can be used as a test of the model. Mean grain size can in this case be interpreted as a measure of the ability of the depositing current to carry sediment, and thus the velocity of the current. In this case the main control on current velocity is distance from the source as the slope of the lake bottom is fairly uniform over the

region of sampling, and thus proximal deposits should have a larger mean grain size than distal deposits. Similarly the graphic standard deviation can be interpreted as a measure of the variability of the current depositing the sediment, and in this case increasing distance from the source should have a smoothing effect on this variability. Thus sorting would be expected to increase with distance from source.

Using these measures it can be predicted from the model that a plot of mean grain size against sorting should be a straight line if mean grain size is measured in phi units, with the most proximal deposits at the coarse and poorly sorted end of the line. Figure 16 shows this, with facies B3 plotting at the proximal end of the line, and facies C at the distal. Table 8 is the mean values for these parameters for each facies state analysed, and this shows that the position and current action ascribed to each facies in the model is correct, the order of proximity being B2-B3-B4-C. A regression was performed on the data (from facies C only), and this gave a value of 0.95 for the correlation coefficient, 0.32 for the slope, and 0.21 for the intercept on the graphic standard deviation axis. The regression was significant at alpha = 0.01.

If the laminated silt unit is considered, the position of source during the deposition of this unit is considered to be constant, at the maximum lake level. Thus the distance of the source from the section can be estimated (Appendix 11). If mean grain size or sorting is plotted against this,

Table 8: Mean grain size and sorting of facies

Given below are the means for each of four facies of Folk-Ward parameters mean grain size (Mg) and graphic standard deviation (D). Both are measured in phi units.

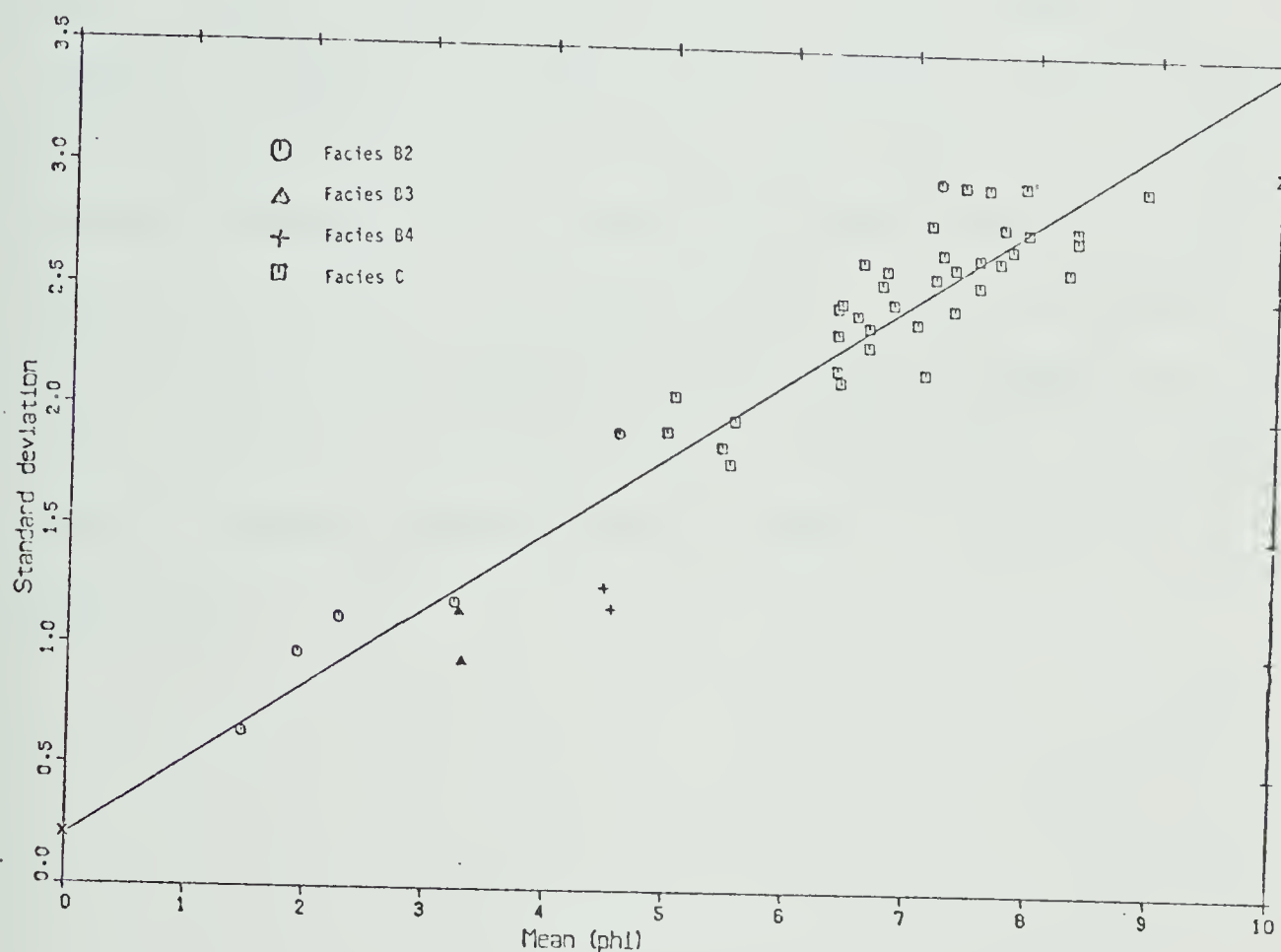
FACIES	Mg	D
B2	3.44	1.47
B3	3.28	1.04
B4	4.50	1.21
C	6.40	2.51

Figure 16: Graph of mean grain size /standard deviation

This graph plots graphic Folk-Ward parameters against each other. The correlation coefficient for this relationship is 0.95, and the regression equation obtained for facies C samples is

$$\text{Sorting} = 0.325 \text{ (Mean)} + 0.215.$$

Both are measured in phi units.



a straight line should result (Figures 17, 18). A regression analysis was performed on both these relationships, using data from facies C only. There is a correlation coefficient of 0.67 between mean grain size and distance from source, and an F test shows the regression to be significant at alpha = 0.01. The correlation coefficient between sorting and distance from source is 0.45, and the regression is significant at alpha = 0.01 also. In both cases the residuals showed no trend. On the graphs it can be seen that the points which do not fit with this model are either of another facies, or at a great distance from the source (sections D18,19). An examination of Figure 5 shows that D18, and D19 are probably dominated by sedimentation from minor stream 2, which explains the poor fit. Thus these results support the sedimentary model of deposition from underflow.

Figure 17: Graph of mean grain size / proximity

The correlation coefficient for this relationship is 0.67.

The equation of the regression line drawn on the graph is

$$\text{Distance} = 274.5 \text{ (Mean)} - 1014.$$

Data from facies C alone were used for this analysis.

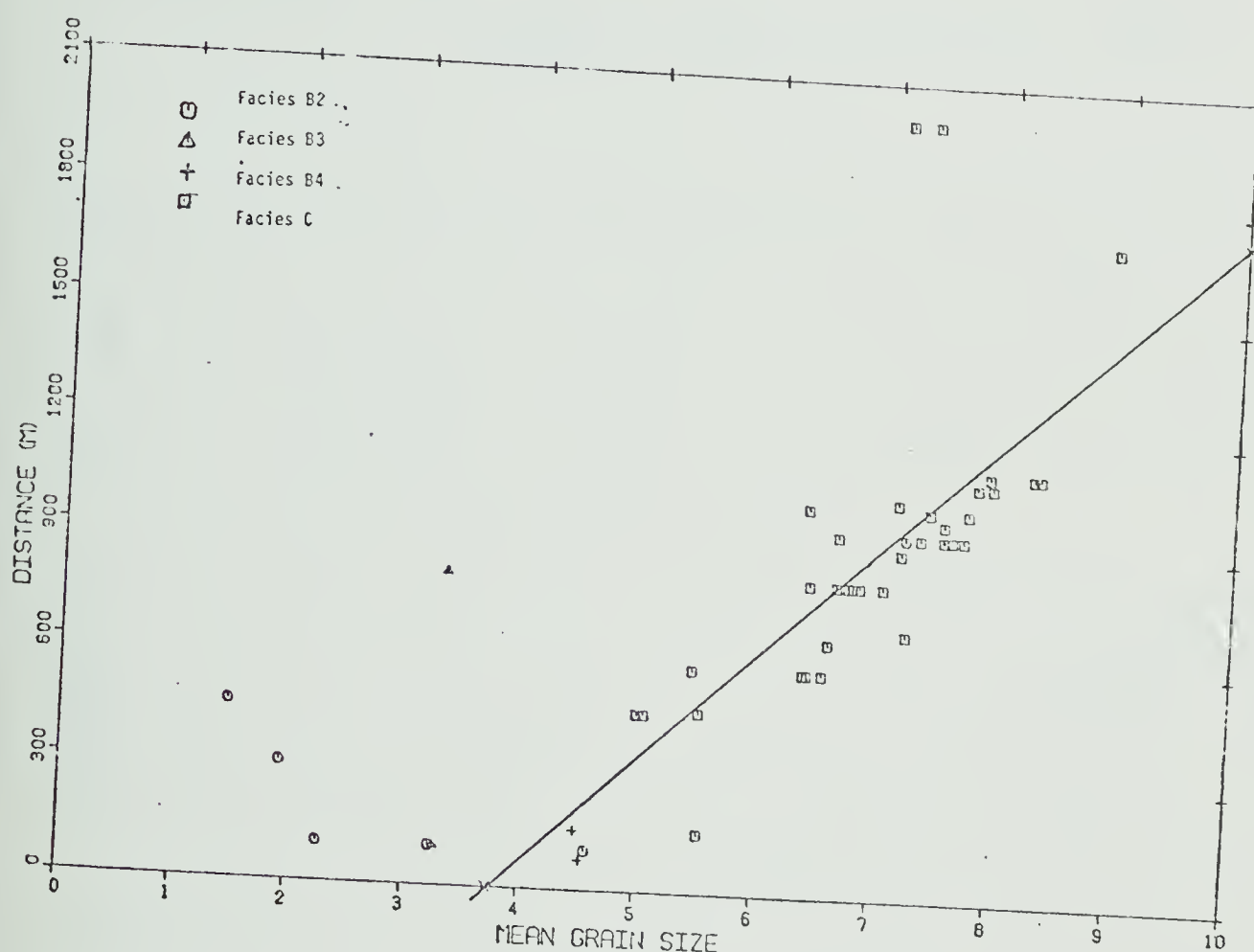
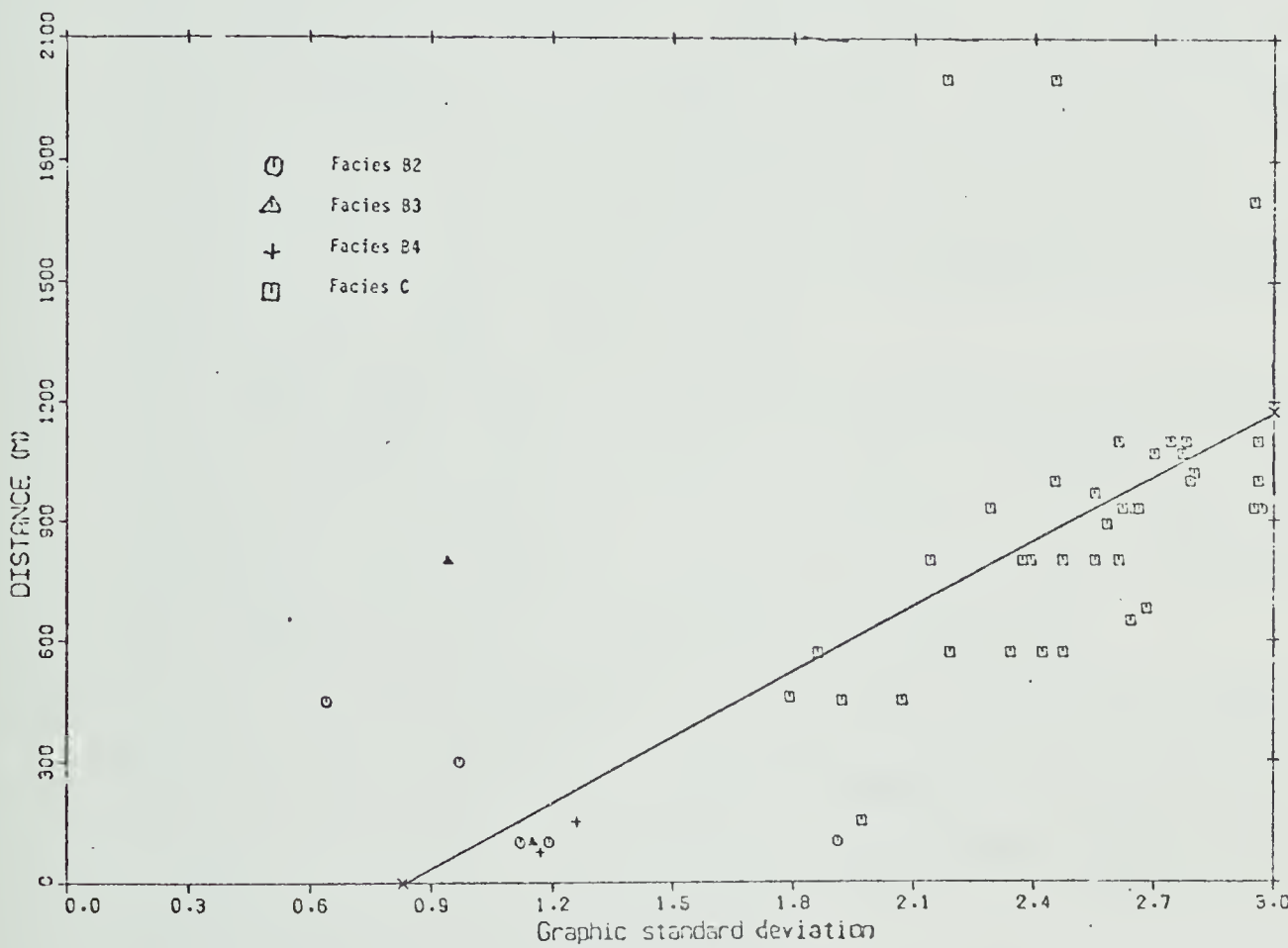


Figure 18: Graph of standard deviation /proximity

This graph plots graphic standard deviation against distance from source. Standard deviation is measured in phi units. The correlation coefficient for this relationship is 0.45, and the equation of the regression line drawn for the data from facies C is

$$\text{distance} = 542.3 \text{ (sorting)} - 452.4$$



VI. Conclusions and suggestions for further work

A summary of conclusions made in this study is given below:

1. The Nye model as adapted by Clarke is supported by the results obtained in the 1979 field season.
2. The 1978 and 1979 floods were very similar in discharge characteristics, indicating that the model is applicable through time i.e. the physical parameters of the flood do not change from year to year.
3. The value of the Manning roughness coefficient n' found by Clarke of $n'=0.009$ is supported by the results of 1979, although it is suggested that incomplete tunnel closure results in a misleading value for this coefficient due to its effect on the potential gradient used as an input to the model.
4. The main constraint on predicting dates of drainage using a model based on the floatation hypothesis is an adequate knowledge of the water balance of the lake, and the mass balance of the confining glacier.
5. Tunnel drainage appears to be established up to 20 days before the jokulhlaup becomes apparent. Thus the early stages of tunnel drainage are relatively important in prediction of drainage dates.
6. The period of stability dominates sedimentation in the lake, and the cyclic drainage produces no characteristic sediments.
7. The dominant process of sedimentation in the lake is that of deposition from turbid underflow.

8. The lake is unstratified with regard to temperature, and the volume of sediment preserved in the water column is insufficient to allow deposition of classical varves.

Suggestions for further work

1. A close monitoring of the inflow streams, and the overflow if operating could lead to a better prediction of drainage dates, and a description of the early stages of tunnel drainage.
2. It seems possible that the closure of the tunnel after drainage could be modelled, and the hypothesis of partial closure tested. This could result in the calibration and general application of the Nye model.
3. A more detailed sampling program could lead to the identification of the effects of the annual cycle in discharge on the lake sediments.
4. Use of a coring device whilst the lake is full could enable the effects of the drainage of the lake on the sediments to be investigated.

VII. References

- ALLEN J.R.L. 1970a. Studies in fluviatile sedimentation: a comparison of fining upwards cyclothsems with special reference to coarse member composition and interpretation. *Journal of Sedimentary Petrology*, 40, pp.298-323.
- AGTERBERG F.P. and BANERJEE I. 1969. Stochastic model for the deposition of varves in glacial Lake Barlow-Objibway, Ontario, Canada. *Canadian Journal of Earth Sciences*, 6, pp.625-652.
- ASHLEY G.M. 1975. Rhythmic sedimentation in glacial lake Hitchcock, Massachusetts-Conneticut. in *Glaciofluvial and Glaciolacustrine Sedimentation*. A.V. Jopling and B.C. MacDonald (eds.). Society of Economic Paleontologists and Mineralogists, Special Publication, 23, pp.304-319.
- ANTEVS E. 1931. Late-glacial clay chronology of North America. *Annual Report, Smithsonian Institute Publication* 3142, pp.313-324.
- BATES C.C. 1953. Rational theory of delta formation. *American Association of Petroleum Geologists Bulletin*, 37, pp.2119-2162.
- BELL H.S. 1942. Density currents as an agent for transporting sediments. *Journal of Geology*, 50, pp.512-547.
- BJORNSSON H. 1975. Explanation of jokulhlaups from Grimsvotn, Vatnajokull, Iceland. *Jokull*, 24, pp.1-26.
- BRETZ J.H. 1923. Glacial drainage on the Columbia plateau. *Bulletin of the Geological Society of America*, 34, pp. 373-608.
- BRETZ J.H. 1969. The Lake Missoula floods and the channelled scablands. *Journal of Geology*, 77, pp. 505-543.
- BROOK D. 1971. Scree benches around ice dammed lakes in South Georgia. *British Antarctic Survey Bulletin*, 26, pp.31-35
- BIRKELAND P. 1964. Pleistocene glaciation of the North Sierra Nevada, north of Lake Tahoe, California. *Journal of Geology*, 72, pp.810-825.

- CHURCH M.A., and GILBERT R. 1975. Proglacial fluvial and lacustrine environments. in Glaciofluvial and Glaciolacustrine Sedimentation. A.V. Jopling and B.C. MacDonald (eds.). Society of Economic Paleontologists and Mineralogists, Special Publication, 23, pp.22-100.
- CLAGUE J.J. 1974. Sedimentology and paleohydrology of late Wisconsinan outwash in the Rocky Mountain Trench, S.E. B.C.. in Glaciofluvial and Glaciolacustrine Sedimentation. A.V. Jopling and B.C. MacDonald (eds.). Society of Economic Paleontologists and Mineralogists, Special Publication, 23, pp.223-236.
- CLAGUE J.J. and MATHEWS W.H. 1973. The magnitude of jokulhlaups. Journal of Glaciology., 12, pp.501-504.
- CLARKE G.K.C. 1980a. An estimate of the magnitude of glacier outburst floods from Lake Donjek, Yukon Territory, Canada. Unpublished report to the Department of Indian and Northern Affairs, 90p.
- CLARKE G.K.C. 1980b. Glacier outburst floods from "Hazard Lake", Yukon Territory, and the problem of flood magnitude prediction. In press.
- COLLINS S.G. and CLARKE G.K.C. 1978. History and bathymetry of a surge dammed lake. Arctic, 30, pp.217-224
- DE GEER G. 1912. A geochronology of the last 12,000 years. Compte Rendu, 11th International Geological Conference (Stockholm, 1910), p241-258.
- EMBLETON C. and KING C.A.M. 1975. Glacial Geomorphology. Publ. Edward Arnold, 573p.
- FABER T. 1972. Hydrological study of the Rusty Glacier. Icefield Ranges Research Project; Scientific results, 3, pp.83-92. Arctic Institute of North America.
- FOLK R.L. 1959. Petrology of the Sedimentary Rocks. Austin, Hemphill. 153 p..
- FOLK R.L. and WARD W.C. 1957. Brazos River Bar: A study in the significance of grain size parameters. Journal of Sedimentary Petrology, 27, pp.3-26
- GILBERT R. 1971. Observations on ice dammed Summit Lake, B.C. Journal of Glaciology, 10, pp.316-356.
- GILBERT R. 1973. Drainings of ice dammed Summit Lake, B.C. Scientific Series no. 20, Inland Water Directorate, Water Resources Board. Environment Canada, 17p.

GILBERT R. 1975b. Sedimentation in Lillooet Lake, British Columbia. Canadian Journal of Earth Sciences, 12, pp.1697-1717

GLEN J.W. 1954. The stability of ice dammed lakes and other water filled holes in glaciers. Journal of Glaciology., 2, pp.316-318.

GUSTAVSON T.C. 1975. Sedimentation and physical limnology in proglacial Malaspina Lake, southeastern Alaska. in Glaciofluvial and Glaciolacustrine Sedimentation. A.V. Jopling and B.C. MacDonald (eds.). Society of Economic Paleontologists and Mineralogists, Special Publication, 23, pp.249-263.

GUSTAVSON T.C., BOOTHROYD J.C., and ASHLEY G.M. 1975. Depositional sequences in glaciolacustrine deltas. in Glaciofluvial and Glaciolacustrine Sedimentation. A.V. Jopling and B.C. MacDonald (eds.). Society of Economic Paleontologists and Mineralogists, Special Publication, 23, pp.264-280

HIGGINS A.H. 1970. On some ice dammed lakes in the Frederikshab district, S.W. Greenland. Denmark, Komissionen fur Videnskbelige Undersogelser, Gronland; Meddeleser om Gronland, 19, pp 378-397.

HOWARTH P. 1968. A supraglacial extension of an ice dammed lake, Tursbergdalsbreen, Norway. Journal of Glaciology., 7, pp.414-419.

JOPLING A.V. and WALKER R.G. 1968. Morphology and origin of ripple drift cross lamination with examples from the Pleistocene of Massachusetts. Journal of Sedimentary Petrology, 38, pp.971-984.

KERR F.A. 1934. The ice dam and floods of the Talsekwe, B.C. Geographical Review, 24, pp.643-645.

KRUMBEIN W.C. and PETTIJOHN F.J. 1938. Manual of sedimentary petrography. Publisher Appleton Century, New York, 549p.

KUENEN Ph.H. 1951. Mechanics of varve formation and the action of turbidity currents. Geologiska Foreningen, Stockholm; Forandlinger, 73, pp.91-127.

Liestøl O. 1955. Glacier dammed lakes in Norway. Norsk Geografisk Tidsskrift, 15, pp.122-149.

LINDSAY J.F. 1966. Observations on the level of a self draining lake on the Casement Glacier, Alaska. Journal of Glaciology, 6, pp.443-445.

- MAAG H.U. 1963. Ice dammed lakes on Axel Heiberg Island. Axel Heiberg Island Research Reports, preliminary report 1961-2, pp.151-160.
- MARCUS M.G. 1960. Periodic drainage of glacier dammed Tulsequah Lake, B.C. Geographical Review, 50, pp.89-106.
- MARCUS M.G. 1968. Effects of glacier dammed lakes in the Chugach and Kenai mountains in the Great Alaska Earthquake of 1964. Hydrology publication 1603, National Academy of Science, pp.329-347.
- MATHEWS W.H. 1965. Two self dumping ice dammed lakes in B.C. Geographical Review, 55, pp.46-52.
- MATHEWS W.H. 1973. The record of two jokulhlaup. in Symposium on the Hydrology of Glaciers, Sept., 1969, Glaciological Society, England.
- NICHOLS R.L. and MILLER M.M. 1952. The Moreno Glacier, Lago Argentino, Patagonia; Advancing glaciers and nearly simultaneously retreating glaciers. Journal of Glaciology., 2, pp.43-51
- NYE J.F. 1951. The flow of glaciers and ice sheets as a problem in plasticity. Proceedings of the Royal Society, A207, pp.554-572.
- NYE J.F. 1976. Water flow in glaciers; jokulhlaups, tunnels, and veins. Journal of Glaciology, 17, pp.181-207.
- ØESTREM G. and STANLEY A.D. 1969. Glacier mass balance measurements; a manual for field and office work. Joint publication of Canada; Dept. of Energy, Mines and Resources and Norwegian Water Resources and Electricity board. 87p.
- PARDEE J.T. 1947. Unusual currents in glacial Lake Missoula, Montana. Bulletin of the Geological Society of America, 53 , pp.1569-1599.
- RABOT C. 1905. Glacial reservoirs and their outbursts. Geographical Journal, 25, pp.534-548.
- RIST S. 1974. Jokulhlaupaannall 1971, 1972 og 1973. Jokull, 23, pp.55-60.
- ROTHLISBERGER H. 1972. Water pressure in intra and subglacial channels. Journal of Glaciology, 11, pp.177-203.
- SHARP R.P. 1947. The Wolf Creek glaciers, St. Elias Range. Geographical Review, 37, pp.26-52.

- SHAW J. 1975. Sedimentary successions in ice marginal lakes. in Glaciofluvial and Glaciolacustrine Sedimentation. A.V. Jopling and B.C. MacDonald (eds.). Society of Economic Paleontologists and Mineralogists, Special Publication, 23, pp.281-303.
- SHAW J., GILBERT R., ARCHER J.J.J., 1978. Proglacial lacustrine sedimentation during winter. Arctic and Alpine Research, 10, pp.689-699.
- SHREVE R.L. 1972. Movement of water in glaciers. Journal of Glaciology., 11, pp.205-214.
- SMITH N.D. 1978. Sedimentation processes and patterns in a glacier fed lake with low sediment input. Canadian Journal of Earth Sciences, 15, pp.741-756.
- STANLEY A.D. 1969. Observations of the surge of the Steele Glacier. Canadian Journal of Earth Sciences, 6, pp.819-830.
- STENBORG R. 1969. Studies of the internal drainage of glaciers. Geografiska Annaler Series A, 51, pp.13-41.
- STONE K.H. 1963a. Alaskan ice dammed lakes. Annals of the Association of American Geographers, 53, pp.332-349.
- STONE K.H. 1963b. The annual emptying of Lake George, Alaska. Arctic, 16, pp.26-40.
- STONE P. 1975. Observations on an ice dammed lake, Hindle Glacier, South Georgia. British Antarctic Survey Bulletin, 40, pp.69-73.
- STRØM K.M. 1938. The catastrophic emptying of a glacier dammed lake in Norway, 1937. Geologie der Meere und Binnengewässer, 2, pp.443-444.
- STURM M. 1979. Origin and composition of clastic varves. in Moraines and Varves, ed Ch. Schlüter, A.A. Balkema, Rotterdam. pp.281-285.
- SWAN D., CLAGUE J.J., and LUTERNAUER J. L., 1978. Grain size studies I; evaluation of the Folk-Ward graphic measures. Journal of Sedimentary Petrology, 48, pp.863-875.
- THORARINSSON S. 1939. The ice dammed lakes of Iceland with reference to their value as indicators of glacial oscillations. Geografiska Annaler, 21, pp.216-242.
- WANKIEWICZ P.M. 1979. Sedimentation in Sunwapta Lake, Jasper National Park, Alberta. Unpublished M.Sc thesis, Department of Geography, University of Alberta.

- WOOD W.A. 1936. The Wood Yukon expedition; an experiment in photographic mapping. Geographical Review, 26, pp.228-46.
- WOOD W.A. 1972. Steele Glacier, 1935-1968. Icefield Ranges Research Project; Scientific results, 3, pp.1-8. Arctic Institute of North America.
- WHALLEY W.B. 1971. Observations of the drainage of an ice dammed lake, Strupvatnet, Trøns, Norway. Norsk Geografisk Tidsskrift, 25, pp.165-174

VIII. Appendix 1

A. Section descriptions

These descriptions are field notes. Unless stated beds are flat lying, and contacts sharp. For location of the sections see Figure 5. Sections are described from the top downwards, and are measured in metres. The nomenclature of Jopling and Walker (1969) has been applied to ripple drift cross lamination.

Section D1

0-0.21

Medium grained poorly sorted sand underlying thin veneer of clay on surface. Roughly bedded, thickness=1cm.

Sample D1A.

0.21-0.26

Sharp contact over interbedded very coarse and medium sand.

0.26-0.35

Fining down bed of coarse sand to silt, laminated.

0.35-0.51

Poorly bedded medium grained sand, fining in lowest 3cm to fine sand.

0.51-0.68

Poorly sorted gravel, average grain size 1cm diameter, poorly bedded. Sample D1B.

0.68-0.91

Gradational contact into coarse sand with pebbles,

massive.

0.91-0.94

Massive fine grained sand/silt, fines downwards. Sample D1C.

0.95-

Coarse grained flat bedded sand with pebbles, poorly sorted.

Section D2

This section lies below D1, lying 2m north. It is suggested that the first three units described correlate with the last three units of D1.

0-0.09

Massive coarse sand with pebbles up to 1 cm diameter.

0.09-0.16

Gradational contact into unit fining downward from fine sand to silt, laminated. Sample D2A.

0.16-0.21

Very coarse sand with pebbles, poorly sorted.

0.21-0.23

Medium grained well sorted sand.

0.23-0.29

Undulating rippled contact leads into fine, well sorted sands. Cross laminated (?).

0.29-0.33

Type B cross laminated medium grained sand.

0.33-0.39

As above but with occasional draping of silt/clay over

laminae.

0.39-0.40

Massive coarse sand

0.40-?

Resistant, partly consolidated silt, with roots embedded in surface.

Sample 2B is a channel sample from 0.23-0.39m.

Section D3

0.00-0.05

Type A cross laminated medium grained sands, fining downward.

0.05-0.09

Finely laminated silt.

0.09-0.36

Roughly bedded medium and coarse sands. Sample D3A.

0.36-?

Gravel, pebble diameters ranging from 0.5-10cm.

Section D4

0.00-0.06

Coarse sand with pebbles underlying rippled upper surface.

0.06-0.13

Thinly bedded fine sands (thickness=1cm).

0.13 0.15

Medium grained sand, poorly bedded.

0.15-0.19

Rippled contact overlies cross laminated (?) fine sand.

0.19-0.39

Medium grained sand grades downward into laminated silts. Sample D4A from base of unit.

0.39-?

Gravel

Section D5

0.00-0.01

Fine silt/clay draping rippled surface .

0.01-0.04

Fining upward sequence from very coarse to medium sand.

0.04-0.25

Sequence of graded beds, 0.5-5 cm in thickness, as a whole fining downwards from predominantly medium sand to fine sand.

0.25-0.45

Gradational contact leads into laminated silts. Sample D5A is a channel sample through the unit.

0.45-0.55

sequence of graded beds grading from coarse to fine sand.

0.55-0.58

Poorly bedded silts.

Section D6

This section lies three metres away from section D5, and the first unit of D6 lies directly below the last unit of D5.

0.00-0.30

Medium coarse sand, poorly bedded. Sample 6B is a channel sample through this unit.

0.30-0.41

Laminated silts interbedded with fine sand. Sample D6A is a channel sample through the unit.

0.41-0.55

Cross laminated fine sand/silt.

0.55-0.59

Medium to coarse grained sand, massive.

Section D7

0.00-0.03

Finely laminated clay draped over rippled surface.

0.03-0.15

Coarse sand poorly bedded with a concentration of pebbles towards the base.

0.15-0.22

Sequence of graded beds, thickness 1.5 cm, grade from coarse to medium sand.

0.22-0.23

Medium grained sand, cross bedded (?).

0.23-0.27

Coarse, massive sand.

0.27-0.31

Graded beds, coarse to medium sand, thickness 2cm.

0.31-0.51

Interbedded fine/medium sands, fining downwards.

0.51-0.81

Laminated silt/clay. Sample D7A from 0.53-0.55; sample D7B from 0.60-0.65; sample D7c from 0.66-0.72; sample D7D from 0.77-0.81.

0.81-?

Coarse gravel with boulders.

Section D8

0.00-0.02

Massive fine sand

0.02-0.52

Coarse sand/gravel, structureless, coarsening towards base.

0.52-0.84

Laminated silts. Sample D8A is a channel sample through the unit.

0.84-?

Gravel.

Section D9

0.00-0.19

Roughly bedded fine to medium grained sand. Sample D9A.

0.19-0.83

Laminated silts. Sample D9B from 0.20-0.28; sample D9C from 0.28-0.40; sample D9D from 0.68-0.73; sample D9E from 0.80-0.83.

0.83-?

Gravel.

Section D10

0.00-0.20

Underlying thin veneer of clay, coarse gravel, with pebbles up to 5cm diameter.

0.20-0.23

Flat bedded coarse sand.

0.23-0.25

Graded beds, thickness=1cm, grading from coarse to fine sand.

0.25-0.26

Fne sand, structureless.

0.26-0.29

Medium sand, massive.

0.29-0.33

Graded beds (sand-silt), sample D10A.

0.33-0.50

Laminated silts, sample D10B from base.

0.50-?

Gravel/coarse sand.

Section D11

0.00-0.10

Finely bedded fine sand.

0.10-0.35

Massive coarse sand.

0.35-0.40

Cross bedded (tabular) medium grained sand.

0.40-0.60

Interbedded medium and fine sands, type B cross laminated, draping of clay over some laminae.

0.60-0.72

Very fine sand/silt, horizontally bedded, shows some grading. Sample D11A.

0.72-0.79

Massive sand, fining downwards from medium to fine.

0.79-0.81

Coarse sand, structureless.

0.81-?

Gravel.

Section D12

0.00-0.08

Laminated clay.

0.08-0.09

Fine sand.

0.09-0.12

Laminated clay/silt.

0.12-0.13

Fine sand.

0.13-0.17

Laminated silts.

0.17-0.28

Type A cross laminated fine sand. Sample D12A.

0.28-0.84

Gradational contact into laminated silts. Sample D12B from 0.30-0.35; sample D12C from 0.40-0.45; sample D12D from 0.50-0.55; sample D12E from 0.60-0.65; sample D12F from 0.70-0.75; sample D12G from base of unit.

0.84-?

Gravel.

Section D13

0.00-0.01

Structureless fine sand.

0.01-0.27

Laminated silts. Sample D13A is a channel sample through the unit.

0.27-?

Coarse gravel.

Section D14

0.00-0.01

Clay, laminated.

0.01-0.46

Laminated silt, sample D14A is a channel sample through the unit.

0.46-?

Gravel.

Section D 15

0.00-0.005

Clay, massive?

0.005-0.18

Fine sand, bedded, (thickness=3cm), contains leaves, and twigs.

0.18-0.58

Laminated silts. Sample D15A is a channel sample through the unit.

0.58-?

Gravel

Section D16

0.00-0.01

Fine sand, cross laminated.

0.01-0.03

Massive clay.

0.03-0.06

Flat bedded medium sand.

0.06-0.11

Fining down sequence from fine sand to silt.

0.11-0.90

Laminated silts. Sample D16A from 0.11-0.15; sample D16B from 0.45-0.50; sample D16C from 0.85 to 0.90.

0.90-?

Gravel.

Section D17

0.00-0.03

Massive clay.

0.03-0.55

Laminated silts, sample D17A is a channel sample through unit.

0.55-?

Gravel.

Section D18

0.00-0.0025

Laminated clay.

0.0025-0.03

medium sand.

0.03-0.06

Fining up bed from coarse to medium sand.

0.06-0.20

Laminated silts. Sample D18A is a channel sample through the unit.

0.20-?

Gravels.

Section D19

0.00-0.40

Laminated silts. Sample D19A is a channel sample.

0.40-?

Partly consolidated gravel.

Section D20

0.00-0.005

Massive clay.

0.005-0.05

Flat bedded fine sand.

0.05-0.70

Laminated silts, base not seen but estimated thickness 1.30m. Sample D20A is a channel sample through entire section; sample D20B is from 0.10-0.15; sample D20C 0.20-0.25; sample D20D from 0.40-0.45; sample D20E from 0.65-0.70.

Section D21

0.00-0.10

Massive clay.

0.10-0.11

Fine sand.

0.11-1.21

Laminated silts. Sample D21A is a channel sample. Base of unit not exposed.

Section D21

0.00-0.01

Structureless clay.

0.01-0.41

Laminated silts. Sample D22A is a channel sample through the unit. Base of unit not exposed.

IX. Appendix 2

Raw data, grain size analysis

This appendix tabulates the results of grain size analysis performed on the samples collected. Under the heading "hydrometer readings" are six columns. These are:

1. EL. TIME; time at which the reading was taken, given in minutes since settling commenced.
2. HYDR.; Hydrometer reading at this point.
3. CORRN.; Correction factor (the hydrometer reading in a settling cylinder containing only distilled water and dispersant).
4. T DEG C; the temperature of the correction cylinder
5. PHI; The diameter of the particle settling at this time, in phi units.
6. PCT. FNR. The percentage of the sample finer than this phi value.

The sieve results are given in a similar fashion. The meaning of the column headings in this case is:

1. DIAM. MM.; the mesh size of the sieve in mm.
2. WT. GMS.; the weight of sample retained in the sieve
3. PHI; the particle diameter in phi units.
4. PER CENT.; The percentage of the total sample retained in the sieve
5. PCT. FNR.; as above.

D1A

HYDROMETER RESULTS

NONE

SIEVE RESULTS

DIAM. MM.	WT. GMS.	PHI	PER CENT	PCT. FNR.
4.000	0.0	-2.00	0.0	100.00
2.000	1.59	-1.00	1.56	98.44
1.000	3.13	-0.0	3.07	95.38
0.710	2.51	0.49	2.46	92.92
0.500	3.71	1.00	3.63	89.29
0.300	12.93	1.74	12.66	76.62
0.250	10.45	2.00	10.24	66.39
0.180	25.27	2.47	24.75	41.64
0.125	21.29	3.00	20.85	20.78
0.090	11.31	3.47	11.08	9.71
0.063	4.51	3.99	4.42	5.29

D1C

HYDROMETER RESULTS

EL.	TIME	HYDR.	CORRN	T DEG C	PHI	PCT. FNR.
	15.0	11.5	4.0	24.0	6.31	15.00
	49.0	9.4	4.0	24.0	7.15	10.80
	96.0	8.5	4.0	24.0	7.63	9.00
	182.0	7.8	3.5	24.0	8.08	8.60
	320.0	8.0	4.0	24.0	8.49	8.00
	1400.0	7.8	4.0	24.0	9.55	7.60

SIEVE RESULTS

DIAM. MM.	WT. GMS.	PHI	PER CENT	PCT. FNR.
2.000	0.0	-1.00	0.0	100.00
1.000	0.19	-0.0	0.38	99.62
0.700	0.13	0.51	0.26	99.36
0.500	0.24	1.00	0.48	98.88
0.354	0.35	1.50	0.70	98.18
0.250	0.65	2.00	1.30	96.88
0.177	0.87	2.50	1.74	95.14
0.125	2.65	3.00	5.30	89.84
0.088	4.74	3.51	9.48	80.36
0.063	5.05	3.99	10.10	70.26

D2A

HYDROMETER RESULTS

EL.	TIME	HYDR.	CORRN	T DEG C	PHI	PCT. FNR.
	0.5	26.5	5.5	24.0	4.00	19.94
	1.0	20.0	5.5	24.0	4.44	13.77
	2.0	15.5	5.5	24.0	4.89	9.50
	4.0	11.2	5.5	24.0	5.36	5.41
	7.0	9.8	5.5	24.0	5.75	4.08

SIEVE RESULTS

DIAM. MM.	WT. GMS.	PHI	PER CENT	PCT. FNR.
4.000	0.0	-2.00	0.0	100.00
2.000	1.07	-1.00	1.02	98.98
1.000	1.38	-0.0	1.31	97.67
0.700	1.03	0.51	0.98	96.70
0.500	1.46	1.00	1.39	95.31
0.300	3.88	1.74	3.68	91.62
0.250	3.42	2.00	3.25	88.38
0.180	12.30	2.47	11.68	76.70
0.125	20.02	3.00	19.01	57.68
0.090	20.27	3.47	19.25	38.43
0.063	12.61	3.99	11.98	26.46

D2B

HYDROMETER RESULTS

EL.	TIME	HYDR.	CORRN	T DEG C	PHI	PCT. FNR.
	0.5	25.5	5.5	24.0	3.99	20.07
	1.0	19.0	5.5	24.0	4.42	13.54
	2.0	14.0	5.5	24.0	4.88	8.53
	4.0	11.0	5.5	24.0	5.36	5.52
	8.0	9.5	5.5	24.0	5.84	4.01

SIEVE RESULTS

DIAM. MM.	WT. GMS.	PHI	PER CENT	PCT. FNR.
2.000	0.0	-1.00	0.0	100.00
1.000	0.02	-0.0	0.02	99.98
0.700	0.47	0.51	0.47	99.51
0.500	0.76	1.00	0.76	98.75
0.300	3.24	1.74	3.25	95.50
0.180	18.49	2.47	18.55	76.94
0.063	49.45	3.99	49.61	27.33

D3A

HYDROMETER RESULTS

NONE

SIEVE RESULTS

DIAM. MM.	WT. GMS.	PHI	PER CENT	PCT. FNR.
4.000	0.0	-2.00	0.0	100.00
2.000	1.23	-1.00	1.14	98.86
1.000	2.79	-0.0	2.60	96.26
0.710	3.09	0.49	2.87	93.39
0.500	5.82	1.00	5.41	87.97
0.300	30.53	1.74	28.40	59.57
0.250	17.70	2.00	16.47	43.11
0.180	23.24	2.47	21.62	21.49
0.125	12.06	3.00	11.22	10.27
0.090	5.19	3.47	4.83	5.44
0.063	2.08	3.99	1.93	3.51

D4A

HYDROMETER RESULTS

EL.	TIME	HYDR.	CORRN	T DEG C	PHI	PCT. FNR.
	0.5	58.5	3.5	24.0	4.41	67.52
	1.0	52.5	3.5	24.0	4.81	60.15
	2.0	45.0	3.5	24.0	5.21	50.95
	4.0	35.0	3.5	24.0	5.58	38.67
	8.0	26.0	3.5	24.0	5.99	27.62
	15.0	20.0	3.5	24.0	6.39	20.26
	30.0	17.0	3.5	24.0	6.86	16.57

SIEVE RESULTS

DIAM. MM.	WT. GMS.	PHI	PER CENT	PCT. FNR.
4.000	0.0	-2.00	0.0	100.00
2.000	0.01	-1.00	0.02	99.98
1.000	0.01	-0.0	0.02	99.96
0.700	0.03	0.51	0.06	99.90
0.500	0.03	1.00	0.06	99.84
0.354	0.06	1.50	0.12	99.72
0.250	0.10	2.00	0.20	99.52
0.177	0.10	2.50	0.20	99.32
0.125	0.35	3.00	0.70	98.62
0.088	0.95	3.51	1.90	96.72
0.063	1.59	3.99	3.18	93.54

D5A

HYDROMETER RESULTS

EL.	TIME	HYDR.	CORRN	T DEG C	PHI	PCT. FNR.
	16.0	13.8	4.0	24.0	6.38	19.60
	49.0	10.9	4.0	24.0	7.16	13.80
	98.0	10.1	4.0	24.0	7.66	12.20
	184.0	9.2	4.0	24.0	8.11	10.40
	318.0	8.8	4.0	24.0	8.49	9.60
	1414.0	8.6	4.0	24.0	9.57	9.20
	0.5	37.5	5.5	24.0	4.11	64.00
	1.0	31.5	5.5	24.0	4.55	52.00
	2.0	25.0	5.5	24.0	4.98	39.00
	4.0	19.0	5.5	24.0	5.42	27.00
	8.0	15.5	5.5	24.0	5.89	20.00
	18.0	12.5	5.5	24.0	6.45	14.00
	42.0	10.5	5.5	24.0	7.05	10.00
	157.0	10.0	5.5	24.0	7.99	9.00

SIEVE RESULTS

DIAM. MM.	WT. GMS.	PHI	PER CENT	PCT. FNR.
1.000	0.02	-0.0	0.04	99.96
0.700	0.03	0.51	0.06	99.90
0.500	0.03	1.00	0.06	99.84
0.354	0.05	1.50	0.10	99.74
0.250	0.26	2.00	0.52	99.22
0.177	0.16	2.50	0.32	98.90
0.125	0.81	3.00	1.62	97.28
0.088	2.79	3.51	5.58	91.70

0.063	4.83	3.99	9.66	82.04
-------	------	------	------	-------

D6A

HYDROMETER RESULTS

EL.	TIME	HYDR.	CORRN	T DEG C	PHI	PCT. FNR.
	0.5	36.5	4.0	24.0	4.10	65.00
	1.0	30.5	4.0	24.0	4.54	53.00
	2.0	25.0	4.0	24.0	4.98	42.00
	4.0	19.0	4.0	24.0	5.42	30.00
	8.0	16.0	4.0	24.0	5.90	24.00
	14.0	13.0	4.0	24.0	6.28	18.00
	16.0	11.8	4.0	24.0	6.36	15.60
	50.0	10.1	4.0	24.0	7.17	12.20
	98.0	9.5	4.0	24.0	7.65	11.00
	181.0	9.7	3.0	24.0	8.09	13.40
	318.0	9.1	4.0	24.0	8.50	10.20
	1412.0	8.4	4.0	24.0	9.57	8.80

SIEVE RESULTS

DIAM. MM.	WT. GMS.	PHI	PER CENT	PCT. FNR.
2.000	0.0	-1.00	0.0	100.00
1.000	0.08	-0.0	0.16	99.84
0.700	0.06	0.51	0.12	99.72
0.500	0.07	1.00	0.14	99.58
0.354	0.08	1.50	0.16	99.42
0.250	0.18	2.00	0.36	99.06
0.177	0.43	2.50	0.86	98.20
0.125	1.68	3.00	3.36	94.84
0.088	3.95	3.51	7.90	86.94
0.063	4.95	3.99	9.90	77.04

D6B

HYDROMETER RESULTS

NONE

SIEVE RESULTS

DIAM. MM.	WT. GMS.	PHI	PER CENT	PCT. FNR.
4.000	0.0	-2.00	0.0	100.00
2.000	0.03	-1.00	0.03	99.97
1.000	1.46	-0.0	1.33	98.64
0.710	5.36	0.49	4.90	93.74
0.500	17.11	1.00	15.64	78.10
0.300	50.16	1.74	45.85	32.25
0.250	16.33	2.00	14.93	17.32
0.180	13.81	2.47	12.62	4.70
0.125	4.01	3.00	3.67	1.03
0.090	0.59	3.47	0.54	0.49
0.063	0.08	3.99	0.07	0.42

D7A

HYDROMETER RESULTS

EL.	TIME	HYDR.	CORRN	T DEG C	PHI	PCT. FNR.
	0.5	52.0	4.0	24.0	4.30	96.00
	1.5	50.5	4.0	24.0	5.08	93.00
	2.0	49.5	4.0	24.0	5.27	91.00
	4.0	46.5	4.0	24.0	5.72	85.00
	8.0	42.0	4.0	24.0	6.17	76.00
	15.0	38.0	4.0	24.0	6.57	68.00
	16.0	38.5	3.5	24.0	6.62	70.00
	30.0	34.0	4.5	24.0	7.03	59.00
	49.0	31.2	4.0	24.0	7.35	54.40
	96.0	28.0	4.0	24.0	7.80	48.00
	183.0	25.2	3.0	24.0	8.24	44.40
	319.0	23.0	4.0	24.0	8.62	38.00
	1414.0	18.5	4.0	24.0	9.65	29.00

SIEVE RESULTS

DIAM. MM.	WT. GMS.	PHI	PER CENT	PCT. FNR.
2.000	0.04	-1.00	0.00	100.00
1.000	0.06	-0.0	0.12	99.88
0.500	0.05	1.00	0.10	99.78
0.250	0.06	2.00	0.12	99.66
0.125	0.15	3.00	0.30	99.36
0.063	0.14	3.99	0.28	99.08

D7B

HYDROMETER RESULTS

EL.	TIME	HYDR.	CORRN	T DEG C	PHI	PCT. FNR.
	0.5	53.0	3.5	24.0	4.32	99.00
	1.0	52.0	3.5	24.0	4.80	97.00
	2.0	51.0	3.5	24.0	5.29	95.00
	4.0	48.5	3.5	24.0	5.75	90.00
	8.0	43.0	4.0	24.0	6.18	78.00
	15.0	40.0	4.5	24.0	6.60	71.00
	30.0	36.5	4.5	24.0	7.06	64.00
	53.0	29.5	4.0	24.0	7.39	51.00
	96.0	26.8	4.0	24.0	7.79	45.60
	183.0	22.8	3.0	24.0	8.22	39.60
	318.0	21.0	4.0	24.0	8.60	34.00
	1413.0	17.2	4.0	24.0	9.65	26.40

SIEVE RESULTS

DIAM. MM.	WT. GMS.	PHI	PER CENT	PCT. FNR.
2.000	0.0	-1.00	0.0	100.00
1.000	0.02	-0.0	0.04	99.96
0.500	0.04	1.00	0.08	99.88
0.250	0.10	2.00	0.20	99.68
0.125	0.15	3.00	0.30	99.38
0.063	0.03	3.99	0.06	99.32

D7C

HYDROMETER RESULTS

EL.	TIME	HYDR.	CORRN	T DEG C	PHI	PCT. FNR.
	0.5	51.5	4.0	24.0	4.30	95.00
	1.0	50.5	4.0	24.0	4.79	93.00
	2.0	49.7	4.0	24.0	5.27	91.40
	4.0	47.0	4.0	24.0	5.73	86.00
	8.0	42.0	5.0	24.0	6.17	74.00
	15.0	38.5	5.0	24.0	6.58	67.00
	18.0	35.5	4.0	24.0	6.67	63.00
	51.0	30.2	4.0	24.0	7.37	52.40
	98.0	27.2	4.0	24.0	7.81	46.40
	185.0	25.0	3.0	24.0	8.25	44.00
	329.0	22.7	4.0	24.0	8.64	37.40
	1415.0	18.2	4.0	24.0	9.65	28.40

SIEVE RESULTS

DIAM. MM.	WT. GMS.	PHI	PER CENT	PCT. FNR.
2.000	0.0	-1.00	0.0	100.00
1.000	0.10	-0.0	0.20	99.80
0.500	0.12	1.00	0.24	99.56
0.250	0.16	2.00	0.32	99.24
0.125	0.17	3.00	0.34	98.90
0.063	0.12	3.99	0.24	98.66

D7D

HYDROMETER RESULTS

EL.	TIME	HYDR.	CORRN	T DEG C	PHI	PCT. FNR.
	0.5	49.0	4.0	24.0	4.26	90.00
	1.0	48.0	4.0	24.0	4.75	88.00
	2.0	46.5	4.0	24.0	5.22	85.00
	4.0	43.0	4.0	24.0	5.68	78.00
	8.0	38.5	4.0	24.0	6.12	69.00
	15.0	34.5	4.5	24.0	6.53	60.00
	16.0	34.8	4.0	24.0	6.58	61.60
	38.0	30.0	5.0	24.0	7.15	50.00
	50.0	28.0	4.0	24.0	7.33	48.00
	97.0	25.0	4.0	24.0	7.78	42.00
	183.0	22.1	3.0	24.0	8.22	38.20
	319.0	20.2	4.0	24.0	8.60	32.40
	1414.0	16.2	4.0	24.0	9.64	24.40

SIEVE RESULTS

DIAM. MM.	WT. GMS.	PHI	PER CENT	PCT. FNR.
4.000	0.0	-2.00	0.0	100.00
2.000	0.49	-1.00	0.98	99.02
1.000	0.26	-0.0	0.52	98.50
0.500	0.35	1.00	0.70	97.80
0.250	0.44	2.00	0.88	96.92
0.125	0.46	3.00	0.92	96.00
0.063	0.27	3.99	0.54	95.46

D9A

HYDROMETER RESULTS

EL.	TIME	HYDR.	CORRN	T DEG C	PHI	PCT. FNR.
	0.5	47.0	4.0	24.0	4.23	86.00
	1.0	45.5	4.0	24.0	4.71	83.00
	2.0	42.0	4.0	24.0	5.17	76.00
	4.0	36.5	4.0	24.0	5.60	65.00
	8.0	30.5	4.0	24.0	6.04	53.00
	15.0	26.5	4.5	24.0	6.45	44.00
	28.0	23.5	4.5	24.0	6.87	38.00
	53.0	22.5	4.0	24.0	7.32	37.00
	96.0	20.8	4.0	24.0	7.73	33.60
	182.0	18.2	3.0	24.0	8.18	30.40
	316.0	17.5	4.0	24.0	8.57	27.00
	1412.0	15.0	4.0	24.0	9.62	22.00

SIEVE RESULTS

DIAM. MM.	WT. GMS.	PHI	PER CENT	PCT. FNR.
4.000	0.0	-2.00	0.0	100.00
2.000	0.22	-1.00	0.44	99.56
1.000	0.43	-0.0	0.86	98.70
0.500	0.12	1.00	0.24	98.46
0.250	0.40	2.00	0.80	97.66
0.125	0.64	3.00	1.28	96.38
0.063	0.54	3.99	1.08	95.30

D9B

HYDROMETER RESULTS

EL.	TIME	HYDR.	CORRN	T DEG C	PHI	PCT. FNR.
	0.5	50.0	5.0	24.0	4.28	90.00
	1.0	48.0	5.0	24.0	4.75	86.00
	2.0	46.0	5.0	24.0	5.22	82.00
	4.0	41.5	5.0	24.0	5.66	73.00
	9.0	34.0	5.0	24.0	6.16	58.00
	15.0	29.5	5.0	24.0	6.48	49.00
	50.0	24.0	5.0	24.0	7.29	38.00
	160.0	20.0	5.0	24.0	8.10	30.00

SIEVE RESULTS

DIAM. MM.	WT. GMS.	PHI	PER CENT	PCT. FNR.
2.000	0.0	-1.00	0.0	100.00
1.000	0.02	-0.0	0.04	99.96
0.500	0.06	1.00	0.12	99.84
0.700	0.06	0.51	0.12	99.72
0.354	0.06	1.50	0.12	99.60
0.250	0.07	2.00	0.14	99.46
0.177	0.08	2.50	0.16	99.30
0.125	0.10	3.00	0.20	99.10
0.088	0.09	3.51	0.18	98.92
0.063	0.02	3.99	0.04	98.88

D9C

HYDROMETER RESULTS

EL.	TIME	HYDR.	CORRN	T DEG C	PHI	PCT. FNR.
	0.5	51.5	6.0	24.0	4.30	91.00
	1.0	50.0	6.0	24.0	4.78	88.00
	2.0	47.0	6.0	24.0	5.23	82.00
	4.0	41.2	6.0	24.0	5.66	70.40
	8.0	35.0	6.0	24.0	6.08	58.00
	13.0	31.0	6.0	24.0	6.39	50.00
	29.0	27.0	6.0	24.0	6.93	42.00
	59.0	23.8	5.5	24.0	7.41	36.60
	159.0	20.0	6.0	24.0	8.09	28.00
	270.0	18.8	6.0	24.0	8.46	25.60
	443.0	17.2	6.0	24.0	8.81	22.40
	1413.0	15.2	6.0	24.0	9.63	18.40

SIEVE RESULTS

DIAM. MM.	WT. GMS.	PHI	PER CENT	PCT. FNR.
2.000	0.0	-1.00	0.0	100.00
0.063	0.88	3.99	1.76	98.24

D9D

HYDROMETER RESULTS

EL.	TIME	HYDR.	CORRN	T DEG C	PHI	PCT. FNR.
	0.5	52.0	5.7	24.0	4.30	92.60
	1.0	50.5	5.7	24.0	4.79	89.60
	2.0	48.2	5.7	24.0	5.25	85.00
	6.0	40.2	5.7	24.0	5.94	69.00
	8.0	37.0	5.7	24.0	6.11	62.60
	15.0	32.0	5.7	24.0	6.50	52.60
	50.0	25.5	5.7	24.0	7.31	39.60
	101.0	21.5	5.7	24.0	7.78	31.60
	242.0	20.0	5.7	24.0	8.39	28.60
	371.0	18.2	5.7	24.0	8.69	25.00
	1358.0	16.0	5.7	24.0	9.60	20.60

SIEVE RESULTS

DIAM. MM.	WT. GMS.	PHI	PER CENT	PCT. FNR.
2.000	0.0	-1.00	0.0	100.00
0.063	0.88	3.99	1.76	98.24

D9D

HYDROMETER RESULTS

EL.	TIME	HYDR.	CORRN	T DEG C	PHI	PCT. FNR.
	0.5	52.0	5.5	24.0	4.30	93.00
	1.0	50.5	5.5	24.0	4.79	90.00
	2.0	49.0	5.5	24.0	5.26	87.00
	4.0	44.8	5.5	24.0	5.70	78.60
	8.0	39.5	5.5	24.0	6.14	68.00
	15.0	35.0	6.0	24.0	6.54	58.00
	32.0	30.0	6.0	24.0	7.03	48.00
	54.0	25.7	5.5	24.0	7.36	40.40
	153.0	27.5	5.5	24.0	8.13	44.00
	267.0	20.5	6.0	24.0	8.47	29.00
	439.0	19.5	6.0	24.0	8.82	27.00
	1412.0	17.0	6.0	24.0	9.64	22.00

SIEVE RESULTS

DIAM. MM.	WT. GMS.	PHI	PER CENT	PCT. FNR.
2.000	0.0	-1.00	0.0	100.00
0.250	0.42	2.00	0.84	99.16
0.063	0.27	3.99	0.54	98.62

D9E

HYDROMETER RESULTS

EL.	TIME	HYDR.	CORRN	T DEG C	PHI	PCT. FNR.
	0.5	50.5	6.0	24.0	4.29	89.00
	1.0	49.0	6.0	24.0	4.76	86.00
	2.0	45.0	6.0	24.0	5.21	78.00
	4.0	38.5	6.0	24.0	5.62	65.00
	8.0	32.0	6.0	24.0	6.05	52.00
	14.0	26.8	6.0	24.0	6.40	41.60
	27.0	23.5	6.0	24.0	6.84	35.00
	54.0	20.1	6.0	24.0	7.32	28.20
	146.0	16.5	6.0	24.0	8.00	21.00
	260.0	15.0	6.0	24.0	8.40	18.00
	432.0	14.0	6.0	24.0	8.76	16.00
	1410.0	12.5	6.0	24.0	9.60	13.00

SIEVE RESULTS

DIAM. MM.	WT. GMS.	PHI	PER CENT	PCT. FNR.
2.000	0.0	-1.00	0.0	100.00
0.355	0.33	1.49	0.66	99.34
0.063	0.39	3.99	0.78	98.56

D10A

HYDROMETER RESULTS

EL.	TIME	HYDR.	CORRN	T DEG C	PHI	PCT. FNR.
	0.5	36.0	6.0	24.0	4.10	60.00
	1.0	22.0	6.0	24.0	4.45	32.00
	2.0	19.0	6.0	24.0	4.92	26.00
	4.0	15.0	6.0	24.0	5.39	18.00
	8.0	11.5	6.0	24.0	5.86	11.00
	15.0	10.2	6.0	24.0	6.30	8.40
	30.0	10.0	6.0	24.0	6.80	8.00
	54.0	9.5	6.0	24.0	7.22	7.00
	138.0	8.5	5.5	24.0	7.89	6.00
	253.0	8.0	6.0	24.0	8.32	4.00
	425.0	8.0	6.0	24.0	8.70	4.00
	1407.0	8.0	6.0	24.0	9.56	4.00

SIEVE RESULTS

DIAM. MM.	WT. GMS.	PHI	PER CENT	PCT. FNR.
2.000	0.0	-1.00	0.0	100.00
1.000	0.01	-0.0	0.02	99.98
0.500	0.02	1.00	0.04	99.94
0.250	0.09	2.00	0.18	99.76
0.125	1.73	3.00	3.46	96.30
0.063	10.50	3.99	21.00	75.30

D11A

HYDROMETER RESULTS

EL.	TIME	HYDR.	CORRN	T DEG C	PHI	PCT. FNR.
	0.5	27.5	3.0	24.0	4.01	36.30
	1.0	25.0	3.0	24.0	4.48	32.59
	2.0	20.0	3.0	24.0	4.94	25.19
	4.0	15.0	3.0	24.0	5.39	17.78
	8.0	12.0	3.0	24.0	5.87	13.33
	15.0	9.5	3.0	24.0	6.30	9.63

SIEVE RESULTS

DIAM. MM.	WT. GMS.	PHI	PER CENT	PCT. FNR.
2.000	0.0	-1.00	0.0	100.00
1.000	0.10	-0.0	0.20	99.80
0.700	0.08	0.51	0.16	99.64
0.500	0.02	1.00	0.04	99.60
0.354	0.06	1.50	0.12	99.48
0.250	0.13	2.00	0.26	99.22
0.177	0.33	2.50	0.66	98.56
0.125	1.59	3.00	3.18	95.38
0.088	4.56	3.51	9.12	86.26
0.063	6.54	3.99	13.08	73.18

D12A

HYDROMETER RESULTS

EL.	TIME	HYDR.	CORRN	T DEG C	PHI	PCT. FNR.
	0.5	17.0	6.0	24.0	3.91	22.00
	1.0	12.0	6.0	24.0	4.37	12.00
	2.0	9.5	6.0	24.0	4.84	7.00
	4.0	8.0	6.0	24.0	5.33	4.00
	8.0	7.2	6.0	24.0	5.83	2.40
	17.0	7.0	6.0	24.0	6.37	2.00
	55.0	7.0	6.0	24.0	7.21	2.00
	133.0	7.0	6.0	24.0	7.85	2.00
	246.0	7.0	6.0	24.0	8.29	2.00
	418.0	7.0	6.0	24.0	8.68	2.00
	1404.0	6.8	6.0	24.0	9.55	1.60

SIEVE RESULTS

DIAM. MM.	WT. GMS.	PHI	PER CENT	PCT. FNR.
2.000	0.0	-1.00	0.0	100.00
1.000	0.01	-0.0	0.02	99.98
0.500	0.06	1.00	0.12	99.86
0.250	2.43	2.00	4.86	95.00
0.125	13.70	3.00	27.40	67.60
0.063	17.80	3.99	35.60	32.00

D12B

HYDROMETER RESULTS

EL.	TIME	HYDR.	CORRN	T DEG C	PHI	PCT. FNR.
	0.5	47.0	4.0	24.0	4.23	86.00
	1.0	44.0	4.0	24.0	4.69	80.00
	2.0	37.5	4.0	24.0	5.11	67.00
	4.0	30.0	4.0	24.0	5.53	52.00
	8.0	22.5	4.5	24.0	5.96	36.00
	14.0	20.0	4.5	24.0	6.34	31.00
	15.0	19.5	4.5	24.0	6.38	30.00
	24.0	15.5	4.5	24.0	6.69	22.00
	47.0	14.3	4.0	24.0	7.16	20.60
	94.0	13.0	4.0	24.0	7.65	18.00
	181.0	12.2	3.0	24.0	8.12	18.40
	1410.0	10.0	4.0	24.0	9.58	12.00

SIEVE RESULTS

DIAM. MM.	WT. GMS.	PHI	PER CENT	PCT. FNR.
2.000	0.0	-1.00	0.0	100.00
1.000	0.10	-0.0	0.20	99.80
0.700	0.04	0.51	0.08	99.72
0.500	0.03	1.00	0.06	99.66
0.354	0.05	1.50	0.10	99.56
0.250	0.24	2.00	0.48	99.08
0.177	0.14	2.50	0.28	98.80
0.125	0.12	3.00	0.24	98.56
0.088	0.17	3.51	0.34	98.22
0.063	0.27	3.99	0.54	97.68

D12C

HYDROMETER RESULTS

EL.	TIME	HYDR.	CORRN	T DEG C	PHI	PCT. FNR.
	0.5	48.2	5.0	24.0	4.25	86.40
	1.0	45.5	5.0	24.0	4.71	81.00
	2.0	40.0	5.0	24.0	5.15	70.00
	4.0	33.0	5.0	24.0	5.56	56.00
	8.0	27.5	5.0	24.0	6.01	45.00
	14.0	23.2	4.0	24.0	6.37	38.40
	15.0	22.0	5.0	24.0	6.41	34.00
	30.0	20.0	5.0	24.0	6.89	30.00
	51.0	17.2	4.0	24.0	7.25	26.40
	94.0	15.1	4.0	24.0	7.67	22.20
	181.0	14.3	3.0	24.0	8.14	22.60
	324.0	13.5	4.0	24.0	8.55	19.00
	1410.0	12.5	4.0	23.0	9.58	17.00

SIEVE RESULTS

DIAM. MM.	WT. GMS.	PHI	PER CENT	PCT. FNR.
4.000	0.0	-2.00	0.0	100.00
2.000	1.01	-1.00	2.02	97.98
1.000	0.40	-0.0	0.80	97.18
0.700	0.11	0.51	0.22	96.96
0.500	0.13	1.00	0.26	96.70
0.354	0.20	1.50	0.40	96.30
0.250	0.21	2.00	0.42	95.88
0.125	0.18	3.00	0.36	95.52
0.177	0.21	2.50	0.42	95.10

0.088	0.28	3.51	0.56	94.54
0.063	0.31	3.99	0.62	93.92

D12D

HYDROMETER RESULTS

EL.	TIME	HYDR.	CORRN	T DEG C	PHI	PCT. FNR.
	0.5	52.0	5.5	24.0	4.30	93.00
	2.0	44.0	5.5	24.0	5.19	77.00
	4.0	36.5	5.5	24.0	5.60	62.00
	8.0	29.5	5.5	24.0	6.03	48.00
	14.0	24.0	5.5	24.0	6.37	37.00
	30.0	20.1	5.5	24.0	6.89	29.20
	65.0	17.5	5.5	24.0	7.42	24.00
	120.0	15.5	5.5	24.0	7.85	20.00
	234.0	14.5	6.0	24.0	8.32	17.00
	406.0	13.2	6.0	24.0	8.71	14.40
	1396.0	12.0	6.0	24.0	9.59	12.00

SIEVE RESULTS

DIAM. MM.	WT. GMS.	PHI	PER CENT	PCT. FNR.
2.000	0.0	-1.00	0.0	100.00
0.355	0.02	1.49	0.04	99.96
0.063	0.16	3.99	0.32	99.64

D12E

HYDROMETER RESULTS

EL.	TIME	HYDR.	CORRN	T DEG C	PHI	PCT. FNR.
	0.5	50.0	5.0	24.0	4.28	90.00
	1.0	47.0	5.0	24.0	4.73	84.00
	2.0	41.5	5.0	24.0	5.16	73.00
	4.0	34.0	5.0	24.0	5.58	58.00
	8.0	26.0	5.0	24.0	5.99	42.00
	12.0	23.0	4.0	24.0	6.26	38.00
	15.0	21.0	5.0	24.0	6.39	32.00
	23.0	20.0	4.0	24.0	6.70	32.00
	65.0	15.0	5.0	24.0	7.40	20.00
	67.0	15.5	4.0	24.0	7.43	23.00
	116.0	15.0	4.0	24.0	7.82	22.00
	241.0	14.0	4.0	24.0	8.34	20.00
	385.0	13.5	4.0	24.0	8.67	19.00
	1422.0	12.0	4.0	23.0	9.59	16.00

SIEVE RESULTS

DIAM. MM.	WT. GMS.	PHI	PER CENT	PCT. FNR.
2.000	0.0	-1.00	0.0	100.00
1.000	0.0	-0.0	0.0	100.00
0.500	0.0	1.00	0.0	100.00
0.250	0.05	2.00	0.10	99.90
0.125	0.08	3.00	0.16	99.74
0.063	0.13	3.99	0.26	99.48

D12F

HYDROMETER RESULTS

EL.	TIME	HYDR.	CORRN	T DEG C	PHI	PCT. FNR.
	0.5	51.0	4.0	24.0	4.29	94.00
	1.0	48.0	4.0	24.0	4.75	88.00
	2.0	43.0	4.0	24.0	5.18	78.00
	4.0	36.0	4.0	24.0	5.60	64.00
	8.0	28.0	4.0	24.0	6.01	48.00
	11.0	23.0	4.0	24.0	6.19	38.00
	15.0	22.0	4.0	24.0	6.41	36.00
	22.0	19.0	4.0	24.0	6.65	30.00
	30.0	19.0	4.0	24.0	6.88	30.00
	66.0	15.0	4.0	24.0	7.41	22.00
	115.0	13.5	4.0	24.0	7.80	19.00
	240.0	12.5	4.0	24.0	8.32	17.00
	383.0	11.5	4.0	24.0	8.65	15.00
	1421.0	11.0	4.0	23.0	9.58	14.00

SIEVE RESULTS

DIAM. MM.	WT. GMS.	PHI	PER CENT	PCT. FNR.
2.000	0.02	-1.00	0.00	100.00
1.000	0.02	-0.0	0.04	99.96
0.500	0.01	1.00	0.02	99.94
0.250	0.02	2.00	0.04	99.90
0.125	0.05	3.00	0.10	99.80
0.063	0.07	3.99	0.14	99.66

D12G

HYDROMETER RESULTS

EL.	TIME	HYDR.	CORRN	T DEG C	PHI	PCT. FNR.
	0.5	51.5	4.0	24.0	4.30	95.00
	1.0	50.0	4.0	24.0	4.78	92.00
	2.0	46.5	4.0	24.0	5.22	85.00
	4.0	40.0	4.0	24.0	5.65	72.00
	8.0	33.0	4.0	24.0	6.06	58.00
	13.0	27.5	4.0	24.0	6.36	47.00
	14.0	27.0	4.0	24.0	6.40	46.00
	24.0	22.5	4.0	24.0	6.75	37.00
	30.0	22.0	4.0	24.0	6.91	36.00
	68.0	17.0	4.0	24.0	7.45	26.00
	117.0	15.2	4.0	24.0	7.83	22.40
	242.0	13.5	4.0	24.0	8.34	19.00
	386.0	13.0	4.0	24.0	8.67	18.00
	1424.0	12.0	4.0	23.0	9.59	16.00

SIEVE RESULTS

DIAM. MM.	WT. GMS.	PHI	PER CENT	PCT. FNR.
2.000	0.05	-1.00	0.00	100.00
1.000	0.05	-0.0	0.10	99.90
0.500	0.06	1.00	0.12	99.78
0.250	0.07	2.00	0.14	99.64
0.125	0.05	3.00	0.10	99.54
0.063	0.07	3.99	0.14	99.40

D13A

HYDROMETER RESULTS

EL.	TIME	HYDR.	CORRN	T DEG C	PHI	PCT. FNR.
	0.5	50.0	6.0	24.0	4.28	88.00
	1.0	49.0	6.0	24.0	4.76	86.00
	2.0	47.0	6.0	24.0	5.23	82.00
	4.0	42.2	6.0	24.0	5.68	72.40
	8.0	36.5	6.0	24.0	6.10	61.00
	15.0	32.0	6.0	24.0	6.50	52.00
	35.0	26.0	6.0	24.0	7.06	40.00
	59.0	23.2	5.5	24.0	7.41	35.40
	114.0	20.5	6.0	24.0	7.85	29.00
	228.0	18.5	6.0	24.0	8.34	25.00
	400.0	17.0	6.0	24.0	8.73	22.00
	1393.0	14.5	6.0	24.0	9.61	17.00

SIEVE RESULTS

DIAM. MM.	WT. GMS.	PHI	PER CENT	PCT. FNR.
2.000	0.0	-1.00	0.0	100.00
0.063	0.36	3.99	0.72	99.28

D13A

HYDROMETER RESULTS

EL.	TIME	HYDR.	CORRN	T DEG C	PHI	PCT. FNR.
	0.5	52.0	5.5	24.0	4.30	93.00
	1.0	51.0	5.5	24.0	4.79	91.00
	2.0	38.0	5.5	24.0	5.12	65.00
	4.0	37.5	5.5	24.0	5.61	64.00
	8.0	35.2	5.5	24.0	6.09	59.40
	15.0	30.8	5.5	24.0	6.49	50.60
	49.0	24.3	5.5	24.0	7.28	37.60
	103.0	21.0	5.5	24.0	7.78	31.00
	217.0	19.0	6.0	24.0	8.31	26.00
	389.0	17.5	6.0	24.0	8.72	23.00
	1386.0	15.0	6.0	24.0	9.61	18.00

SIEVE RESULTS

DIAM. MM.	WT. GMS.	PHI	PER CENT	PCT. FNR.
2.000	0.0	-1.00	0.0	100.00
0.250	0.23	2.00	0.46	99.54
0.063	0.20	3.99	0.40	99.14

D14A

HYDROMETER RESULTS

EL.	TIME	HYDR.	CORRN	T DEG C	PHI	PCT. FNR.
	0.5	52.0	5.5	24.0	4.30	93.00
	1.0	51.0	5.5	24.0	4.79	91.00
	2.0	38.0	5.5	24.0	5.12	65.00
	4.0	37.5	5.5	24.0	5.61	64.00
	8.0	35.2	5.5	24.0	6.09	59.40
	15.0	30.8	5.5	24.0	6.49	50.60
	49.0	24.3	5.5	24.0	7.28	37.60
	103.0	21.0	5.5	24.0	7.78	31.00
	217.0	19.0	6.0	24.0	8.31	26.00
	389.0	17.5	6.0	24.0	8.72	23.00
	1386.0	15.0	6.0	24.0	9.61	18.00

SIEVE RESULTS

DIAM. MM.	WT. GMS.	PHI	PER CENT	PCT. FNR.
2.000	0.0	-1.00	0.0	100.00
0.250	0.23	2.00	0.46	99.54
0.063	0.20	3.99	0.40	99.14

D15A

HYDROMETER RESULTS

EL.	TIME	HYDR.	CORRN	T DEG C	PHI	PCT. FNR.
	0.5	52.0	6.0	24.0	4.30	92.00
	1.0	51.0	6.0	24.0	4.79	90.00
	2.0	49.5	6.0	24.0	5.27	87.00
	4.0	45.2	6.0	24.0	5.71	78.40
	8.0	40.0	6.0	24.0	6.15	68.00
	15.0	35.0	6.0	24.0	6.54	58.00
	43.0	28.5	5.5	24.0	7.23	46.00
	96.0	24.2	6.0	24.0	7.77	36.40
	210.0	22.0	6.0	24.0	8.31	32.00
	382.0	20.2	6.0	24.0	8.73	28.40
	1380.0	17.3	6.0	24.0	9.63	22.60

SIEVE RESULTS

DIAM. MM.	WT. GMS.	PHI	PER CENT	PCT. FNR.
2.000	0.0	-1.00	0.0	100.00
0.300	0.05	1.74	0.10	99.90
0.063	0.21	3.99	0.42	99.48

D15A

HYDROMETER RESULTS

EL.	TIME	HYDR.	CORRN	T DEG C	PHI	PCT. FNR.
	0.5	52.0	4.0	24.0	4.30	96.00
	1.0	50.5	4.0	24.0	4.79	93.00
	2.0	48.5	4.0	24.0	5.25	89.00
	4.0	44.5	4.0	24.0	5.70	81.00
	8.0	38.5	4.0	24.0	6.12	69.00
	13.0	35.2	4.0	24.0	6.44	62.40
	14.0	35.0	4.0	24.0	6.49	62.00
	24.0	31.5	4.0	24.0	6.84	55.00
	29.0	30.0	4.5	24.0	6.96	51.00
	68.0	25.0	4.0	24.0	7.52	42.00
	117.0	23.0	4.0	24.0	7.90	38.00
	241.0	21.0	4.0	24.0	8.40	34.00
	385.0	19.5	4.0	24.0	8.72	31.00
	1423.0	17.0	4.0	23.0	9.63	26.00

SIEVE RESULTS

DIAM. MM.	WT. GMS.	PHI	PER CENT	PCT. FNR.
2.000	0.0	-1.00	0.0	100.00
1.000	0.0	-0.0	0.0	100.00
0.500	0.01	1.00	0.02	99.98
0.250	0.02	2.00	0.04	99.94
0.125	0.03	3.00	0.06	99.88
0.063	0.05	3.99	0.10	99.78

D16A

HYDROMETER RESULTS

EL.	TIME	HYDR.	CORRN	T DEG C	PHI	PCT. FNR.
	0.5	47.0	4.5	24.0	4.23	85.00
	1.0	43.5	4.5	24.0	4.69	78.00
	2.0	39.5	4.5	24.0	5.14	70.00
	4.0	34.0	4.5	24.0	5.58	59.00
	8.0	26.0	4.5	24.0	5.99	43.00
	12.0	22.5	4.0	24.0	6.25	37.00
	15.0	20.0	4.5	24.0	6.39	31.00
	24.0	19.0	4.0	24.0	6.72	30.00
	67.0	15.0	4.0	24.0	7.43	22.00
	117.0	14.0	4.0	24.0	7.82	20.00
	241.0	13.0	4.0	24.0	8.33	18.00
	385.0	12.0	4.0	24.0	8.66	16.00
	1423.0	11.5	4.0	23.0	9.58	15.00

SIEVE RESULTS

DIAM. MM.	WT. GMS.	PHI	PER CENT	PCT. FNR.
2.000	0.0	-1.00	0.0	100.00
1.000	0.01	-0.0	0.02	99.98
0.500	0.02	1.00	0.04	99.94
0.250	0.10	2.00	0.20	99.74
0.125	0.42	3.00	0.84	98.90
0.063	2.20	3.99	4.40	94.50

D16B

HYDROMETER RESULTS

EL.	TIME	HYDR.	CORRN	T DEG C	PHI	PCT. FNR.
	0.5	50.0	5.5	24.0	4.28	89.00
	1.5	46.0	5.5	24.0	5.01	81.00
	2.0	44.0	5.5	24.0	5.19	77.00
	4.0	38.5	5.5	24.0	5.62	66.00
	8.0	32.0	5.5	24.0	6.05	53.00
	15.0	26.5	5.5	24.0	6.45	42.00
	16.0	30.0	4.0	24.0	6.53	52.00
	28.0	26.0	4.0	24.0	6.90	44.00
	30.0	22.0	5.5	24.0	6.91	33.00
	72.0	22.0	4.0	24.0	7.54	36.00
	121.0	20.0	4.0	24.0	7.89	32.00
	391.0	17.0	4.0	24.0	8.71	26.00
	1429.0	15.5	4.0	23.0	9.62	23.00

SIEVE RESULTS

DIAM. MM.	WT. GMS.	PHI	PER CENT	PCT. FNR.
2.000	0.0	-1.00	0.0	100.00
1.000	0.05	-0.0	0.10	99.90
0.700	0.05	0.51	0.10	99.80
0.500	0.03	1.00	0.06	99.74
0.354	0.04	1.50	0.08	99.66
0.250	0.02	2.00	0.04	99.62
0.177	0.01	2.50	0.02	99.60
0.125	0.06	3.00	0.12	99.48
0.088	0.04	3.51	0.08	99.40

0.063 0.07 3.99 0.14 99.26

D16C

HYDROMETER RESULTS

EL.	TIME	HYDR.	CORRN	T DEG C	PHI	PCT. FNR.
	0.5	52.0	4.0	24.0	4.30	96.00
	1.0	50.0	4.0	24.0	4.78	92.00
	2.0	47.0	4.0	24.0	5.23	86.00
	4.0	41.5	4.0	24.0	5.66	75.00
	8.0	35.5	4.5	24.0	6.09	62.00
	15.0	33.2	4.0	24.0	6.52	58.40
	15.0	31.0	4.5	24.0	6.50	53.00
	27.0	29.0	4.0	24.0	6.90	50.00
	30.0	26.0	4.5	24.0	6.95	43.00
	71.0	23.0	4.0	24.0	7.54	38.00
	120.0	21.0	4.0	24.0	7.89	34.00
	245.0	19.0	4.0	24.0	8.39	30.00
	389.0	17.5	4.0	24.0	8.72	27.00
	1428.0	16.0	4.0	24.0	9.64	24.00

SIEVE RESULTS

DIAM. MM.	WT. GMS.	PHI	PER CENT	PCT. FNR.
2.000	0.04	-1.00	0.00	100.00
1.000	0.02	-0.0	0.04	99.96
0.500	0.03	1.00	0.06	99.90
0.250	0.05	2.00	0.10	99.80
0.125	0.12	3.00	0.24	99.56
0.063	0.15	3.99	0.30	99.26

D17A

HYDROMETER RESULTS

EL.	TIME	HYDR.	CORRN	T DEG C	PHI	PCT. FNR.
	0.5	51.0	4.0	24.0	4.29	94.00
	1.0	49.5	4.0	24.0	4.77	91.00
	2.0	45.5	4.0	24.0	5.21	83.00
	4.0	39.5	4.5	24.0	5.64	70.00
	8.0	32.5	4.5	24.0	6.06	56.00
	12.0	26.8	4.0	24.0	6.29	45.60
	15.0	26.0	4.0	24.0	6.45	44.00
	23.0	22.8	4.0	24.0	6.72	37.60
	30.0	23.0	3.5	24.0	6.92	39.00
	66.0	18.0	4.0	24.0	7.44	28.00
	115.0	16.5	4.0	24.0	7.83	25.00
	240.0	15.0	4.0	24.0	8.35	22.00
	384.0	14.0	4.0	24.0	8.67	20.00
	1428.0	13.0	4.0	23.0	9.59	18.00

SIEVE RESULTS

DIAM. MM.	WT. GMS.	PHI	PER CENT	PCT. FNR.
2.000	0.04	-1.00	0.00	100.00
1.000	0.04	-0.0	0.08	99.92
0.500	0.01	1.00	0.02	99.90
0.250	0.01	2.00	0.02	99.88
0.125	0.02	3.00	0.04	99.84
0.063	0.02	3.99	0.04	99.80

D18A

HYDROMETER RESULTS

EL.	TIME	HYDR.	CORRN	T DEG C	PHI	PCT. FNR.
	0.5	51.5	3.5	24.0	4.30	96.00
	1.0	50.5	3.5	24.0	4.79	94.00
	2.0	47.5	3.5	24.0	5.24	88.00
	4.0	43.0	3.5	24.0	5.68	79.00
	8.0	36.0	3.5	24.0	6.10	65.00
	14.0	31.5	4.0	24.0	6.45	55.00
	15.0	29.5	3.5	24.0	6.48	52.00
	26.0	25.5	4.0	24.0	6.84	43.00
	30.0	24.0	4.0	24.0	6.92	40.00
	69.0	19.0	4.0	24.0	7.48	30.00
	118.0	17.0	4.0	24.0	7.85	26.00
	243.0	14.0	4.0	24.0	8.34	20.00
	387.0	13.0	4.0	24.0	8.67	18.00
	1426.0	12.5	4.0	24.0	9.61	17.00

SIEVE RESULTS

DIAM. MM.	WT. GMS.	PHI	PER CENT	PCT. FNR.
2.000	0.0	-1.00	0.0	100.00
1.000	0.05	-0.0	0.10	99.90
0.500	0.07	1.00	0.14	99.76
0.250	0.06	2.00	0.12	99.64
0.125	0.03	3.00	0.06	99.58
0.063	0.05	3.99	0.10	99.48

D18A

HYDROMETER RESULTS

EL.	TIME	HYDR.	CORRN	T DEG C	PHI	PCT. FNR.
	0.5	53.0	5.5	24.0	4.32	95.00
	1.0	51.5	5.5	24.0	4.80	92.00
	2.0	48.5	5.5	24.0	5.25	86.00
	4.0	43.5	5.5	24.0	5.69	76.00
	8.0	32.5	5.5	24.0	6.06	54.00
	15.0	31.5	5.5	24.0	6.50	52.00
	34.0	25.5	5.5	24.0	7.03	40.00
	87.0	19.8	5.5	24.0	7.65	28.60
	201.0	16.7	6.0	24.0	8.23	21.40
	373.0	15.0	6.0	24.0	8.66	18.00
	1373.0	12.7	6.0	24.0	9.58	13.40

SIEVE RESULTS

DIAM. MM.	WT. GMS.	PHI	PER CENT	PCT. FNR.
2.000	0.0	-1.00	0.0	100.00
0.063	0.23	3.99	0.46	99.54

D19A

HYDROMETER RESULTS

EL.	TIME	HYDR.	CORRN	T DEG C	PHI	PCT. FNR.
	0.5	52.5	6.0	24.0	4.31	93.00
	1.0	51.5	6.0	24.0	4.80	91.00
	2.0	51.0	6.0	24.0	5.29	90.00
	4.0	50.1	6.0	24.0	5.79	88.20
	8.0	47.8	6.0	24.0	6.24	83.60
	12.0	46.0	6.0	24.0	6.51	80.00
	27.0	44.0	5.5	24.0	7.07	77.00
	79.0	36.5	6.0	24.0	7.76	61.00
	193.0	32.5	6.0	24.0	8.35	53.00
	365.0	29.0	6.0	24.0	8.78	46.00
	1367.0	23.7	6.0	24.0	9.67	35.40

SIEVE RESULTS

DIAM. MM.	WT. GMS.	PHI	PER CENT	PCT. FNR.
2.000	0.0	-1.00	0.0	100.00
0.300	0.34	1.74	0.68	99.32
0.063	0.95	3.99	1.90	97.42

D20A

HYDROMETER RESULTS

EL.	TIME	HYDR.	CORRN	T DEG C	PHI	PCT. FNR.
	0.5	50.0	5.5	24.0	4.28	89.00
	1.0	46.5	5.5	24.0	4.72	82.00
	2.0	40.5	5.5	24.0	5.15	70.00
	4.0	32.5	5.5	24.0	5.56	54.00
	8.0	25.5	5.5	24.0	5.99	40.00
	18.0	20.0	5.5	24.0	6.52	29.00
	72.0	15.0	5.5	24.0	7.48	19.00
	173.0	13.2	6.0	24.0	8.09	14.40
	358.0	12.2	6.0	24.0	8.61	12.40
	1364.0	10.2	6.0	24.0	9.56	8.40

SIEVE RESULTS

DIAM. MM.	WT. GMS.	PHI	PER CENT	PCT. FNR.
2.000	0.0	-1.00	0.0	100.00
0.500	0.02	1.00	0.04	99.96
0.250	0.06	2.00	0.12	99.84
0.063	0.43	3.99	0.86	98.98

D20B

HYDROMETER RESULTS

EL.	TIME	HYDR.	CORRN	T DEG C	PHI	PCT. FNR.
	0.5	46.0	6.0	24.0	4.22	80.00
	1.0	41.0	6.0	24.0	4.65	70.00
	2.0	33.5	6.0	24.0	5.07	55.00
	4.0	26.0	6.0	24.0	5.49	40.00
	8.0	19.8	6.0	24.0	5.93	27.60
	13.0	16.0	6.0	24.0	6.25	20.00
	54.0	12.8	6.0	24.0	7.25	13.60
	164.0	10.5	6.0	24.0	8.03	9.00
	350.0	10.5	6.0	24.0	8.58	9.00
	1359.0	10.0	6.0	24.0	9.55	8.00

SIEVE RESULTS:

DIAM. MM.	WT. GMS.	PHI	PER CENT	PCT. FNR.
2.000	0.0	-1.00	0.0	100.00
0.700	0.03	0.51	0.06	99.94
0.300	0.26	1.74	0.52	99.42
0.063	3.43	3.99	6.86	92.56

D20C

HYDROMETER RESULTS

EL. TIME	HYDR.	CORRN	T DEG C	PHI	PCT. FNR.
0.5	47.5	4.5	24.0	4.24	86.00
1.0	44.5	4.5	24.0	4.70	80.00
2.0	36.5	4.5	24.0	5.10	64.00
4.0	29.0	4.5	24.0	5.52	49.00
8.0	22.0	4.5	24.0	5.95	35.00
15.0	20.5	4.5	24.0	6.39	32.00
16.0	20.5	4.0	24.0	6.44	33.00
29.0	17.5	4.0	24.0	6.84	27.00
72.0	15.0	4.0	24.0	7.48	22.00
122.0	13.5	4.0	24.0	7.84	19.00
246.0	12.5	4.0	24.0	8.34	17.00
381.0	12.0	4.0	24.0	8.65	16.00
1430.0	11.5	4.0	23.0	9.59	15.00

SIEVE RESULTS

DIAM. MM.	WT. GMS.	PHI	PER CENT	PCT. FNR.
2.000	0.0	-1.00	0.0	100.00
1.000	0.01	-0.0	0.02	99.98
0.500	0.04	1.00	0.08	99.90
0.250	0.04	2.00	0.08	99.82
0.125	0.11	3.00	0.22	99.60
0.063	0.25	3.99	0.50	99.10

D20D

HYDROMETER RESULTS

EL.	TIME	HYDR.	CORRN	T DEG C	PHI	PCT. FNR.
	0.5	48.7	5.0	24.0	4.25	87.40
	1.0	45.5	5.0	24.0	4.71	81.00
	2.0	38.7	5.0	24.0	5.12	67.40
	4.0	31.5	5.0	24.0	5.55	53.00
	8.0	23.0	5.0	24.0	5.96	36.00
	14.0	20.8	4.0	24.0	6.34	33.60
	15.0	19.0	5.5	24.0	6.38	27.00
	27.0	18.0	4.0	24.0	6.80	28.00
	36.0	16.5	5.5	24.0	6.99	22.00
	72.0	15.2	4.0	24.0	7.48	22.40
	121.0	14.0	4.0	24.0	7.84	20.00
	245.0	13.0	4.0	24.0	8.34	18.00
	390.0	12.0	4.0	24.0	8.67	16.00
	1428.0	11.0	4.0	23.0	9.58	14.00

SIEVE RESULTS

DIAM. MM.	WT. GMS.	PHI	PER CENT	PCT. FNR.
4.000	0.0	-2.00	0.0	100.00
2.000	0.25	-1.00	0.50	99.50
1.000	0.18	-0.0	0.36	99.14
0.700	0.07	0.51	0.14	99.00
0.500	0.03	1.00	0.06	98.94
0.354	0.02	1.50	0.04	98.90
0.250	0.04	2.00	0.08	98.82
0.177	0.05	2.50	0.10	98.72

0.125	0.05	3.00	0.10	98.62
0.088	0.06	3.51	0.12	98.50
0.063	0.05	3.99	0.10	98.40

D20E

HYDROMETER RESULTS

EL.	TIME	HYDR.	CORRN	T DEG C	PHI	PCT. FNR.
	0.5	49.0	4.5	24.0	4.26	89.00
	1.0	47.0	4.5	24.0	4.73	85.00
	2.0	40.5	4.5	24.0	5.15	72.00
	4.0	33.0	4.5	24.0	5.56	57.00
	8.0	26.0	4.5	24.0	5.99	43.00
	14.0	21.5	4.0	24.0	6.35	35.00
	26.0	17.5	4.0	24.0	6.76	27.00
	30.0	17.0	4.0	24.0	6.86	26.00
	68.0	14.5	4.0	24.0	7.43	21.00
	117.0	13.5	4.0	24.0	7.81	19.00
	243.0	12.5	4.0	24.0	8.33	17.00
	387.0	12.0	4.0	24.0	8.66	16.00
	1424.0	11.5	4.0	23.0	9.58	15.00

SIEVE RESULTS

DIAM. MM.	WT. GMS.	PHI	PER CENT	PCT. FNR.
2.000	0.0	-1.00	0.0	100.00
1.000	0.01	-0.0	0.02	99.98
0.500	0.02	1.00	0.04	99.94
0.250	0.03	2.00	0.06	99.88
0.125	0.08	3.00	0.16	99.72
0.063	0.16	3.99	0.32	99.40

D21A

HYDROMETER RESULTS

EL.	TIME	HYDR.	CORRN	T DEG C	PHI	PCT. FNR.
	0.5	48.5	4.5	24.0	4.25	88.00
	1.0	44.0	4.5	24.0	4.69	79.00
	2.0	37.0	4.5	24.0	5.11	65.00
	4.0	29.0	4.5	24.0	5.52	49.00
	8.0	22.5	4.5	24.0	5.96	36.00
	13.0	22.0	4.0	24.0	6.30	36.00
	14.0	19.5	4.5	24.0	6.33	30.00
	25.0	18.0	4.0	24.0	6.74	28.00
	68.0	15.5	4.0	24.0	7.44	23.00
	117.0	14.0	4.0	24.0	7.82	20.00
	242.0	13.0	4.0	24.0	8.33	18.00
	386.0	12.5	4.0	24.0	8.67	17.00
	1424.0	12.0	4.0	23.0	9.59	16.00

SIEVE RESULTS

DIAM. MM.	WT. GMS.	PHI	PER CENT	PCT. FNR.
2.000	0.01	-1.00	0.00	100.00
1.000	0.04	-0.0	0.08	99.92
0.500	0.04	1.00	0.08	99.84
0.250	0.07	2.00	0.14	99.70
0.125	0.10	3.00	0.20	99.50
0.063	0.25	3.99	0.50	99.00

D22A

HYDROMETER RESULTS

EL.	TIME	HYDR.	CORRN	T DEG C	PHI	PCT. FNR.
	0.5	50.5	4.0	24.0	4.29	93.00
	2.0	44.0	4.0	24.0	5.19	80.00
	4.0	37.5	4.0	24.0	5.61	67.00
	7.0	32.0	4.0	24.0	5.95	56.00
	14.0	28.2	4.0	24.0	6.42	48.40
	15.0	25.0	4.5	24.0	6.43	41.00
	25.0	23.0	4.0	24.0	6.79	38.00
	69.0	18.0	4.0	24.0	7.47	28.00
	117.0	16.5	4.0	24.0	7.84	25.00
	243.0	15.5	4.0	24.0	8.36	23.00
	387.0	14.5	4.0	24.0	8.69	21.00
	1425.0	13.5	4.0	23.0	9.60	19.00

SIEVE RESULTS

DIAM. MM.	WT. GMS.	PHI	PER CENT	PCT. FNR.
2.000	0.0	-1.00	0.0	100.00
1.000	0.02	-0.0	0.04	99.96
0.500	0.10	1.00	0.20	99.76
0.250	0.17	2.00	0.34	99.42
0.125	0.04	3.00	0.08	99.34
0.063	0.05	3.99	0.10	99.24

1A1

HYDROMETER RESULTS

EL.	TIME	HYDR.	CORRN	T DEG C	PHI	PCT. FNR.
	0.5	40.5	5.7	24.0	4.15	69.60
	1.0	33.0	5.7	24.0	4.56	54.60
	2.0	26.5	5.7	24.0	5.00	41.60
	4.0	22.0	5.7	24.0	5.45	32.60
	8.0	18.0	5.7	24.0	5.92	24.60
	13.0	16.0	5.7	24.0	6.25	20.60
	34.0	13.8	5.7	24.0	6.92	16.20
	58.0	13.2	5.7	24.0	7.31	15.00
	114.0	12.5	5.7	24.0	7.79	13.60
	201.0	11.5	5.7	24.0	8.19	11.60
	331.0	10.5	5.7	24.0	8.54	9.60
	457.0	10.2	5.7	24.0	8.77	9.00
	1412.0	9.8	5.7	24.0	9.58	8.20

SIEVE RESULTS

DIAM. MM.	WT. GMS.	PHI	PER CENT	PCT. FNR.
2.000	0.0	-1.00	0.0	100.00
0.700	0.07	0.51	0.14	99.86
0.250	0.37	2.00	0.74	99.12
0.125	1.11	3.00	2.22	96.90
0.063	5.93	3.99	11.86	85.04

1A2A

HYDROMETER RESULTS

EL.	TIME	HYDR.	CORRN	T DEG C	PHI	PCT. FNR.
	0.5	49.0	5.7	24.0	4.26	86.60
	1.0	45.5	5.7	24.0	4.71	79.60
	2.0	38.0	5.7	24.0	5.12	64.60
	4.0	30.0	5.7	24.0	5.53	48.60
	8.0	23.0	5.7	24.0	5.96	34.60
	15.0	18.5	5.7	24.0	6.37	25.60
	29.0	16.5	5.7	24.0	6.83	21.60
	70.0	13.5	5.7	24.0	7.44	15.60
	195.0	12.0	5.7	24.0	8.17	12.60
	325.0	11.0	5.7	24.0	8.53	10.60
	450.0	11.0	5.7	24.0	8.76	10.60
	1410.0	10.2	5.7	24.0	9.58	9.00

SIEVE RESULTS

DIAM. MM.	WT. GMS.	PHI	PER CENT	PCT. FNR.
2.000	0.0	-1.00	0.0	100.00
0.063	1.70	3.99	3.40	96.60

1A2B

HYDROMETER RESULTS

EL.	TIME	HYDR.	CORRN	T DEG C	PHI	PCT. FNR.
	0.5	48.0	5.7	24.0	4.25	84.60
	1.0	44.0	5.7	24.0	4.69	76.60
	2.0	37.0	5.7	24.0	5.11	62.60
	4.0	30.0	5.7	24.0	5.53	48.60
	8.0	23.0	5.7	24.0	5.96	34.60
	15.0	18.3	5.7	24.0	6.37	25.20
	36.0	16.0	5.7	24.0	6.98	20.60
	64.0	14.2	5.7	24.0	7.39	17.00
	189.0	12.8	5.7	24.0	8.15	14.20
	318.0	11.8	5.7	24.0	8.52	12.20
	444.0	11.5	5.7	24.0	8.76	11.60
	1405.0	10.5	5.7	24.0	9.58	9.60

SIEVE RESULTS

DIAM. MM.	WT. GMS.	PHI	PER CENT	PCT. FNR.
2.000	0.0	-1.00	0.0	100.00
0.300	0.15	1.74	0.30	99.70
0.063	3.20	3.99	6.40	93.30

1A3

HYDROMETER RESULTS

EL.	TIME	HYDR.	CORRN	T DEG C	PHI	PCT. FNR.
	0.5	48.0	5.7	24.0	4.25	84.60
	1.0	44.0	5.7	24.0	4.69	76.60
	2.0	37.5	5.7	24.0	5.11	63.60
	4.0	29.5	5.7	24.0	5.53	47.60
	8.0	23.0	5.7	24.0	5.96	34.60
	15.0	19.0	5.7	24.0	6.38	26.60
	30.0	16.2	5.7	24.0	6.86	21.00
	87.0	13.8	5.7	24.0	7.60	16.20
	182.0	12.0	5.7	24.0	8.12	12.60
	311.0	11.5	5.7	24.0	8.50	11.60
	437.0	11.2	5.7	24.0	8.75	11.00
	1400.0	10.2	5.7	24.0	9.58	9.00

SIEVE RESULTS

DIAM. MM.	WT. GMS.	PHI	PER CENT	PCT. FNR.
2.000	0.0	-1.00	0.0	100.00
0.063	3.25	3.99	6.50	93.50

1A4

HYDROMETER RESULTS

EL.	TIME	HYDR.	CORRN	T DEG C	PHI	PCT. FNR.
	0.5	36.0	5.7	24.0	4.10	60.60
	1.0	33.5	5.7	24.0	4.57	55.60
	2.0	29.3	5.7	24.0	5.03	47.20
	4.0	24.5	5.7	24.0	5.48	37.60
	8.0	20.0	5.7	24.0	5.94	28.60
	15.0	16.2	5.7	24.0	6.36	21.00
	79.0	11.8	5.7	24.0	7.51	12.20
	173.0	10.9	5.7	24.0	8.07	10.40
	303.0	10.0	5.7	24.0	8.47	8.60
	429.0	9.9	5.7	24.0	8.72	8.40
	1396.0	9.0	5.7	24.0	9.57	6.60

SIEVE RESULTS

DIAM. MM.	WT. GMS.	PHI	PER CENT	PCT. FNR.
2.000	0.0	-1.00	0.0	100.00
0.700	0.13	0.51	0.26	99.74
0.300	2.88	1.74	5.76	93.98
0.106	5.03	3.24	10.06	83.92
0.063	2.50	3.99	5.00	78.92

1A5

HYDROMETER RESULTS

EL.	TIME	HYDR.	CORRN	T DEG C	PHI	PCT. FNR.
	0.5	50.5	5.7	24.0	4.29	89.60
	1.0	49.5	5.7	24.0	4.77	87.60
	2.0	43.5	5.7	24.0	5.19	75.60
	4.0	36.5	5.7	24.0	5.60	61.60
	8.0	29.0	5.7	24.0	6.02	46.60
	13.0	23.5	5.7	24.0	6.32	35.60
	32.0	19.8	5.7	24.0	6.93	28.20
	59.0	17.0	5.7	24.0	7.35	22.60
	152.0	14.2	5.7	24.0	8.01	17.00
	283.0	13.5	5.7	24.0	8.45	15.60
	409.0	13.0	5.7	24.0	8.71	14.60
	1383.0	11.8	5.7	24.0	9.58	12.20

SIEVE RESULTS

DIAM. MM.	WT. GMS.	PHI	PER CENT	PCT. FNR.
2.000	0.0	-1.00	0.0	100.00
0.063	0.81	3.99	1.62	98.38

1B1

HYDROMETER RESULTS

EL.	TIME	HYDR.	CORRN	T DEG C	PHI	PCT. FNR.
	0.5	51.0	5.7	24.0	4.29	90.60
	1.0	49.0	5.7	24.0	4.76	86.60
	2.0	42.0	5.7	24.0	5.17	72.60
	4.0	37.0	5.7	24.0	5.61	62.60
	8.0	31.5	5.7	24.0	6.05	51.60
	14.0	26.0	5.7	24.0	6.40	40.60
	62.0	21.5	5.7	24.0	7.42	31.60
	166.0	15.5	5.7	24.0	8.08	19.60
	295.0	15.0	5.7	24.0	8.49	18.60
	422.0	14.0	5.7	24.0	8.74	16.60
	1393.0	12.5	5.7	24.0	9.59	13.60

SIEVE RESULTS

DIAM. MM.	WT. GMS.	PHI	PER CENT	PCT. FNR.
2.000	0.0	-1.00	0.0	100.00
0.063	0.54	3.99	1.08	98.92

1B2

HYDROMETER RESULTS

EL.	TIME	HYDR.	CORRN	T DEG C	PHI	PCT. FNR.
	0.5	17.5	5.7	24.0	3.91	23.60
	1.0	15.5	5.7	24.0	4.39	19.60
	2.0	14.0	5.7	24.0	4.88	16.60
	4.0	12.0	5.7	24.0	5.37	12.60
	8.0	10.5	5.7	24.0	5.85	9.60
	14.0	10.0	5.7	24.0	6.25	8.60
	38.0	9.5	5.7	24.0	6.97	7.60
	65.0	8.8	5.7	24.0	7.35	6.20
	159.0	8.0	5.7	24.0	7.99	4.60
	289.0	7.8	5.7	24.0	8.41	4.20
	415.0	7.8	5.7	24.0	8.68	4.20
	1389.0	7.0	5.7	24.0	9.54	2.60

SIEVE RESULTS

DIAM. MM.	WT. GMS.	PHI	PER CENT	PCT. FNR.
4.000	0.0	-2.00	0.0	100.00
2.000	3.08	-1.00	6.16	93.84
1.000	1.27	-0.0	2.54	91.30
0.500	7.03	1.00	14.06	77.24
0.250	12.10	2.00	24.20	53.04
0.125	7.73	3.00	15.46	37.58
0.063	4.07	3.99	8.14	29.44

1B5

HYDROMETER RESULTS

EL.	TIME	HYDR.	CORRN	T DEG C	PHI	PCT. FNR.
	0.5	45.5	5.7	24.0	4.21	79.60
	1.0	41.5	5.7	24.0	4.66	71.60
	2.0	37.5	5.7	24.0	5.11	63.60
	4.0	33.2	5.7	24.0	5.57	55.00
	8.0	29.0	5.7	24.0	6.02	46.60
	15.0	26.2	5.7	24.0	6.45	41.00
	43.0	21.5	5.7	24.0	7.16	31.60
	69.0	20.0	5.7	24.0	7.49	28.60
	143.0	18.0	5.7	24.0	8.00	24.60
	273.0	16.5	5.7	24.0	8.45	21.60
	400.0	16.0	5.7	24.0	8.72	20.60
	1378.0	13.5	5.7	24.0	9.59	15.60

SIEVE RESULTS

DIAM. MM.	WT. GMS.	PHI	PER CENT	PCT. FNR.
2.000	0.0	-1.00	0.0	100.00
0.300	0.51	1.74	1.02	98.98
0.063	7.57	3.99	15.14	83.84

1C2

HYDROMETER RESULTS

EL.	TIME	HYDR.	CORRN	T DEG C	PHI	PCT. FNR.
	0.5	47.5	5.7	24.0	4.24	83.60
	1.0	45.5	5.7	24.0	4.71	79.60
	2.0	42.8	5.7	24.0	5.18	74.20
	4.0	39.0	5.7	24.0	5.63	66.60
	8.0	35.0	5.7	24.0	6.08	58.60
	16.0	31.2	5.7	24.0	6.55	51.00
	36.0	26.1	5.7	24.0	7.08	40.80
	71.0	22.1	5.7	24.0	7.53	32.80
	136.0	20.0	5.7	24.0	7.98	28.60
	383.0	17.0	5.7	24.0	8.70	22.60
	1372.0	14.8	5.7	24.0	9.60	18.20

SIEVE RESULTS

DIAM. MM.	WT. GMS.	PHI	PER CENT	PCT. FNR.
2.000	0.0	-1.00	0.0	100.00
0.063	4.32	3.99	8.64	91.36

1E2

HYDROMETER RESULTS

EL.	TIME	HYDR.	CORRN	T DEG C	PHI	PCT. FNR.
	0.5	53.5	5.7	24.0	4.33	95.60
	1.0	53.0	5.7	24.0	4.82	94.60
	2.0	52.5	5.7	24.0	5.31	93.60
	4.0	52.0	5.7	24.0	5.80	92.60
	8.0	50.5	5.7	24.0	6.29	89.60
	15.0	49.2	5.7	24.0	6.72	87.00
	27.0	47.0	5.7	24.0	7.11	82.60
	64.0	42.0	5.7	24.0	7.67	72.60
	129.0	38.2	5.7	24.0	8.13	65.00
	247.0	34.8	5.7	24.0	8.55	58.20
	376.0	32.2	5.7	24.0	8.83	53.00
	1367.0	27.0	5.7	24.0	9.71	42.60

SIEVE RESULTS

DIAM. MM.	WT. GMS.	PHI	PER CENT	PCT. FNR.
2.000	0.02	-1.00	0.00	100.00
0.063	0.89	3.99	1.78	98.22

1F2

HYDROMETER RESULTS

EL.	TIME	HYDR.	CORRN	T DEG C	PHI	PCT. FNR.
	0.5	39.5	5.7	24.0	4.14	67.60
	1.0	32.8	5.7	24.0	4.56	54.20
	2.0	25.0	5.7	24.0	4.98	38.60
	4.0	19.2	5.7	24.0	5.43	27.00
	8.0	14.8	5.7	24.0	5.89	18.20
	16.0	13.2	5.7	24.0	6.38	15.00
	55.0	10.8	5.7	24.0	7.24	10.20
	108.0	10.0	5.7	24.0	7.72	8.60
	249.0	10.0	5.7	24.0	8.33	8.60
	378.0	9.0	5.7	24.0	8.62	6.60
	1363.0	8.8	5.7	24.0	9.54	6.20

SIEVE RESULTS

DIAM. MM.	WT. GMS.	PHI	PER CENT	PCT. FNR.
2.000	0.0	-1.00	0.0	100.00
0.250	0.22	2.00	0.44	99.56
0.106	2.87	3.24	5.74	93.82
0.063	5.81	3.99	11.62	82.20

X. Appendix 3

Data from cumulative curves

Tabulated below are the phi values at various cumulative percentages, measured directly from cumulative curves plotted from grain size analyses. P95 refers to the phi value at which point 95% of the sample is coarser than that value. Also given is the percent sand and silt in the sample.

Sample	P95	P84	P75	P50	P25	P16	P5	Sand	Silt
D1A	4.3	3.3	3.0	2.3	1.8	1.2	0.4	83	7
D1C	11.0	5.9	5.2	4.4	3.8	3.4	2.5	19	65
D2A	5.6	4.3	4.0	3.2	2.6	2.2	1.2	73	27
D2B	5.6	4.4	4.0	3.3	2.6	2.1	1.8	73	27
D3A	4.0	2.8	2.4	1.9	1.3	1.1	0.4	95	5
D4A	11.2	6.9	6.2	5.3	4.5	4.3	3.7	6	87
D5A	11.4	6.5	5.6	4.6	4.0	3.8	3.2	18	74
D6A	11.7	6.7	5.8	4.7	4.0	3.7	3.0	23	68
D6B	2.5	2.1	1.9	1.5	1.1	0.8	0.4	99	1
D7A	13.3	11.6	10.2	7.6	6.2	5.8	4.8	2	64
D7B	13.3	11.5	9.9	7.4	6.3	5.9	5.3	1	68
D7C	13.4	11.6	10.3	7.6	6.1	5.8	4.6	2	65
D7D	13.5	11.3	9.6	7.2	5.9	5.2	4.0	8	66
D9A	13.2	10.8	8.9	6.2	5.2	4.6	3.8	8	67

D9B	13.6	11.2	9.5	6.5	5.8	5.1	4.2	5	68
D9C	12.8	10.4	9.4	6.4	5.6	5.2	4.1	10	67
D9D	13.0	10.8	9.1	6.9	5.8	5.4	4.4	4	70
D9D	12.9	10.6	7.7	6.7	5.8	5.3	4.1	2	74
D9E	12.3	8.9	7.6	6.1	5.2	4.9	3.8	6	78
D10A	8.1	5.6	5.0	4.2	4.0	3.6	3.1	4	72
D10B	11.5	7.4	6.0	5.0	4.4	4.2	3.8	7	82
D11A	7.5	5.6	4.9	4.4	3.9	3.6	3.1	27	70
D12A	5.1	4.2	3.9	3.4	2.7	2.3	2.0	82	16
D12B	12.0	9.5	6.6	5.6	5.0	4.8	4.1	7	80
D12C	12.9	9.8	7.5	5.8	5.0	4.7	4.1	4	79
D12D	12.2	8.5	7.4	5.9	5.3	4.8	4.2	0	86
D12E	13.0	9.6	7.2	5.8	5.1	4.8	4.1	3	80
D12F	13.1	9.5	7.2	6.0	5.2	5.0	4.2	1	85
D12G	12.8	9.6	7.5	6.3	5.6	5.2	4.3	1	85
D13A	13.0	9.9	9.4	7.6	5.6	5.1	4.1	3	77
D14A	12.8	10.2	8.4	6.5	4.9	4.7	3.4	2	79
D15A	13.2	11.0	9.3	7.0	5.8	5.4	4.6	1	72
D15A	13.2	11.3	9.8	7.0	5.9	5.5	4.5	1	70
D16A	12.3	9.0	7.2	5.8	4.9	4.3	3.9	6	78
D16B	13.1	11.1	9.0	6.4	5.2	4.7	4.1	2	73
D16C	13.1	11.2	9.3	6.7	5.6	5.3	4.4	1	73
D17A	12.8	10.2	7.8	6.2	5.5	5.1	4.2	1	80
D18A	13.1	10.0	7.9	6.6	5.8	5.4	4.5	1	81
D18A	12.4	9.2	8.0	6.7	5.8	5.4	4.3	1	82
D19A	13.8	12.1	11.0	8.5	7.1	6.1	4.2	2	56
D20A	11.3	8.9	6.9	5.7	4.9	4.5	4.1	1	88

D20B	11.0	6.9	6.1	5.2	4.5	4.2	3.2	7	84
D20C	12.5	9.2	7.1	5.6	4.8	4.4	4.1	1	83
D20D	12.3	8.9	7.1	5.7	4.9	4.5	4.1	2	83
D20E	12.6	9.1	7.0	5.8	5.0	4.7	3.9	1	83
D21A	12.6	9.8	7.2	5.5	4.8	4.4	4.1	1	82
D22A	12.8	10.4	7.9	6.4	5.4	4.9	4.2	1	78
1A1	11.2	7.2	5.9	4.7	4.1	4.0	3.2	15	75
1A2A	11.4	7.5	6.5	5.6	4.8	4.4	4.2	2	87
1A2B	12.6	7.9	6.4	5.5	5.3	4.8	3.4	7	81
1A3	11.3	7.7	6.5	5.5	4.7	4.3	3.0	6	83
1A4	10.8	7.1	6.2	4.9	4.1	3.2	1.5	21	71
1A5	12.1	9.6	7.2	6.0	5.2	4.9	3.6	6	80
1B1	12.4	9.1	7.8	6.1	5.1	4.8	4.3	1	83
1B2	8.0	5.1	4.0	2.7	1.3	0.9	0.1	64	32
1B5	12.6	9.6	7.9	5.8	4.5	4.0	2.4	16	66
1C2	12.7	10.3	8.5	6.6	5.1	4.1	2.4	14	64
1E2	13.4	12.5	11.4	9.0	7.6	7.0	4.9	2	49
1F2	10.5	6.3	5.6	4.7	4.1	3.8	3.0	11	75

XI. Appendix 4

Lake water temperatures

Temperatures are in degrees centigrade and depths in metres

Location	Depth	Temperature
A1	0	7.5
A1	5	6.0
A1	10	5.7
A2 (July 3)	0	7.0
A2 "	5	6.0
A2 "	10	5.7
A2 (July 4)	0	6.5
A2 "	5	6.5
A2 "	10	6.5
A3	0	6.7
A3	5	5.5
A3	10	5.8
A4	0	6.5
A4	5	5.5
A4	10	5.5

A5	0	7.0
A5	5	5.8
A5	10	5.5
B2	0	6.5
B2	5	5.8
B2	10	5.8
C2	0	6.5
C2	5	5.5
C2	10	5.5
C2	20	5.2
C2	30	5.5
D2	0	6.5
D2	5	6.0
D2	10	5.5
E2	0	7.0
E2	5	5.5
E2	10	5.0
E2	20	5.0

XII. Appendix 5

Suspended sediment concentration, lake water

"Surface" refers to samples taken from the lake surface, otherwise the number following the location refers to the depth below the lake surface.

Location	Suspended sediment concentration (g/l)

D2, surface	0.297
D2, 5m	0.082
D2, 10m	0.060

E2, surface	0.139
E2, 5m	0.040
E2, 10m	0.053
E2, 20m	0.095

C2, surface	0.038
C2, 5m	0.069
C2, 10m	0.063
C2, 20m	0.053
C2, 30m	0.070

B2, surface	0.007
B2, 5m	0.055
B2, 10m	0.041

A2, surface	0.038
A2, 5m	0.051
A2, 10m	0.122
F2, surface	0.051
F2, 5m	0.056

XIII. Appendix 6

Suspended sediment content, inflow streams

This table contains the data obtained from an hourly sampling of Hazard Creek between 08.00 and 19.00 hours on July 18th, and also samples obtained from three minor inflow streams on the afternoon of July 8th.

Location	Time	Suspended sediment concentration (g/l)
Hazard Creek	08.00	0.280
Hazard Creek	09.00	0.206
Hazard Creek	10.00	0.283
Hazard Creek	11.00	0.260
Hazard Creek	12.00	0.473
Hazard Creek	13.00	1.211
Hazard Creek	14.00	1.957
Hazard Creek	15.00	1.488
Hazard Creek	16.00	1.883
Hazard Creek	17.00	1.388
Hazard Creek	18.00	1.119
Hazard Creek	19.00	1.335
Stream 1	13.00	0.186
Stream 2	14.30	2.879
Stream 3	15.30	1.832

XIV. Appendix 7

Stage measurements, July 4th-22nd

The measurements tabulated are in metres below or above an arbitrary zero point, taken as being the stage at which the first measurement was made.

Date	Time	Stage
4th July	15.45	0
5th July	18.30	0
6th July	17.40	-0.07
7th July	18.00	-0.17
8th July	17.50	-0.20
9th July	17.50	-0.17
11th July	17.30	-0.13
12th July	17.45	+0.03
13th July	18.00	+0.03
14th July	18.00	0
15th July	17.05	-0.17
17th July	17.00	-0.05
18th July	15.40	-0.15
19th July	17.00	-0.05
20th July	15.40	-0.15
21st July	14.00	-0.05
22nd July	19.30	0

XV. Appendix 8

Stage measurements, July 18th

Below are the results of hourly observations of stage made on July 18th, from 08.00 to 20.00 hrs. The stage is measured in metres from an arbitrary zero point.

Time	Stage
08.00	-0.25
09.00	-0.23
10.00	-0.23
11.00	-0.21
12.00	-0.17
13.00	-0.15
14.00	-0.12
15.00	-0.09
16.00	-0.05
17.00	-0.05
18.00	-0.07
19.00	-0.07
20.00	-0.07

XVI. Appendix 9

Estimates of daily discharge

Tabulated below are estimates made of the inflow into the lake over a 24 hour period, used as a correction to estimate the volume of water escaping through the sub-glacial tunnel Q_i is given in metres³/second.

TIME	DISCHARGE	TIME	DISCHARGE
0.00	14.0	13.00	16.0
01.00	13.0	14.00	19.0
02.00	11.0	15.00	21.0
03.00	9.0	16.00	23.0
04.00	8.0	17.00	23.0
05.00	7.0	18.00	21.0
06.00	6.0	19.00	20.0
07.00	6.0	20.00	19.0
08.00	7.0	21.00	18.0
09.00	8.0	22.00	16.0
10.00	10.0	23.00	15.0
11.00	12.0		
12.00	14.0		

XVII. Appendix 10

Discharge calculations and data

D is the lake level measured in metres from an arbitrary zero point, three centimetres below the maximum level attained. dD is the difference in lake level between successive measurements, in metres. dt is the time difference between measurements, in thousands of seconds. A is the surface area of the lake at a lake level halfway between the bracketing measurements, in metres² × 10⁵, calculated using the methods described in the text. Qa is the overall discharge from the lake, calculated by $Q_a = dD/dt \cdot A$, and is given in cubic metres/second as is Qi and Qt. Qi is the discharge into the lake from the inflow streams as estimated in the text, and Qt is the discharge through the sub-glacial tunnel, given by $Q_t = Q_a + Q_i$. V is the volume discharged from the lake at the depth of interest, calculated by the methods of the text, and given in cubic metres × 10⁶.

Date	Time	D	dD	dt	A	Qa	Qi	Qt	V
1st	17.20	1.02							
			0.08	13.5	1.126	-6.6	19.0	12.4	1.050
21.05	0.94								
			0.13	42.0	1.133	-3.5	10.0	6.5	0.935
2nd	8.45	0.81							
			-0.04	10.5	1.139	-4.3	8.0	3.7	0.851
	11.40	0.77							
			-0.14	25.8	1.145	-6.2	21.0	14.6	0.755
	18.50	0.63							

-0.31 48.3 1.161 -7.5 Lake full,outflow

3rd 08.15 0.32 operating and thus
 -0.07 19.5 1.174 -4.2 estimate of tunnel
 13.40 0.25 discharge not
 -0.07 22.2 1.179 -3.7 possible
 19.50 0.18
 -0.02 43.5 1.183 -0.5

4th 07.55 0.16
 0.00 14.1 1.183 0
 11.50 0.16
 -0.15 27.6 1.189 -6.5
 19.30 -0.01
 -0.04 8.4 1.274 -6.1
 21.50 -0.03
 0.10 34.8 1.193 3.4

5th 07.30 0.07
 0.01 24.0 1.189 0.5
 14.10 0.08
 -0.07 15.5 1.194 -5.5
 18.25 0.01
 0.11 53.1 1.190 2.5

6th 09.10 0.12
 0.01 10.2 1.186 1.0
 12.00 0.13
 -0.01 12.0 1.186 -1.2
 15.20 0.12
 -0.04 24.0 1.188 -2.0

			0.07	4.5	1.096	17.1	21.0	38.1	1.505
15.45		1.46							
			0.04	2.7	1.092	16.2	23.0	39.2	1.566
16.30		1.50							
			0.07	3.6	1.089	21.1	23.0	54.1	1.617
17.30		1.57							
			0.06	3.6	1.084	18.1	21.0	38.1	1.688
18.30		1.63							
			0.06	3.6	1.081	18.0	20.0	38.0	1.748
1930		1.69							
			0.08	3.6	1.076	23.9	19.0	42.9	1.818
20.30		1.77							
			0.10	3.9	1.070	29.7	18.0	48.7	1.909
21.30		1.87							
			0.09	3.6	1.063	26.6	16.0	42.6	2.008
22.30		1.98							
			0.12	3.6	1.055	35.2	15.0	50.2	2.147
23.30		2.10							
			0.15	3.6	1.048	43.7	14.0	57.7	2.255
10th	00.30	2.25							
			0.16	3.6	1.038	46.1	13.0	59.1	2.412
01.30		2.41							
			0.90	14.4	1.005	62.8	9.5	72.4	2.920
05.30		3.31							
			0.32	3.6	0.969	86.1	7.0	93.1	3.479
06.30		3.63							
			0.38	3.6	0.948	100.1	6.0	106.1	3.806

		0.71	2.3	0.680	211.8	22.0	233.8	8.088
15.33	9.67							
		0.31	0.7	0.660	284.0	23.0	307.0	8.425
16.00	10.25							
		0.51	1.5	0.633	215.2	23.0	238.2	8.861
16.25	10.76							
		0.83	2.1	0.608	240.2	23.0	263.2	9.275
17.00	11.59							
		0.95	1.8	0.574	303.1	22.0	325.1	9.831
17.30	12.54							
		0.55	1.5	0.550	201.8	21.0	222.8	10.23
17.55	13.09							
		1.27	3.6	0.520	183.0	20.0	203.0	10.72
18.55	14.36							
		2.24	3.6	0.468	291.4	19.0	310.4	11.61
19.55	16.60							
		2.77	3.9	0.404	286.7	18.0	304.7	12.70
21.00	19.37							
		7.90	3.6	0.291	689.0	17.0	706.0	14.66
22.00	27.23							

XVIII. Appendix 11

Distances of sections from source

The distance from the mouth of the inflow stream
is given in metres.

Section	Distance	Section	Distance
D1	100	D12	800
D2	100	D13	970
D3	300	D14	1020
D4	460	D15	1070
D5	450	D16	1000
D6	450	D17	890
D7	1100	D18	2000
D9	930	D19	1700
D10	150	D20	570
D11	75	D21	650
		D22	680

I. Appendix 12

Sample descriptions and locations; sections

Unless stated all samples are channel samples through the intervals given.

Sample Number	Depth (m)	Description
D1A	0.00-0.21	Massive sand
D1B	0.51-0.68	Gravel, massive
D1C	0.91-0.94	Massive fine grained sand/silt
D2A	0.09-0.16	Laminated silts/sand
D2B	0.36-0.39	Cross laminated sands
D3A	0.09-0.36	Poorly bedded medium/coarse sands
D4A	0.36-0.39	Laminated silts
D5A	0.25-0.45	Laminated silts
D6A	0.30-0.41	Laminated silts/fine sand
D7A	0.53-0.55	Laminated silts
D7B	0.60-0.65	Laminated silts
D7C	0.66-0.72	Laminated silts
D7D	0.77-0.81	Laminated silts
D8A	0.52-0.84	Laminated silts
D9A	0.00-0.19	Poorly bedded sand
D9B	0.20-0.28	Laminated silts
D9C	0.28-0.40	Laminated silts
D9D	0.68-0.73	Laminated silts
D9E	0.80-0.83	Laminated silts

D10A	0.29-0.33	Graded beds, sand/silt
D10b	0.45-0.50	Laminated silts
D11A	0.60-0.72	Sand/silt, flat bedded
D12A	0.17-0.28	Cross laminated sand
D12B	0.30-0.35	Laminated silts
D12C	0.40-0.45	Laminated silts
D12D	0.50-0.55	Laminated silts
D12E	0.60-0.65	Laminated silts
D12F	0.70-0.75	Laminated silts
D12G	0.80-0.84	Laminated silts
D13A	0.01-0.27	Laminated silts
D14A	0.01-0.46	Laminated silts
D15A	0.18-0.58	Laminated silts
D16A	0.11-0.15	Laminated silts
D16B	0.45-0.50	Laminated silts
D16C	0.85-0.90	Laminated silts
D17A	0.03-0.55	Laminated silts
D18A	0.06-0.20	Laminated silts
D19A	0.00-0.40	Laminated silts
D20A	0.05-0.70	Laminated silts
D20B	0.10-0.15	Laminated silts
D20C	0.20-0.25	Laminated silts
D20D	0.40-0.45	Laminated silts
D20E	0.65-0.70	Laminated silts
D21A	0.11-1.21	Laminated silts
D22A	0.01-0.41	Laminated silts

B30302